**Protein Turnover and Quality Control of Cardiac Myosin Binding Protein C
in Hypertrophic Cardiomyopathy**

by

Amelia Ann Glazier

A dissertation submitted in partial fulfillment
of the requirements for the degree of
Doctor of Philosophy
(Molecular and Integrative Physiology)
in the University of Michigan
2019

Doctoral Committee:

      Associate Professor Sharlene M. Day, Co-chair
      Professor Daniel E. Michele, Co-chair
      Professor Daniel A. Beard
      Professor Andrew P. Lieberman
      Professor Henry L. Paulson

"Life need not be easy, provided only that it is not empty."

– Lise Meitner

"The poets did well to conjoin music and medicine, in Apollo, because the office of medicine is but to tune the curious harp of man's body and reduce it to harmony."

– Sir Francis Bacon

"I encourage you to look at the world around you and think about how it works. My friends, you can go forth and make this world a better place."

– Bill Nye

Amelia A. Glazier

glaziera@umich.edu

ORCID ID: 0000-0002-3248-5773

Dedicated to Dolores Glazier, who gave me my first microscope.

ACKNOWLEDGEMENTS

First and foremost, I must thank my graduate mentor, Dr. Sharlene Day, for six wonderful years in her lab. She has very much supported my journey to become a better scientist and communicator through her own mentorship and enthusiasm for my research. Pursuing this project has allowed me to broaden my horizons and learn how to synthesize techniques and concepts from different biomedical disciplines, from biophysics to translational medicine, into my scientific thinking. I am also very grateful to Dr. Dan Michele, both as my co-mentor and as graduate program chair, for his invaluable scientific advice and commitment to scientific education. Thank you to the members of my dissertation committee, whose varied perspectives always provided well-rounded and constructive critiques at committee meetings, and Dr. Sue Moenter and Dr. Margaret Westfall for the encouragement you gave me when I doubted myself.

I am grateful to the entire Department of Molecular and Integrative Physiology; I cannot imagine a more welcoming and collaborative environment for graduate students. I have also greatly appreciated my experiences with the Systems & Integrative Biology training grant and the chaperone hub of the Protein Folding Diseases Initiative, for challenging me to think outside my normal wheelhouse, and with the University of Michigan Life Sciences Orchestra, who let me sustain my passion for playing music for 5

years of wonderful concerts. Having the privilege to play Beethoven symphonies with the physician who invented ECMO truly made me appreciate being a part of Michigan's amazingly talented science community.

I owe special thanks to many current and former denizens of the 7th floor of MSRBIII: our lab manager Jaime Yob, for running a tight ship and helping me with tissue preps practically weekly for three years; Neha Hafeez, for meticulous benchwork while assisting with experiments; Vi Tang, for cloning wizardry and his ability to befriend anyone; Juliani Rodriguez, for her inextinguishable positive attitude and joy of learning; Andrea Thompson, for words of encouragement throughout the process of writing this dissertation; Kristina Carpenter, for always being on top of all things administrative; and Hannah Hill, for being my late night lab companion and sharing many sincere conversations about the important things in life. Thank you to all Day Lab and Helms Lab members for creating a collegial and congenial environment that was a pleasure to be a part of.

And to my family: thank you to my parents and grandparents, all of whom fostered my twin loves of art and science in different ways. And to my sister Jessica, I dedicate what's left of my mental energy after my defense as she pursues her own PhD in developmental and social psychology at the University of Washington. Finally, to everyone who still believed in me when I couldn't believe in myself, words cannot express my gratitude for your support and advice. You are all the catalysts that allowed me to reach the activation energy I needed to complete my PhD when I was stuck in a low-energy transition state.

TABLE OF CONTENTS

LIST OF FIGURES

LIST OF TABLES

ABSTRACT

The cardiac sarcomere is a complex matrix of molecular machinery that is responsible for contraction of the heart. Proper contractile function relies on maintenance of rigid stoichiometry of myofilament proteins and multiple protein quality control (PQC) pathways. Though PQC is undeniably essential to sarcomere protein homeostasis (proteostasis), there are many gaps in our knowledge of factors that regulate turnover of sarcomere proteins. Mutations in many of these proteins cause hypertrophic cardiomyopathy (HCM), which is often designated a "sarcomeropathy." HCM and is characterized by thickening of the left ventricular free wall and intraventricular septum, myocardial fibrosis, and diastolic dysfunction. The most commonly mutated gene in HCM is cardiac myosin binding protein C (*MYBPC3*). The primary pathogenic mechanisms associated with MYBPC3 mutations remain unresolved. PQC and protein turnover are central to two hypotheses with the most supportive evidence: haploinsufficiency of MYBPC3 in the sarcomere, and proteotoxicity of truncated MYBPC3 protein products. However, very little is known about how MYBPC3 interacts with PQC networks in either physiological or pathological conditions. The goal of this thesis was to investigate pathogenic mechanisms associated with different MYBPC3 mutations, explore the roles of protein homeostasis and turnover with respect to these mechanisms, and identify PQC factors which are involved in MYBPC3 turnover.

Using affinity purification-mass spectrometry, we identified several molecular chaperones as potential novel interactors with MYBPC3, including αB-crystallin and HSP27, and the inducible and constitutive isoforms of the ubiquitous heat shock protein 70kDa family (HSP70 and HSC70, respectively). We then confirmed that HSP70 chaperones regulate proteasomal degradation of MYBPC3 by modulating their expression and activity and observing effects on MYBPC3 protein half-life in a primary cardiomyocyte culture system. This represents to our knowledge the first identification of a chaperone associated with MYBPC3.

To determine the extent to which proteotoxicity of truncated MYBPC3 contributes to HCM pathogenesis in isolation from haploinsufficiency, we explored the effects of acute and chronic expression of truncated MYBPC3 on cardiomyocyte PQC using primary cell culture and a transgenic mouse model, respectively. We reported no deleterious effects of truncated MYBPC3 expression on proteostasis *in vitro* or *in vivo*. Further, chronic expression of a truncating MYBPC3 transgene in mice up to 12 months of age was not sufficient to elicit hypertrophic remodeling. These results challenge the hypothesis that truncated MYBPC3 is directly proteotoxic and suggest a "poison peptide" mechanism may not be relevant to HCM pathogenesis without concurrent MYBPC3 haploinsufficiency.

Lastly, we investigated the locus-dependency of protein stability in non-truncating MYBPC3 mutations. Novel analysis of genotypes using the Sarcomeric Human Cardiomyopathy Registry (SHaRe) of HCM patients uncovered putative clusters of missense mutations in the C3, C6 and C10 domains of MYBPC3. We identified a consistent pattern in C10 mutants of lack of sarcomere incorporation and markedly rapid degradation. This was in contrast to C3 and C6 mutants, which were generally equally

stable as WT MYBPC3 and localized correctly within the sarcomere. These findings demonstrate that mutation locus significantly influences protein stability and turnover, and further dissect pathogenic mechanisms associated with non-truncating mutations.

With these studies, we have moved toward clarifying pathogenic mechanisms in MYBPC3-linked HCM, which will inform future development of targeted interventions for patients with different genotypes. Furthermore, we have identified new potential therapeutic targets to restore normal stoichiometry to haploinsufficient sarcomeres. Finally, we have contributed to our understanding of the enigmatic process of sarcomere protein quality control.

CHAPTER 1

Introduction

1.1   Hypertrophic Cardiomyopathy: presentation and etiology

1.1.1 Characteristics of hypertrophic cardiomyopathy. Familial hypertrophic cardiomyopathy (HCM) is the most common form of the inherited cardiomyopathies, occurring in about 1 in 500 individuals[Maron 1995, Zou 2004]. HCM is a monogenic disease with autosomal dominant inheritance, and is primarily considered a sarcomeropathy, as the vast majority of HCM mutations occur in proteins of the cardiac sarcomere. HCM is therefore distinct from hypertrophy associated with extrinsic factors such as hypertension. The primary feature of HCM is hypertrophic remodeling of the left ventricle and intraventricular septum to a thickness ≥15mm[Jacoby 2013]. In contrast to physiologic hypertrophy in which the LV chamber volume increases along with LV wall thickness, pathologic hypertrophy in HCM leads to a reduction in LV chamber volume.

Functionally, HCM is characterized by diastolic dysfunction associated with impaired myocardial relaxation and reduced filling. LV outflow tract obstruction also frequently occurs in HCM as a result of septal hypertrophy and mitral valve abnormalities[Maron 2002, Shah 1969]. These features can lead to heart failure, arrhythmias and sudden cardiac death. Histological analyses of HCM hearts reveal interstitial fibrosis and

myocardial disorganization[Teare 1958, Yutani 1987]. This disorganization extends to the ultrastructural level; transmission electron microscopy of HCM tissue shows disordered myofilaments and out-of-register Z-disks[Razzaque 2013].

HCM is noted be a particularly heterogeneous disease in several aspects, such as age of onset, magnitude of hypertrophy, cardiac morphology, and severity of symptoms. Mutations are often incompletely penetrant within families, with some mutation carriers developing severe phenotypes while others remain asymptomatic. The disease has been found to first manifest in both children and octogenarians with a median onset at ~45 years of age[Ho 2018]. HCM most commonly presents as asymmetrical LV hypertrophy with the intraventricular septum disproportionally affected, but concentric, apical, and other morphologies can occur[Baxi 2016]. Broad heterogeneity of clinical presentation in HCM makes it difficult to anticipate who will develop disease and which therapeutic interventions to employ. Currently available treatment options include beta-blockers, Ca^{2+} channel inhibitors, implantable cardioverter-defibrillators for patients vulnerable to arrhythmias, and heart transplant for end-stage HCM that has progressed to heart failure.

1.1.2 Genetics of hypertrophic cardiomyopathy. The sarcomere is the basic contractile unit of muscle. HCM-associated mutations occur in the genes for almost all the key contractile and regulatory cardiac sarcomere proteins including cardiac myosin binding protein C (*MYBPC3*) β-myosin heavy chain (*MYH7*), ventricular myosin essential and regulatory light chains (*MYL3* and *MYL2*), α-actin (*ACTC1*), α-tropomyosin (*TPM1*), cardiac troponin C, T, and I (*TNNC1, TNNI3,* and *TNNT2*), and titin (*TTN*)[Kimura 2016]. A number of genes encoding Z-disk associated proteins, such as obscurin (*OBSCN*), four-and-a-half LIM protein-1 (*FHL1*), and muscle LIM protein (*CSRP3*)[Marston 2017, Theis 2006], and

2

proteins related to Ca^{2+} signaling such as phospholamban (*PLN*)[Landstrom 2012] also carry HCM mutations. Despite the increasingly long list of HCM-associated genes, no mutations are detected in about half of HCM cases, though many variants of uncertain significance have been identified. Of cases where a mutation is found, MYBPC3 mutations constitute about 50%[Alfares 2015]. While multiple studies have aimed to differentiate disease severity, progression, and phenotype with specific sub-classes of mutations; there is currently no consensus regarding MYBPC3 mutations being predictive of any particular phenotype or prognosis[Lopes 2013]. Likewise, it has not yet been shown that the location of truncating mutations or missense mutations within MYBPC3 are predictive of clinical outcomes. The majority of patients with MYBPC3-linked HCM are heterozygous for the causative mutation. Compound heterozygotes occur rarely, and are associated with worse clinical outcomes[Hodatsu 2014, Wessels 2015]. Homozygous individuals typically develop severe cardiomyopathy as neonates that is typically lethal by age 1; heart transplant is the only treatment option[Xin 2007, Zahka 2008].

1.1.3 History of research into hypertrophic cardiomyopathy. Physicians as far back as the early 18th century made records of occurrences of sudden death with ventricular hypertrophy or dilation discovered *post mortem*, likely caused by HCM or DCM[Coats 2008]. However, the underlying cause of this cardiac remodeling remained elusive well into the 20th century. Physicians noted that this condition often ran in families, and was not associated with hypertension or aortic valve defects, known stimuli of cardiac hypertrophy. Several terms were proposed as names for the disease, including "idiopathic cardiac hypertrophy," "familial cardiomegaly," and "muscular subaortic stenosis", each reflecting prominent aspects of HCM, but none capturing the whole picture[Coats 2008].

3

Finally, a modern understanding of HCM was first clinically described by pathologist Donald Teare in 1958 based on examination of eight case histories of patients aged 14-45 years with asymmetrical cardiac hypertrophy identified *post mortem*[Teare 1958]. His description includes many of the hallmarks of HCM which are still today used as diagnostic criteria: hypertrophy primarily of the intraventricular septum and left ventricular free wall, extensive myocardial fibrosis, myocyte disarray, and arrhythmia. Additionally, one patient had evidence of outflow tract obstruction and seven of the eight patients experienced sudden cardiac death. More evidence of the inheritability HCM came when the sudden death of one of the patients' brothers revealed highly similar pathologies in both siblings. Subsequent studies of the initial patient's and additional families with histories of heart disease and sudden death supported an autosomal dominant mode of inheritance, and took note of incomplete disease penetrance and significant heterogeneity of symptoms[Emanuel 1971, Hollman 1960, Pare 1961].

In the late 1980s, genetic linkage analysis of affected families identified likely loci for causative mutations in HCM on several different chromosomes [Jarcho 1989, Solomon 1990]. A locus found on chromosome 14 contained the genes for cardiac α and β myosin heavy chains[Saez 1987], which were compelling and logical targets to investigate for HCM-causing mutations. In 1990, β myosin heavy chain (*MYH7*) was the first gene confirmed to harbor mutations which segregated with HCM in affected families[Geisterfer-Lowrance 1990]. Mutations in cardiac troponin T (*TNNT*) and α-tropomyosin (*TPM1*) were the next to be conclusively associated with HCM, suggesting HCM was a disease of the sarcomere related to aberrant function or expression of mutant cardiac contractile proteins[Thierfelder 1994]. MYBPC3 was proposed to be another affected sarcomere protein after its gene was

mapped to a region on chromosome 11 which overlapped with another HCM locus[Carrier 1993, Gautel 1995]. Subsequently, the first MYBPC3 mutations found to be inherited in families with a history of HCM were discovered[Bonne 1995, Watkins 1995], which led to complete sequencing of the *MYBPC3* gene and protein product[Carrier 1997, Gautel 1995]. Since the initial discovery of the molecular etiology of HCM, over 900 individual disease-causing mutations have been identified in at least 15 genes, with the majority encoding sarcomere proteins[Alfares 2015]. MYBPC3 mutations are found in approximately 50% of gene test-positive patients, making MYBPC3 mutations the most common cause of HCM[Alfares 2015].

1.1.4 Mutations in MYBPC3. The *MYBPC3* gene is uniquely affected mostly by nonsense, frameshift, and splice site mutations that produce premature stop codons, compared to other sarcomere genes. While most other genes involved in HCM, especially sarcomere genes, have >90% non-truncating mutations, the reverse is true for *MYBPC3*, in which >90% of mutations prematurely truncate the protein[Alfares 2015, Morita 2008]. Still, certain non-truncating mutations are highly prevalent, including the Arg502Trp mutation found to be the single most common mutation in HCM[Page 2012, Saltzman 2010], and the Pro1210Cysfs*58 mutation present in up to 4% of the South Asian population[Kuster 2014]. Truncating and non-truncating mutations are hypothesized to act through separate mechanisms which will be discussed below.

1.2. Function of MYBPC3 in cardiac muscle: a key regulator of contraction

1.2.1 Sarcomere localization and structural roles of MYBPC3. MYBPC was initially identified as an impurity of intermediate molecular weight in preparations of myosin from rabbit skeletal muscle[Starr 1971]. MYBPC was first isolated simply as an

attempt to generate more pure preparations of myosin, but its strong interaction with myosin made it of physiological interest[Offer 1973]. Microscopy studies showed that MYBPC localized to a limited region within the A-band and confirmed that it corresponded to 7-9 transverse stripes spaced 43 nm apart in the A-band previously observed in electron microscopy analyses of striated muscle[Craig 1976, Pepe 1975]. The segment of the sarcomere containing MYBPC is referred to as the C-zone. The stoichiometric ratio of MYBPC to myosin molecules has been determined to be approximately 1:7-9[Craig 1976]. This stoichiometry suggests only a relatively small percentage of potential cross-bridges are affected by MYBPC under physiological conditions[Stelzer 2006].

MYBPC3 is expressed exclusively in cardiac muscle, while the two other isoforms MYBPC1 and MYBPC2 are only found in skeletal muscle[Weber 1993]. Additionally, MYBPC3 is expressed throughout development, unlike some sarcomere proteins which have specific fetal isoforms[Gautel 1998]. Importantly, this means loss of MYBPC3 expression cannot be compensated for by developmental or non-cardiac isoforms. MYBPC3 has eleven domains connected by linker sequences: eight immunoglobulin-like and three fibronectin III-like referred to as C0 through C10[Gautel 1995, Okagaki 1993]. The C0 domain is unique to cardiac MYBPC3, as is a 30-amino acid sequence in C5, and the "LAGGGRRIS" sequence found within the M-motif, which contains phosphorylation sites not present in skeletal muscle isoforms[Gautel 1995, Kasahara 1994]. MYBPC3 interacts with a number of other sarcomere components, including the S2 region of myosin heavy chain[Starr 1978], light meromyosin[Moos 1975], F-actin[Moos 1978], titin[Furst 1992, Soteriou 1993], and four-and-a-half LIM domain protein 1 (FHL1), a protein of undetermined function which may regulate hypertrophy signaling pathways[Liang 2018, McGrath 2006]. Specific locations of

interactor binding sites can be found in Figure 1.1A. Broadly speaking, the C-terminal domains (C7-C10) are thought to act by anchoring MYBPC3 to the thick filament, while the N-terminal domains (C0-C2) are hypothesized to switch back and forth between myosin S2 and actin in a phosphorylation dependent manner, thereby acting as a regulator of contraction. Interactions with certain specific titin super-repeats may be responsible for limiting localization of MYBPC3 to the C-zone [Furst 1989, Tonino 2017]. The function of the interior domains is not well understood, but the cardiac-specific insertion of the C5 domain is hypothesized to act as a mobile "hinge" sequence and may have intramolecular interactions with other domains[Idowu 2003, Moolman-Smook 2002]. Further, evidence of missense mutation clusters within C3 and C6 points toward important but unknown roles of these domains (See Figure 1.2) (Thompson et. al., manuscript in preparation).

1.2.2 Interactions of MYBPC3 with myosin and the thick filament. Evidence strongly suggests that MYBPC3 acts as a molecular "brake" on contraction. In vitro motility assays have demonstrated that the velocity of actin filaments sliding along native thick filaments decreases when actin reaches the C-zone[Previs 2012]. In the absence of MYBPC3, the velocity remained constant across the entire thick filament. Similarly, in *ex vivo* papillary muscles from MYBPC3 knockout mice, the duration of the cross-bridge cycle was found to be accelerated when compared to muscles from wild-type mice, suggesting the presence of MYBPC3 normally restrains cycling[Lecarpentier 2008]. The myosin S2 binding domain (C1C2 fragment) appears to be sufficient to produce this inhibitory effect both in vitro and in skinned cardiac fibers[Kampourakis 2014, Kunst 2000, Razumova 2006]. The exact molecular mechanism of the "braking" effect has not been conclusively

shown, but recent findings suggest MYBPC3 may stabilize the super-relaxed (SRX)

conformation of myosin heads. In the SRX state, the myosin heads are tightly bound to

the thick filament backbone and display an extremely slow ATP turnover rate, thereby

severely restricting formation of cross-bridges[McNamara 2015]. Hearts of MYBPC3 knockout

mice were shown to have a significantly smaller proportion of SRX myosin as opposed

to disordered-relaxed (DRX) or active myosin when compared to wild-type

hearts[McNamara 2016]. A reduced SRX:DRX ratio has also been observed in myocardial

tissue from HCM patients with MYBPC3 mutations[McNamara 2017]. Reduced expression of

MYBPC3 would hypothetically destabilize SRX myosin, making more myosin heads

available to form cross-bridges. The physiologic purpose of stabilizing SRX myosin has

been speculated to be to maintain a reserve population of myosin heads which can

become active when necessary, such as under β-adrenergic stimulation[Mamidi 2017,

McNamara 2015, Nagayama 2007]. Therefore, the effect MYBPC3 exerts on myosin directly is

likely critical for precise regulation of cardiomyocyte contraction.

1.2.3 Interactions of MYBPC3 with actin and the thin filament

While MYBPC3 has traditionally been designated a thick filament protein, its

association with actin may be equally as important as its interactions with myosin.

MYBPC3 interacts with actin at its N-terminus (C0-M domain), in a region which overlaps

with the C1C2 myosin S2 binding region [Squire 2003]. The C1C2 fragment was found to

retain the "brake" function in filament sliding assays with only myosin S1 present,

indicating that MYBPC3's interaction with the myosin S2 domain is not the only factor in

its function[Saber 2008, Shaffer 2007]. In these studies, C1C2 co-sedimented with actin, but not

myosin S1. Additionally, sarcomere incorporation of C1C2 results in conformational

changes in the troponins associated with thin filament activation even in the presence of blebbistatin, which prevents formation of strong cross-bridges and inhibits force production. This indicates MYBPC3 also interacts directly with the thin filament to alter contractile function, independent of myosin's conformation. Partial extraction, full ablation, and mutation of MYBPC in several experimental models has repeatedly been shown to increase calcium sensitivity of force generation of the sarcomere[Cazorla 2006, Hofmann 1991, Kulikovskaya 2003, Witt 2001], consistent with the increased calcium sensitivity found in myocardium from HCM patients, although this is not limited to individuals with MYBPC3 mutations. Whether this effect originates directly from loss of MYBPC3 in the sarcomere or is an indirect consequence of remodeling is still unclear. However, several of these studies observed that N-terminal fragments of MYBPC3 which bind to actin are capable of activating force production at low or absent Ca^{2+} concentrations[Harris 2004, Herron 2006, Kampourakis 2014, Razumova 2008, Witt 2001]. Subsequently, Previs et. al. demonstrated that when N-terminal MYBPC3 fragments are bound to the thin filament, tropomyosin is displaced from the blocked position, uncovering the myosin-binding sites on actin in a similar fashion to the displacement induced by Ca^{2+} binding to troponin C[Previs 2012]. This interaction potentially explains the effect of MYBPC3 on Ca^{2+} sensitivity of force. Further, the thin filament activating property may serve to equalize activation status near the M-line, the furthest point from the location of Ca^{2+} release units at the Z-disk and the lowest point in a Ca^{2+} concentration gradient across the sarcomere generated after excitation[Previs 2015]. Recently, it has also been proposed that through this activating property, MYBPC3 may act as a sarcomere length sensor. Skinned myocardium from homozygous MYBPC3 knockout mice was found to have a blunted length-dependent rate of force

redevelopment, implicating MYBPC3 as a major contributor to the length-dependent activation mechanism, wherein sarcomere length influences Ca^{2+} sensitivity and force development.[Mamidi 2014, Pfuhl 2012].

1.2.4 Regulation of MYBPC3 function by phosphorylation. These findings provide substantial evidence that MYBPC3 is a significant regulator of both thick and thin filament function capable of meticulously fine-tuning contraction. This fine-tuning is further controlled by phosphorylation of residues mediated by protein kinase A (PKA), protein kinase C (PKC), protein kinase D (PKD), Ca^{2+}/calmodulin dependent kinase II (CaMKII) and GSK3β (Figure 1.1*A*) [Bardswell 2010, Gautel 1995, Hartzell 1984, Kuster 2013, Mohamed 1998, Venema 1993]. In fact, phosphorylation is essential for proper MYBPC3 function. The phosphorylation sites considered to be most influential in terms of affecting function are found in the cardiac-specific sequence within the C1-C2 linker at Ser275, Ser284, and Ser304 (residue positions represent human MYBPC3). A series of studies from the Sadayappan Lab using phosphonull and/or phosphomimetic mutations at these sites underscore the importance of phosphorylation to MYBPC3 function and the complexity of its consequences on cardiac physiology and disease. Replacement of all three serine residues with alanine in a transgenic mouse model, completely abolishing phosphorylation at these sites, resulted in significant diastolic dysfunction and dilated cardiac morphology comparable to the knockout mouse phenotype, while a full phosphomimetic mouse model with all three serines mutated to aspartic acid residues displayed no adverse phenotype[Gupta 2013, Sadayappan 2005, Sadayappan 2006]. Surprisingly, mimicking phosphorylation at only one site while ablating it at the other two results in three distinct phenotypes: normal (S275A/S284D/S304A), dilated

10

(S275D/S284A/S304A), and hypertrophic (S275A/S284A/S304D)[Sadayappan 2011]. S275D/S284A/S304D transgenic mice developed a hypertrophic phenotype as well[Gupta 2013]. These findings imply that each phosphorylation site exerts its own unique effect on MYBPC3 function, and that maintenance of cardiac function requires a delicate balance of phosphorylation state. This is corroborated by the fact that MYBPC3 total phosphorylation has been observed to be significantly decreased in HCM, end-stage heart failure, pressure overload-induced right heart failure, and myocardial ischemia[Decker 2005, El-Armouche 2007, Jacques 2008, Walker 2011]. Baseline phosphorylation levels of MYBPC3 in human donor myocardium have been reported to be fairly high, at 4-5mol P_i/mol MYBPC3, suggesting a combination of regulatory effects from each phosphoresidue is necessary for proper function[Jacques 2008]. The precise molecular mechanism relevant to each site remains to be determined, but there is evidence that phosphorylation of these sites follows a hierarchical pattern, with phosphorylation of Ser284 significantly enabling accessibility of the other two sites to several kinases[Gautel 1995, Sadayappan 2011].

Overall, phosphorylation affects MYBPC3 by altering its conformation and spatial orientation such that the N-terminal domains interact with either myosin or actin, thus affecting myosin conformation[Weisberg 1996]. Current evidence supports a mechanism in which unphosphorylated MYBPC3 favors N-terminal interactions with myosin S2 associated with the "braking" effect, while phosphorylated MYBPC3 favors interactions with actin associated with thin filament activation[Gruen 1999, Kulikovskaya 2003, Taylor 2016]. Accordingly, phosphorylation blunts the "braking" effect[Previs 2012]. This mechanism is supported by *in vitro* findings indicating that incorporation of phosphonull MYBPC3 into isolated thick filaments promotes ordered arrangement of myosin heads consistent with

the SRX conformation, while phosphomimetic MYBPC3 produces more disordered filaments, suggesting more myosin heads are in the DRX conformation[Kensler 2017]. Phosphomimetic MYBPC3 also reduces myofilament Ca^{2+} sensitivity and enhances the length-dependent activation response in skinned myocardium[Kumar 2015]. Thus, phosphorylation of MYBPC3 acts as a switch to promote either thick filament inactivation or thin filament activation, depending on the prevailing physiological needs.

1.2.5 Roles of MYBPC3 in whole-organ cardiac physiology. The molecular interactions of MYBPC3 with the thick and thin filaments, when translated to the whole organ level, produce both inotropic (affecting force of contraction) and lusitropic (affecting rate of relaxation) effects on the heart[Pohlmann 2007, Winegrad 1999]. Decreased lusitropy can lead to impaired LV filling as less relaxation during diastole allows a reduced volume of blood to enter the LV and can increase intraventricular pressure. Diastolic dysfunction very frequently develops in HCM, highlighting a critical role for MYBPC3 in modulating cardiac lusitropy. MYBPC3's effects on contraction and relaxation are primarily hypothesized to be mediated by changes in the rate of cross-bridge attachment and detachment in response to phosphorylation[Moss 2015, Tong 2004]. Phosphorylation of MYBPC3 by PKA is thought to be a significant contributor the accelerated cross-bridge cycling kinetics and enhanced systolic function induced by β-adrenergic stimulus[Gresham 2017, Gresham 2016, Tong 2008]. Phosphomimetic constitutive phosphorylation of Ser304 largely abolished the positive inotropic effects of dobutamine *in vivo,* again supporting an important role for MYBPC3 in preserving a β-adrenergic contractile reserve [Mamidi 2017]. Additionally, papillary muscles from a phosphomimetic mouse model exhibited a faster relaxation rate, while muscles from phosphonull mice had a slowed relaxation rate as well

12

as diastolic dysfunction[Rosas 2014]. In a separate study, phosphonull MYBPC3 mice exhibited both decreased rates of pressure development in systole and of pressure decline in diastole, as determined by *in situ* pressure-volume analysis[Gresham 2016]. Independently of phosphorylation, total loss of MYBPC3 in mice was associated with lowered end-systolic pressure and abbreviated systole leading to reduced ejection fraction[Nagayama 2007]. As discussed above, MYBPC3 may be involved in length-dependent activation. Impaired length-dependent activation has been observed in HCM patient myocardial tissue, though again, this is not limited to those with MYBPC3 mutations[Sequeira 2013, van Dijk 2012, Vikhorev 2018]. Length-dependent activation is the main cellular mechanism contributing to the Frank-Starling Law of the heart, which defines the directly proportional relationship between end-diastolic volume and stroke volume.

1.3   Proposed primary pathogenic mechanisms in MYBPC3-linked HCM

Despite extensive focus on the biophysical, cellular and physiological functions of MYBPC3, a definitive mechanism linking the effect of mutations in MYBPC3 to hypertrophic myocardial remodeling has not been established. Two hypotheses have received significant emphasis in the literature regarding truncating MYBPC3 mutations specifically, both of which center on homeostasis of MYBPC3 protein. The first of these is the haploinsufficiency hypothesis. Haploinsufficiency occurs when a heterozygous mutation results in single functional copy of a gene that is insufficient to maintain normal function, and is a primary mechanism underlying many Mendelian diseases such as HCM[Deutschbauer 2005]. This hypothesis thus asserts that HCM patients with truncating MYBPC3 mutations express reduced MYBPC3 protein in the myocardium, and that pathogenesis arises from a relative absence of functional protein. Incorporated

sarcomere proteins adhere to strict stoichiometric ratios; therefore, balance between their synthesis and degradation must be precisely regulated. However, the mechanisms fundamental to this stringent regulation are not yet clear. Experiments using exogenous tagged sarcomere proteins have demonstrated the remarkable imperturbability of sarcomere stoichiometry. Overexpression of such proteins leads to replacement of incorporated endogenous protein within the sarcomere without a change in total expression levels or ratios, while excess unincorporated protein is degraded[Gulick 1997, Michele 1999, Rust 1999, Sadayappan 2008, Thompson 2014]. These findings make the question of why MYBPC3 stoichiometry may not be preserved in MYBPC3-linked HCM all the more perplexing. The second hypothesis suggests that truncated mutant MYBPC3 proteins are proteotoxic; that is, they are capable of disrupting normal protein quality control (PQC) systems through aggregation or overload of rate-limiting PQC elements. An overview of the intersecting PQC systems involved in sarcomere protein homeostasis can be found in Figure 1.3. In this case, pathogenesis arises from the presence of non-functional protein. It should be noted that these hypotheses are not mutually exclusive. However, few studies have tried to determine whether either absence of functional protein or presence of non-functional protein, in isolation from the other, are necessary or sufficient for HCM pathogenesis. Existing evidence for and against each hypothesis will be discussed below.

   1.3.1   Evidence for haploinsufficiency of WT MYBPC3. Haploinsufficiency has been suspected as a potential pathogenic mechanism in HCM patients with truncating MYBPC3 mutations since the first truncating mutations were identified in the mid-1990s[Andersen 2004, Yang 1998, Yu 1998]. Over the following twenty years, multiple independent

studies have failed to detect truncated mutant proteins in myocardial tissue of HCM patients[Helms 2014, Jacques 2008, Marston 2009, Rottbauer 1997, Theis 2009, van Dijk 2009, van Dijk 2012]. Most importantly, a majority of studies using patient tissue found reduced wild-type MYBPC3 protein expression (Table 1.1). Allelic imbalance at the mRNA level favoring an increased ratio of wild-type to mutant transcript was also reported in some cases[Helms 2014, Marston 2009, van Dijk 2009]. The combined results indicate that on average, HCM patients with MYBPC3 truncating mutations express roughly 70% of wild-type MYBPC3 protein compared to control individuals. This suggests a compensatory mechanism that incompletely overcomes the loss of mutant allele, but cannot maintain the MYBPC3 sarcomere stoichiometry necessary for normal contractile function.

To test this hypothesis experimentally, several *in vitro* and *in vivo* studies have been performed to show that replacement of functional MYBPC3 in haploinsufficient models can attenuate phenotype, while reduction of functional MYBPC3 can induce hypertrophic responses. Cardiomyocytes derived from human induced pluripotent stem cells (hiPS-CMs) and embryonic stem cells (hES-CMs) are emerging as a powerful tool to study cardiomyopathies in a human model. Though significant variations in methodologies should be recognized, these studies broadly suggest reduction of MYBPC3 may also be present in both patient-derived and genetically engineered hiPS-CMs (A summary of MYBPC3 studies in hiPS-CMs and hES-CMs can be found in Table 1.2). Differentiated cardiomyocyte cultures with reduced MYBPC3 expression showed a mixture of phenotypes including cellular hypertrophy, myofibrillar disarray, reduced force generation, and Ca^{2+} dysregulation. In further support of the haploinsufficiency hypothesis, gene replacement therapy resulting in increased WT MYBPC3 expression

was found to ameliorate hypertrophy and dysfunction in two independent studies within stem cell based systems[Monteiro da Rocha 2016, Prondzynski 2017]. However, some hiPS-CM models have not exhibited any significant reduction in MYBPC3 expression while still displaying phenotypes[Seeger]; therefore it is still unclear whether haploinsufficiency itself is the triggering mechanism.

Several mouse models carrying null or truncating MYBPC3 mutations exist; however, there is considerable variability in severity and onset of phenotype between heterozygotes of different models, with some exhibiting very mild to no phenotype[Carrier 2004, Harris 2002, McConnell 1999, Vignier 2009]. It is possible that this variability is correlated to the amount of wild-type MYBPC3 each model expresses. *In vivo* experiments which have utilized approaches to correct or induce haploinsufficiency have helped mechanistically dissect whether reduction in MYBPC3 expression is a precursor or downstream consequence of cardiac hypertrophy. Heterozygous knock-in mice carrying a G>A transition in the last nucleotide of exon 6, which produces multiple products including a full-length missense transcript, a transcript terminating in exon 9, and a deletion of exon 6, express ~80% of control MYBPC3 levels and display diastolic dysfunction[Fraysse 2012, Vignier 2009]. Exon skipping of exons 5 and 6 via antisense oligoribonucleotide injection increased expression of total MYBPC3 and temporarily rescued cardiomyopathy, though only in neonatal mice[Gedicke-Hornung 2013]. The protein product lacking the sequence encoded by exons 5 and 6 was stable and functional. In the same mouse model, wild-type MYBPC3 gene therapy delivered by adeno-associated virus to neonatal mice was able to partially prevent hypertrophic remodeling in a dose-dependent manner[Mearini 2014]. Conversely, a tamoxifen-inducible homozygous MYBPC3 knockout mouse model was

used to assess the consequences of loss of MYBPC3 expression in adult (12 week-old) mice. By 2 weeks after knockdown, MYBPC3 expression was reduced to ~40% of controls, and diastolic dysfunction was observed. At 20 weeks after knockdown, with MYBPC3 protein at ~10% of controls, left ventricular weight and wall thickness had significantly increased, suggesting that a marked reduction in MYBPC3 can induce significant functional and structural changes. Similarly, morpholino-mediated knockdown of MYBPC3 in *d. rerio* elicited dose-dependent symptoms consistent with hypertrophic remodeling[Chen 2013]. While there is much evidence in the literature that haploinsufficiency of MYBPC3 is sufficient to induce hypertrophic remodeling, variability in mouse model and hiPS-CM phenotypes leaves open the question of whether a "second hit" caused by currently unknown factors is necessary in conjunction with haploinsufficiency.

 1.3.2 Evidence for proteotoxicity of truncated MYBPC3. While truncated MYBPC3 proteins have not yet been observed in myocardium from MYBPC3-linked HCM patients, it is important not to assume that absence of evidence equals evidence of absence. Low or absent truncated protein has been attributed to two different quality surveillance mechanisms: i) nonsense-mediated decay (NMD), a process by which mRNA transcripts with premature termination codons located 50 or more nucleotides upstream of an exon-exon junction are targeted for degradation; and ii) the ubiquitin proteasome system (UPS), through which proteins labeled with ubiquitin are targeted for degradation by the proteasome, a large macromolecular protease complex[Sarikas 2005, Vignier 2009]. However, despite allelic imbalance and NMD, mutant mRNA remains present. Our lab and others have previously shown that potentially ~16-40% of total MYBPC3 mRNA in HCM patient myocardium may originate from the mutant allele, and could provide a

template for truncated protein. Western blotting was the most commonly used detection method cited in studies which looked for truncated MYBPC3 proteins; in some cases the authors established lower detection limits in their experiments varying from 1.5-3.0% of total MYBPC3 protein[Marston 2009, Rottbauer 1997, van Dijk 2009]. This leaves open the possibility that truncated protein is present at levels below the resolution of techniques reported thus far, due to accelerated UPS-mediated degradation. It has been suggested that the need to continually degrade any truncated MYBPC3 that is translated over the lifetime of an HCM patient could cause chronic stress to the proteasome and affect hypertrophic signaling pathways[Carrier 2010, Day 2013]. This hypothesis is supported by findings of UPS dysfunction in myocardial tissue from HCM patients. Our lab has reported that the chymotrypsin- and caspase-like activities of the proteasome were significantly depressed in HCM myocardium, comparably to the activity observed in failing myocardium[Predmore 2010]. Although not tested in isolation from other genotypes, the majority of samples in these experiments were from HCM patients with MYBPC3 truncating mutations. Thottakara *et. al.* also reported a 45% reduction in chymotrypsin-like proteasome activity in samples with MYBPC3 mutations exclusively[Thottakara 2015]. Lastly, observation of preamyloid oligomers in myocytes from patient myocardium suggests that proteostasis may be impaired in HCM[Sanbe 2004].

When expressed in several *in vitro* systems, truncated MYBPC3 proteins have reliably been reported to have lower steady state expression and fail to incorporate into the sarcomere compared to WT MYBPC3[Bahrudin 2008, Flavigny 1999, Sarikas 2005]. These studies have analyzed a range of truncated proteins of varying sizes. Such findings suggest truncated MYBPC3 in general is degraded at a faster rate than WT MYBPC3. Accelerated

degradation could be a function of several factors including lack of sarcomere incorporation, protein folding status, and altered interactions with PQC pathways. Furthermore, some *in vitro* studies have presented evidence that expression of truncated MYBPC3 in neonatal cardiomyocytes is sufficient to induce dysfunction of the UPS, as determined by reduced chymotrypsin-like activity of the 20S proteasome, increased polyubiquitinated proteins, and accumulation of a fluorescent UPS substrate whose expression is inversely proportional to UPS function[Bahrudin 2008, Sarikas 2005]. Limited evidence also exists that truncated MYBPC3 itself can form ubiquitin-positive aggregates of presumably misfolded protein in neonatal cardiomyocytes[Sarikas 2005]. In regards to *in vivo* models, The Carrier Lab reported a compelling series of experiments using both heterozygous truncating MYBPC3 knock-in and heterozygous MYBPC3 knock-out mice. While both knock-in and knock-out mice showed increases in ubiquitinated proteins at baseline, only in the knock-in mice was chymotrypsin-like proteasome activity reduced[Schlossarek 2012]. Further, with the additional challenge of isoprenaline and phenylephrine to induce adrenergic stress, once again only the knock-in mice displayed decreased proteasome activity. In a subsequent study, the MYBPC3 knock-in and knock-out mice were crossed with a Ub^{G76}-GFP UPS reporter line and cardiac phenotype was examined at 1 year of age[Schlossarek 2012]. Knock-in mice, but not knock-out, showed accumulation of the reporter protein, indicating general impairment of the UPS pathway. Additionally, the heart weight/body weight ratio of the knock-in mice was larger than that of either wild-type or knock-out mice. These results suggest that not only can expression of truncated MYBPC3 exacerbate hypertrophy, but it is necessary to cardiac UPS dysfunction in HCM. The caveat to these studies, however, is that truncated protein

expression was induced in a haploinsufficient model, making it unclear whether UPS dysfunction can be caused by truncated protein expression alone.

1.4   Experimental rationale and approach

This project consists of experiments designed to address three specific aims:

(i)   Define physical and functional interactions between MYBPC3 and protein quality control-related factors. (Chapter 2)

(ii)   Assess proteotoxic effects of truncating MYBPC3 mutations *in vitro* and *in vivo.* (Chapter 3)

(iii) Assess mutation locus-dependent protein stability in non-truncating MYBPC3 mutations. (Chapter 4)

Each aim seeks to generate a better understanding of pathogenesis in MYBPC3-linked HCM and on a broader scale to expand our basic knowledge of regarding the roles of proteostasis and protein quality control mechanisms in myocardial physiology.

Chapter 2 presents an unbiased, affinity purification-mass spectrometry screening assay developed to identify novel physical interactions between MYBPC3 and protein quality control factors. Select proteins which passed our specificity criteria were considered candidates for assessment of potential functional interactions. Subsequently, a biochemical pulse-chase assay was used to monitor degradation of MYBPC3 in response to genetic and pharmacological manipulations of candidate interactors using a primary cardiomyocyte culture model. The rationale and significance of this aim was to begin to understand the specific regulation of MYBPC3 protein turnover and degradation. While specific chaperones, co-chaperones, and E3 ligases have been identified for other

important myofilament proteins, literature on MYBPC3 protein quality control has only just scratched the surface.

Chapter 3 presents first a series of experiments using a panel of five disease-causing truncating MYBPC3 mutations expressed in neonatal rat ventricular cardiomyocyte (NRVM) cell culture. These experiments began as an attempt to replicate the ubiquitin proteasome system dysfunction reported by a previous study suggesting that truncated MYBPC3 protein was sufficient to derail proteostasis in cardiomyocytes. Based on findings from Chapter 2, we then expanded these experiments to look at responses of heat shock protein kDa (HSP70) molecular chaperones. After this acute expression-based model system produced no signs of proteostasis being affected, we moved to a transgenic mouse model which expresses truncated MYBPC3 against a non-haploinsufficient background. Chronic, lifetime expression of this mutation was not sufficient to disrupt myocardial proteostasis or induce hypertrophic LV remodeling. The significance of this aim goes toward determining the relative contributions of the two hypothetical pathogenic mechanisms proposed above.

Chapter 4 presents experiments designed to evaluate the stability of a second panel of disease-causing, non-truncating MYBPC3 mutations expressing in NRVMs. The stimuli for this study was the observation in Chapter 2 that a non-truncating mutation in the C10 domain was subject to extremely rapid degradation, combined with novel patient genotype data from the Sarcomeric Human Cardiomyopathy Registery (SHaRe) revealing three putative non-truncating mutation clusters in the C3, C6, and C10 domains. We used a streamlined cycloheximide pulse-chase assay and localization analysis to identify patent indications of protein instability associated with C10, but not C3 or C6

mutants. These results provide surprising evidence that some MYBPC3 missense mutations, research for which is underrepresented in the literature, may share a common pathogenic mechanism with truncating mutations.

FIGURE 1.1
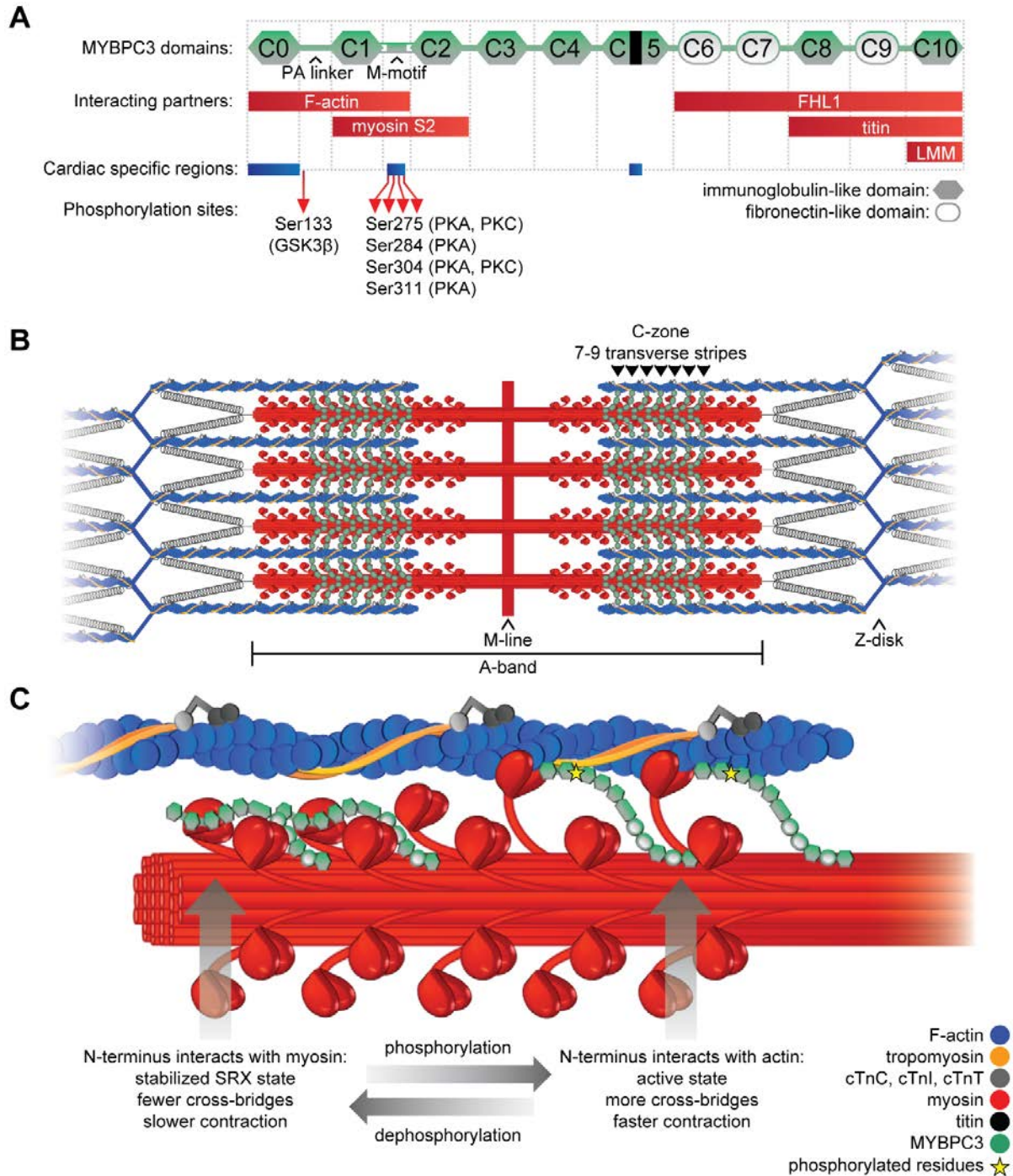
Figure 1.1. Structure, localization, and function of MYBPC3. *(A)* Diagram of MYBPC3 structure highlighting domains associated with known interactors, cardiac-specific sequences, and key phosphorylation sites. References for identification of binding domains: S2:C1-C2[Gruen 1999],LMM:C10[Flashman 2007, Miyamoto 1999]; Actin:C0-C2[Kensler 2011, Shaffer 2009, Squire 2003, Whitten 2008]; Titin:C8-C10[Freiburg 1996]; FHL1:C6-C10[McGrath 2006]. *(B)* MYBPC3 localizes exclusively to 7-9 transverse stripes in the C-zone of the sarcomere. *(C)* MYBPC3 modulates contraction by both inhibiting acto-myosin interactions when unphosphorylated and activating the thin filament when phosphorylated.

FIGURE 1.2
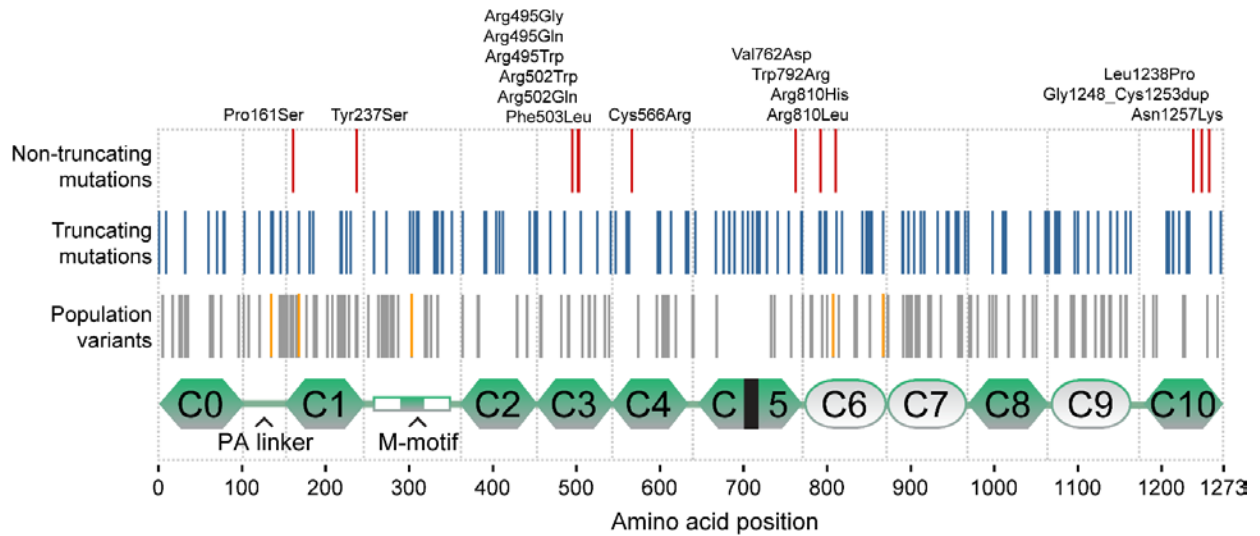
Figure 1.2. *MYBPC3* mutation landscape. Truncating mutations are more abundant and occur along the entire gene. Missense and non-truncating mutations are far less frequent, and may potentially cluster specifically in domains C3, C6, and C10. Genotype analysis was accomplished using de-identified data of a cohort of HCM patients with MYBPC3 mutations from the Sarcomere Human Cardiomyopathy Registry (SHaRe).

FIGURE1.3
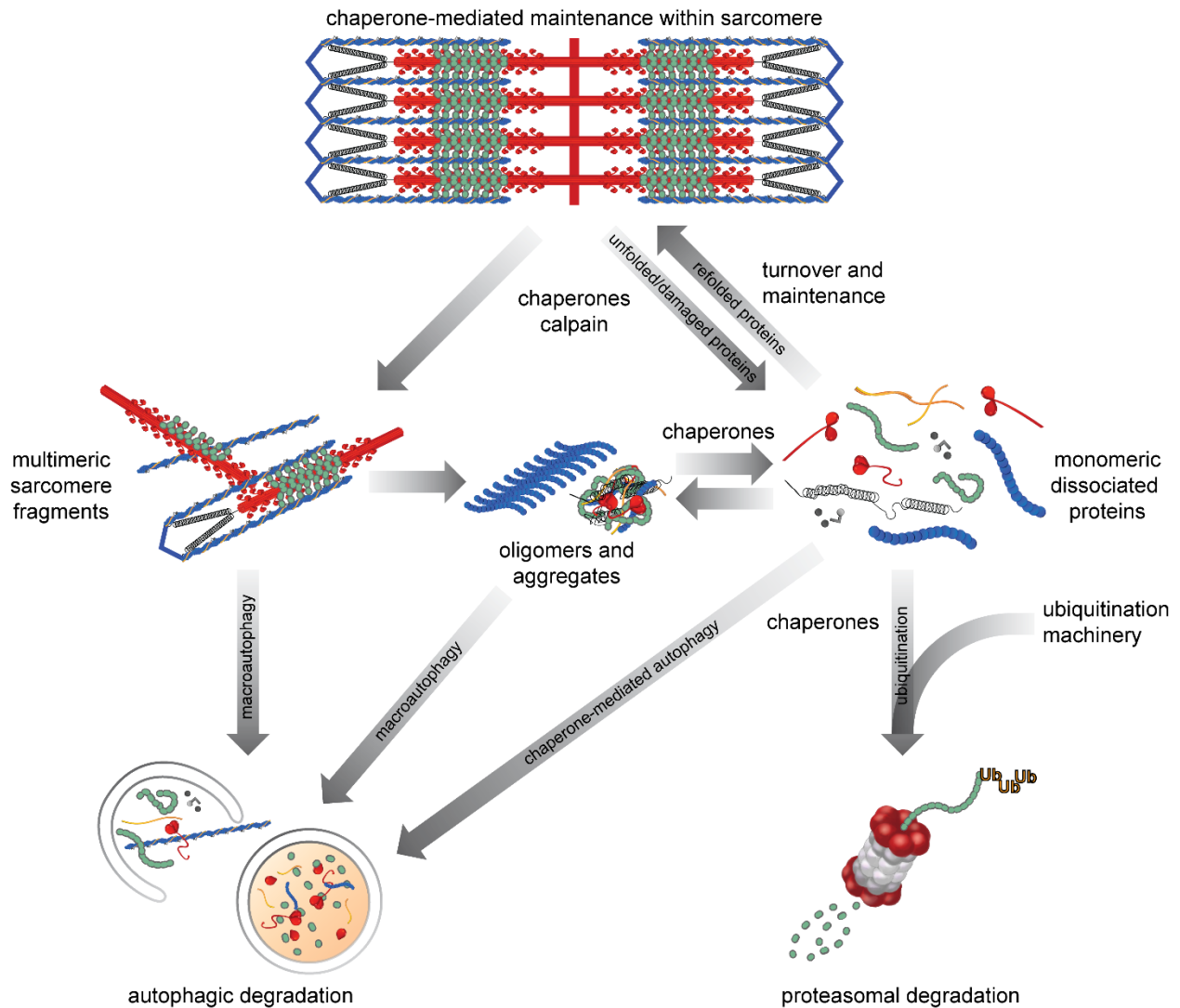
Figure 1.3. Overview of protein quality control pathways for sarcomeric proteins.
Proteostasis of the sarcomere is maintained by activity of sarcomere-associated chaperones/co-chaperones and cytoplasmic chaperone handling of proteins dissociated from the sarcomere. The calpain pathway is thought to facilitate myofilament protein dissociation. Terminally misfolded or damaged proteins must be isolated from the myofilaments in order to undergo proteasomal degradation through the ubiquitin proteasome system (UPS). Single proteins can also be targeted for chaperone-mediated autophagy (CMA) or chaperone-assisted selective autophagy (CASA). Larger, multimeric sarcomere fragments and aggregates that are not disassembled are removed by macroautophagy via autophagosomes and lysosomal degradation.

TABLE 1.1. MYBPC3 haploinsufficiency studies in patient myocardium.

Study	# unique mutations	% mutant MYBPC3 mRNA	% MYBPC3 protein compared to donors	p-value (protein level)	Protein detection method / normalization
[Jacques 2008]	2	Not reported	76±4%	not reported	Immunoblot / actin
[Marston 2009]	5	~40%	76±3%	not reported	Immunoblot / actin
[Theis 2009]	7	Not reported	~200%	p<0.001	Immunoblot / GAPDH
[van Dijk 2009]	2	~20%	67±5%	p<0.05	Immunoblot / α-actinin
[van Dijk 2012]	4	Not reported	67±5%	p<0.0001	SDS-PAGE and SYPRO stain / α-actinin
[van Dijk 2014]	3	Not reported	65±5%	not reported	SDS-PAGE and SYPRO stain / α-actinin
[Helms 2014]	15	16±3%	88±6%	not significant	Immunoblot / GAPDH
[McNamara 2017]	8	Not reported	~68%	p<0.05	Immunoblot / α-actinin

TABLE 1.2. MYBPC3 haploinsufficiency studies in hESC-CMs or hiPS-CMs

Study	Model	Mutation	% mutant MYBPC3 mRNA	% MYBPC3 protein compared to control	p-value (protein level)	Protein detection method / normalization	Phenotype
[Tanaka 2014]	hiPS-CM	p.Gly999_Gln1004del	Not reported	~80% at day 60	p<0.05	Immunoblot / GAPDH	Cellular hypertrophy, myofibrillar disarray
[Birket 2015]	hiPS-CM	c.2373dupG p.Trp792Val fs*41	Not reported	<50% at day 25	p<0.05	Immunoblot / α-actinin	Reduced force generation No cellular hypertrophy
[Monteiro da Rocha 2016]	hES-CM	c.2905+1 G>A	<10%	~50% only at day 17 of differentiation. No difference at day 30.	p=0.04	Immunoblot / α-actinin	Cellular hypertrophy, sarcomere disarray, dysregulated Ca^{2+} homeostasis
[Prondzynski 2017]	hiPS-CM	p.Val454Cys fs*21	Not reported	~50%	p=0.064	Immunoblot / α-actinin	Cellular hypertrophy
[Ribeiro 2017]	hiPS-CM	TALEN-engineered KO via stop codon in exon 1	~50%	Reduced; not quantified	not reported	Immunoblot / α-actinin	Contractile defects, Reduced force generation
[Seeger]	hiPS-CM	p.Arg943*	32.7±0.6%	No difference at days 53-50	not significant	Immunoblot / α-sarcomeric actin	No cellular hypertrophy, elevated diastolic Ca^{2+}

TABLE 1.3. Animal models of MYBPC3-linked HCM.

Model *(species)*	Genetic background	Mutation type	Homozygous phenotype	Heterozygous phenotype	WT MYBPC3 protein levels compared to controls
Mus musculus					
[McConnell 1999] [McConnell 2001] [Fraysse 2012]	Black Swiss	Truncating in exon 30	At 8-12 weeks: • Fibrosis • Diastolic dysfunction • Dilated cardiomyopathy	At >125 weeks: • LV wall hypertrophy • No functional deficits	+/-: 89.9±8.5% -/-: no WT protein
[Harris 2002] [Korte 2003]	C57/BL6	Truncating Removal of exons 3-10	At 12 weeks: • Ca^{2+} sensitivity ↓ • Hypertrophy • Diastolic dysfunction) • accelerated cross-bridge cycling kinetics	• No phenotype	+/-: no reduction -/-: no WT protein
[Carrier 2004] [Schlossarek 2012] [Schlossarek 2012]	C57/BL6 or C57/BL6-Black Swiss mixed	Transcription start site knock out	At ~14 weeks: • Dilated cardiomyopathy • Diastolic dysfunction • Eccentric left ventricular hypertrophy	At 10-11 months: • Asymmetric septal hypertrophy	At 10-11 mo +/-: ~75% -/-: no WT protein
[Vignier 2009] [Fraysse 2012] [Gedicke-Hornung 2013] [Mearini 2014]	Black Swiss	Splice site (c.772G>A) multiple products. truncating and non-truncating Δexon6	• Ca^{2+} sensitivity ↑ • Hypertrophy • Diastolic dysfunction	• Ca^{2+} sensitivity ↑ • Diastolic dysfunction	At 60 weeks +/-: 79% of WT -/-: 10% of WT
[Chen 2012]	C57/BL6	Conditional truncating (tamoxifen induces deletion of exons 3-5)	Knockout induced at 12wk. By 20wk post tamoxifen (32wk): • Myocyte hypertrophy • Fibrosis		Less than 10% of vehicle controls by 8 weeks after tamoxifen treatment
Felis catus					
[Meurs 2005] [Carlos Sampedrano 2009] [van Dijk 2016]	Maine Coon cat	Non-truncating Ala31Pro	• Hypertrophy • Sudden death • Diastolic dysfunction	• Hypertrophy • Longer lifespan than -/-	Allelic imbalance in +/- (WT > A31P). Total MYBPC3 unchanged in both +/- and -/-
Danio rerio					
[Chen 2013]		Knockdown using morpholinos against translation start site	At 72hr post fertilization, dose dependent increase in: • Heart failure • Ventricular wall thickness • Atrial enlargement		Extent of knockdown not determined

1.5 REFERENCES

1.   Alfares AA, Kelly MA, McDermott G, Funke BH, Lebo MS, Baxter SB, Shen J, McLaughlin HM, Clark EH, Babb LJ, Cox SW, DePalma SR, Ho CY, Seidman JG, Seidman CE, Rehm HL. Results of clinical genetic testing of 2,912 probands with hypertrophic cardiomyopathy: Expanded panels offer limited additional sensitivity. *Genetics in medicine : official journal of the American College of Medical Genetics*. 2015

2.   Andersen PS, Havndrup O, Bundgaard H, Larsen LA, Vuust J, Pedersen AK, Kjeldsen K, Christiansen M. Genetic and phenotypic characterization of mutations in myosin-binding protein c (mybpc3) in 81 families with familial hypertrophic cardiomyopathy: Total or partial haploinsufficiency. *European journal of human genetics : EJHG*. 2004;12:673-677

3.   Bahrudin U, Morisaki H, Morisaki T, Ninomiya H, Higaki K, Nanba E, Igawa O, Takashima S, Mizuta E, Miake J, Yamamoto Y, Shirayoshi Y, Kitakaze M, Carrier L, Hisatome I. Ubiquitin-proteasome system impairment caused by a missense cardiac myosin-binding protein c mutation and associated with cardiac dysfunction in hypertrophic cardiomyopathy. *Journal of molecular biology*. 2008;384:896-907

4.   Bardswell SC, Cuello F, Rowland AJ, Sadayappan S, Robbins J, Gautel M, Walker JW, Kentish JC, Avkiran M. Distinct sarcomeric substrates are responsible for protein kinase d-mediated regulation of cardiac myofilament ca2+ sensitivity and cross-bridge cycling. *The Journal of biological chemistry*. 2010;285:5674-5682

5.   Baxi AJ, Restrepo CS, Vargas D, Marmol-Velez A, Ocazionez D, Murillo H. Hypertrophic cardiomyopathy from a to z: Genetics, pathophysiology, imaging, and management. *Radiographics : a review publication of the Radiological Society of North America, Inc.* 2016;36:335-354

6.   Birket MJ, Ribeiro MC, Kosmidis G, Ward D, Leitoguinho AR, van de Pol V, Dambrot C, Devalla HD, Davis RP, Mastroberardino PG, Atsma DE, Passier R, Mummery CL. Contractile defect caused by mutation in mybpc3 revealed under conditions optimized for human psc-cardiomyocyte function. *Cell reports*. 2015;13:733-745

7.   Bonne G, Carrier L, Bercovici J, Cruaud C, Richard P, Hainque B, Gautel M, Labeit S, James M, Beckmann J, Weissenbach J, Vosberg HP, Fiszman M, Komajda M, Schwartz K. Cardiac myosin binding protein-c gene splice acceptor site mutation is associated with familial hypertrophic cardiomyopathy. *Nature genetics*. 1995;11:438-440

8. Carlos Sampedrano C, Chetboul V, Mary J, Tissier R, Abitbol M, Serres F, Gouni V, Thomas A, Pouchelon JL. Prospective echocardiographic and tissue doppler imaging screening of a population of maine coon cats tested for the a31p mutation in the myosin-binding protein c gene: A specific analysis of the heterozygous status. *Journal of veterinary internal medicine*. 2009;23:91-99

9. Carrier L, Bonne G, Bahrend E, Yu B, Richard P, Niel F, Hainque B, Cruaud C, Gary F, Labeit S, Bouhour JB, Dubourg O, Desnos M, Hagege AA, Trent RJ, Komajda M, Fiszman M, Schwartz K. Organization and sequence of human cardiac myosin binding protein c gene (mybpc3) and identification of mutations predicted to produce truncated proteins in familial hypertrophic cardiomyopathy. *Circulation research*. 1997;80:427-434

10. Carrier L, Hengstenberg C, Beckmann JS, Guicheney P, Dufour C, Bercovici J, Dausse E, Berebbi-Bertrand I, Wisnewsky C, Pulvenis D, et al. Mapping of a novel gene for familial hypertrophic cardiomyopathy to chromosome 11. *Nature genetics*. 1993;4:311-313

11. Carrier L, Knoll R, Vignier N, Keller DI, Bausero P, Prudhon B, Isnard R, Ambroisine ML, Fiszman M, Ross J, Jr., Schwartz K, Chien KR. Asymmetric septal hypertrophy in heterozygous cmybp-c null mice. *Cardiovascular research*. 2004;63:293-304

12. Carrier L, Schlossarek S, Willis MS, Eschenhagen T. The ubiquitin-proteasome system and nonsense-mediated mrna decay in hypertrophic cardiomyopathy. *Cardiovascular research*. 2010;85:330-338

13. Cazorla O, Szilagyi S, Vignier N, Salazar G, Kramer E, Vassort G, Carrier L, Lacampagne A. Length and protein kinase a modulations of myocytes in cardiac myosin binding protein c-deficient mice. *Cardiovascular research*. 2006;69:370-380

14. Chen PP, Patel JR, Powers PA, Fitzsimons DP, Moss RL. Dissociation of structural and functional phenotypes in cardiac myosin-binding protein c conditional knockout mice. *Circulation*. 2012;126:1194-1205

15. Chen YH, Pai CW, Huang SW, Chang SN, Lin LY, Chiang FT, Lin JL, Hwang JJ, Tsai CT. Inactivation of myosin binding protein c homolog in zebrafish as a model for human cardiac hypertrophy and diastolic dysfunction. *Journal of the American Heart Association*. 2013;2:e000231

16. Coats CJ, Hollman A. Hypertrophic cardiomyopathy: Lessons from history. *Heart (British Cardiac Society)*. 2008;94:1258-1263

17.   Craig R, Offer G. The location of c-protein in rabbit skeletal muscle. *Proceedings of the Royal Society of London. Series B, Biological sciences*. 1976;192:451-461

18.   Day SM. The ubiquitin proteasome system in human cardiomyopathies and heart failure. *American journal of physiology. Heart and circulatory physiology*. 2013;304:H1283-1293

19.   Decker RS, Decker ML, Kulikovskaya I, Nakamura S, Lee DC, Harris K, Klocke FJ, Winegrad S. Myosin-binding protein c phosphorylation, myofibril structure, and contractile function during low-flow ischemia. *Circulation*. 2005;111:906-912

20.   Deutschbauer AM, Jaramillo DF, Proctor M, Kumm J, Hillenmeyer ME, Davis RW, Nislow C, Giaever G. Mechanisms of haploinsufficiency revealed by genome-wide profiling in yeast. *Genetics*. 2005;169:1915-1925

21.   El-Armouche A, Pohlmann L, Schlossarek S, Starbatty J, Yeh YH, Nattel S, Dobrev D, Eschenhagen T, Carrier L. Decreased phosphorylation levels of cardiac myosin-binding protein-c in human and experimental heart failure. *Journal of molecular and cellular cardiology*. 2007;43:223-229

22.   Emanuel R, Withers R, O'Brien K. Dominant and recessive modes of inheritance in idiopathic cardiomyopathy. *Lancet (London, England)*. 1971;2:1065-1067

23.   Flashman E, Watkins H, Redwood C. Localization of the binding site of the c-terminal domain of cardiac myosin-binding protein-c on the myosin rod. *The Biochemical journal*. 2007;401:97-102

24.   Flavigny J, Souchet M, Sebillon P, Berrebi-Bertrand I, Hainque B, Mallet A, Bril A, Schwartz K, Carrier L. Cooh-terminal truncated cardiac myosin-binding protein c mutants resulting from familial hypertrophic cardiomyopathy mutations exhibit altered expression and/or incorporation in fetal rat cardiomyocytes. *Journal of molecular biology*. 1999;294:443-456

25.   Fraysse B, Weinberger F, Bardswell SC, Cuello F, Vignier N, Geertz B, Starbatty J, Kramer E, Coirault C, Eschenhagen T, Kentish JC, Avkiran M, Carrier L. Increased myofilament ca2+ sensitivity and diastolic dysfunction as early consequences of mybpc3 mutation in heterozygous knock-in mice. *J Mol Cell Cardiol*. 2012;52:1299-1307

26.   Freiburg A, Gautel M. A molecular map of the interactions between titin and myosin-binding protein c. Implications for sarcomeric assembly in familial hypertrophic cardiomyopathy. *European journal of biochemistry*. 1996;235:317-323

27. Furst DO, Nave R, Osborn M, Weber K. Repetitive titin epitopes with a 42 nm spacing coincide in relative position with known a band striations also identified by major myosin-associated proteins. An immunoelectron-microscopical study on myofibrils. *Journal of cell science*. 1989;94 (Pt 1):119-125

28. Furst DO, Vinkemeier U, Weber K. Mammalian skeletal muscle c-protein: Purification from bovine muscle, binding to titin and the characterization of a full-length human cdna. *Journal of cell science*. 1992;102 (Pt 4):769-778

29. Gautel M, Furst DO, Cocco A, Schiaffino S. Isoform transitions of the myosin binding protein c family in developing human and mouse muscles: Lack of isoform transcomplementation in cardiac muscle. *Circulation research*. 1998;82:124-129

30. Gautel M, Zuffardi O, Freiburg A, Labeit S. Phosphorylation switches specific for the cardiac isoform of myosin binding protein-c: A modulator of cardiac contraction? *The EMBO journal*. 1995;14:1952-1960

31. Gedicke-Hornung C, Behrens-Gawlik V, Reischmann S, Geertz B, Stimpel D, Weinberger F, Schlossarek S, Precigout G, Braren I, Eschenhagen T, Mearini G, Lorain S, Voit T, Dreyfus PA, Garcia L, Carrier L. Rescue of cardiomyopathy through u7snrna-mediated exon skipping in mybpc3-targeted knock-in mice. *EMBO molecular medicine*. 2013;5:1128-1145

32. Geisterfer-Lowrance AA, Kass S, Tanigawa G, Vosberg HP, McKenna W, Seidman CE, Seidman JG. A molecular basis for familial hypertrophic cardiomyopathy: A beta cardiac myosin heavy chain gene missense mutation. *Cell*. 1990;62:999-1006

33. Gresham KS, Mamidi R, Li J, Kwak H, Stelzer JE. Sarcomeric protein modification during adrenergic stress enhances cross-bridge kinetics and cardiac output. *Journal of applied physiology (Bethesda, Md. : 1985)*. 2017;122:520-530

34. Gresham KS, Stelzer JE. The contributions of cardiac myosin binding protein c and troponin i phosphorylation to beta-adrenergic enhancement of in vivo cardiac function. *The Journal of physiology*. 2016;594:669-686

35. Gruen M, Gautel M. Mutations in beta-myosin s2 that cause familial hypertrophic cardiomyopathy (fhc) abolish the interaction with the regulatory domain of myosin-binding protein-c. *Journal of molecular biology*. 1999;286:933-949

36. Gruen M, Prinz H, Gautel M. Capk-phosphorylation controls the interaction of the regulatory domain of cardiac myosin binding protein c with myosin-s2 in an on-off fashion. *FEBS letters*. 1999;453:254-259

37. Gulick J, Hewett TE, Klevitsky R, Buck SH, Moss RL, Robbins J. Transgenic remodeling of the regulatory myosin light chains in the mammalian heart. *Circulation research*. 1997;80:655-664

38. Gupta MK, Gulick J, James J, Osinska H, Lorenz JN, Robbins J. Functional dissection of myosin binding protein c phosphorylation. *Journal of molecular and cellular cardiology*. 2013;64:39-50

39. Harris SP, Bartley CR, Hacker TA, McDonald KS, Douglas PS, Greaser ML, Powers PA, Moss RL. Hypertrophic cardiomyopathy in cardiac myosin binding protein-c knockout mice. *Circ Res*. 2002;90:594-601

40. Harris SP, Rostkova E, Gautel M, Moss RL. Binding of myosin binding protein-c to myosin subfragment s2 affects contractility independent of a tether mechanism. *Circulation research*. 2004;95:930-936

41. Hartzell HC, Glass DB. Phosphorylation of purified cardiac muscle c-protein by purified camp-dependent and endogenous ca2+-calmodulin-dependent protein kinases. *The Journal of biological chemistry*. 1984;259:15587-15596

42. Helms AS, Davis FM, Coleman D, Bartolone SN, Glazier AA, Pagani F, Yob JM, Sadayappan S, Pedersen E, Lyons R, Westfall MV, Jones R, Russell MW, Day SM. Sarcomere mutation-specific expression patterns in human hypertrophic cardiomyopathy. *Circulation. Cardiovascular genetics*. 2014;7:434-443

43. Herron TJ, Rostkova E, Kunst G, Chaturvedi R, Gautel M, Kentish JC. Activation of myocardial contraction by the n-terminal domains of myosin binding protein-c. *Circulation research*. 2006;98:1290-1298

44. Ho CY, Day SM, Ashley EA, Michels M, Pereira AC, Jacoby D, Cirino AL, Fox JC, Lakdawala NK, Ware JS, Caleshu CA, Helms AS, Colan SD, Girolami F, Cecchi F, Seidman CE, Sajeev G, Signorovitch J, Green EM, Olivotto I. Genotype and lifetime burden of disease in hypertrophic cardiomyopathy: Insights from the sarcomeric human cardiomyopathy registry (share). *Circulation*. 2018;138:1387-1398

45. Hodatsu A, Konno T, Hayashi K, Funada A, Fujita T, Nagata Y, Fujino N, Kawashiri MA, Yamagishi M. Compound heterozygosity deteriorates phenotypes of hypertrophic cardiomyopathy with founder mybpc3 mutation: Evidence from patients and zebrafish models. *American journal of physiology. Heart and circulatory physiology*. 2014;307:H1594-1604

46.   Hofmann PA, Hartzell HC, Moss RL. Alterations in ca2+ sensitive tension due to partial extraction of c-protein from rat skinned cardiac myocytes and rabbit skeletal muscle fibers. *The Journal of general physiology*. 1991;97:1141-1163

47.   Hollman A, Goodwin JF, Teare D, Renwick JW. A family with obstructive cardiomyopathy (asymmetrical hypertrophy). *British heart journal*. 1960;22:449-456

48.   Idowu SM, Gautel M, Perkins SJ, Pfuhl M. Structure, stability and dynamics of the central domain of cardiac myosin binding protein c (mybp-c): Implications for multidomain assembly and causes for cardiomyopathy. *Journal of molecular biology*. 2003;329:745-761

49.   Jacoby DL, DePasquale EC, McKenna WJ. Hypertrophic cardiomyopathy: Diagnosis, risk stratification and treatment. *CMAJ : Canadian Medical Association journal = journal de l'Association medicale canadienne*. 2013;185:127-134

50.   Jacques A, Hoskins AC, Kentish JC, Marston SB. From genotype to phenotype: A longitudinal study of a patient with hypertrophic cardiomyopathy due to a mutation in the mybpc3 gene. *Journal of muscle research and cell motility*. 2008;29:239-246

51.   Jacques AM, Copeland O, Messer AE, Gallon CE, King K, McKenna WJ, Tsang VT, Marston SB. Myosin binding protein c phosphorylation in normal, hypertrophic and failing human heart muscle. *Journal of molecular and cellular cardiology*. 2008;45:209-216

52.   Jarcho JA, McKenna W, Pare JA, Solomon SD, Holcombe RF, Dickie S, Levi T, Donis-Keller H, Seidman JG, Seidman CE. Mapping a gene for familial hypertrophic cardiomyopathy to chromosome 14q1. *The New England journal of medicine*. 1989;321:1372-1378

53.   Kampourakis T, Yan Z, Gautel M, Sun YB, Irving M. Myosin binding protein-c activates thin filaments and inhibits thick filaments in heart muscle cells. *Proceedings of the National Academy of Sciences of the United States of America*. 2014;111:18763-18768

54.   Kasahara H, Itoh M, Sugiyama T, Kido N, Hayashi H, Saito H, Tsukita S, Kato N. Autoimmune myocarditis induced in mice by cardiac c-protein. Cloning of complementary DNA encoding murine cardiac c-protein and partial characterization of the antigenic peptides. *The Journal of clinical investigation*. 1994;94:1026-1036

55.   Kensler RW, Craig R, Moss RL. Phosphorylation of cardiac myosin binding protein c releases myosin heads from the surface of cardiac thick filaments. *Proceedings*

of the National Academy of Sciences of the United States of America. 2017;114:E1355-E1364

56. Kensler RW, Shaffer JF, Harris SP. Binding of the n-terminal fragment c0-c2 of cardiac mybp-c to cardiac f-actin. *Journal of structural biology.* 2011;174:44-51

57. Kimura A. Molecular genetics and pathogenesis of cardiomyopathy. *Journal of human genetics.* 2016;61:41-50

58. Koizumi T. Turnover rates of structural proteins of rabbit skeletal muscle. *Journal of biochemistry.* 1974;76:431-439

59. Korte FS, McDonald KS, Harris SP, Moss RL. Loaded shortening, power output, and rate of force redevelopment are increased with knockout of cardiac myosin binding protein-c. *Circulation research.* 2003;93:752-758

60. Kulikovskaya I, McClellan G, Flavigny J, Carrier L, Winegrad S. Effect of mybp-c binding to actin on contractility in heart muscle. *The Journal of general physiology.* 2003;122:761-774

61. Kulikovskaya I, McClellan G, Levine R, Winegrad S. Effect of extraction of myosin binding protein c on contractility of rat heart. *American journal of physiology. Heart and circulatory physiology.* 2003;285:H857-865

62. Kumar M, Govindan S, Zhang M, Khairallah RJ, Martin JL, Sadayappan S, de Tombe PP. Cardiac myosin-binding protein c and troponin-i phosphorylation independently modulate myofilament length-dependent activation. *The Journal of biological chemistry.* 2015;290:29241-29249

63. Kunst G, Kress KR, Gruen M, Uttenweiler D, Gautel M, Fink RH. Myosin binding protein c, a phosphorylation-dependent force regulator in muscle that controls the attachment of myosin heads by its interaction with myosin s2. *Circulation research.* 2000;86:51-58

64. Kuster DW, Sadayappan S. Mybpc3's alternate ending: Consequences and therapeutic implications of a highly prevalent 25 bp deletion mutation. *Pflugers Archiv : European journal of physiology.* 2014;466:207-213

65. Kuster DW, Sequeira V, Najafi A, Boontje NM, Wijnker PJ, Witjas-Paalberends ER, Marston SB, Dos Remedios CG, Carrier L, Demmers JA, Redwood C, Sadayappan S, van der Velden J. Gsk3beta phosphorylates newly identified site in the proline-alanine-rich region of cardiac myosin-binding protein c and alters cross-bridge cycling kinetics in human: Short communication. *Circulation research.* 2013;112:633-639

66.   Landstrom AP, Ackerman MJ. Beyond the cardiac myofilament: Hypertrophic cardiomyopathy- associated mutations in genes that encode calcium-handling proteins. *Current molecular medicine*. 2012;12:507-518

67.   Lecarpentier Y, Vignier N, Oliviero P, Guellich A, Carrier L, Coirault C. Cardiac myosin-binding protein c modulates the tuning of the molecular motor in the heart. *Biophysical journal*. 2008;95:720-728

68.   Liang Y, Bradford WH, Zhang J, Sheikh F. Four and a half lim domain protein signaling and cardiomyopathy. *Biophysical reviews*. 2018

69.   Lopes LR, Rahman MS, Elliott PM. A systematic review and meta-analysis of genotype-phenotype associations in patients with hypertrophic cardiomyopathy caused by sarcomeric protein mutations. *Heart (British Cardiac Society)*. 2013;99:1800-1811

70.   Mamidi R, Gresham KS, Li J, Stelzer JE. Cardiac myosin binding protein-c ser(302) phosphorylation regulates cardiac beta-adrenergic reserve. *Science advances*. 2017;3:e1602445

71.   Mamidi R, Gresham KS, Stelzer JE. Length-dependent changes in contractile dynamics are blunted due to cardiac myosin binding protein-c ablation. *Frontiers in physiology*. 2014;5:461

72.   Maron BJ. Hypertrophic cardiomyopathy: A systematic review. *Jama*. 2002;287:1308-1320

73.   Maron BJ, Gardin JM, Flack JM, Gidding SS, Kurosaki TT, Bild DE. Prevalence of hypertrophic cardiomyopathy in a general population of young adults. Echocardiographic analysis of 4111 subjects in the cardia study. Coronary artery risk development in (young) adults. *Circulation*. 1995;92:785-789

74.   Marston S. Obscurin variants and inherited cardiomyopathies. *Biophysical reviews*. 2017;9:239-243

75.   Marston S, Copeland O, Jacques A, Livesey K, Tsang V, McKenna WJ, Jalilzadeh S, Carballo S, Redwood C, Watkins H. Evidence from human myectomy samples that mybpc3 mutations cause hypertrophic cardiomyopathy through haploinsufficiency. *Circulation research*. 2009;105:219-222

76.   Martin AF. Turnover of cardiac troponin subunits. Kinetic evidence for a precursor pool of troponin-i. *The Journal of biological chemistry*. 1981;256:964-968

77. McConnell BK, Fatkin D, Semsarian C, Jones KA, Georgakopoulos D, Maguire CT, Healey MJ, Mudd JO, Moskowitz IP, Conner DA, Giewat M, Wakimoto H, Berul CI, Schoen FJ, Kass DA, Seidman CE, Seidman JG. Comparison of two murine models of familial hypertrophic cardiomyopathy. *Circulation research*. 2001;88:383-389

78. McConnell BK, Jones KA, Fatkin D, Arroyo LH, Lee RT, Aristizabal O, Turnbull DH, Georgakopoulos D, Kass D, Bond M, Niimura H, Schoen FJ, Conner D, Fischman DA, Seidman CE, Seidman JG. Dilated cardiomyopathy in homozygous myosin-binding protein-c mutant mice. *The Journal of clinical investigation*. 1999;104:1235-1244

79. McGrath MJ, Cottle DL, Nguyen MA, Dyson JM, Coghill ID, Robinson PA, Holdsworth M, Cowling BS, Hardeman EC, Mitchell CA, Brown S. Four and a half lim protein 1 binds myosin-binding protein c and regulates myosin filament formation and sarcomere assembly. *The Journal of biological chemistry*. 2006;281:7666-7683

80. McNamara JW, Li A, Dos Remedios CG, Cooke R. The role of super-relaxed myosin in skeletal and cardiac muscle. *Biophysical reviews*. 2015;7:5-14

81. McNamara JW, Li A, Lal S, Bos JM, Harris SP, van der Velden J, Ackerman MJ, Cooke R, Dos Remedios CG. Mybpc3 mutations are associated with a reduced super-relaxed state in patients with hypertrophic cardiomyopathy. *PloS one*. 2017;12:e0180064

82. McNamara JW, Li A, Smith NJ, Lal S, Graham RM, Kooiker KB, van Dijk SJ, Remedios CGD, Harris SP, Cooke R. Ablation of cardiac myosin binding protein-c disrupts the super-relaxed state of myosin in murine cardiomyocytes. *Journal of molecular and cellular cardiology*. 2016;94:65-71

83. Mearini G, Stimpel D, Geertz B, Weinberger F, Kramer E, Schlossarek S, Mourot-Filiatre J, Stoehr A, Dutsch A, Wijnker PJ, Braren I, Katus HA, Muller OJ, Voit T, Eschenhagen T, Carrier L. Mybpc3 gene therapy for neonatal cardiomyopathy enables long-term disease prevention in mice. *Nature communications*. 2014;5:5515

84. Meurs KM, Sanchez X, David RM, Bowles NE, Towbin JA, Reiser PJ, Kittleson JA, Munro MJ, Dryburgh K, Macdonald KA, Kittleson MD. A cardiac myosin binding protein c mutation in the maine coon cat with familial hypertrophic cardiomyopathy. *Human molecular genetics*. 2005;14:3587-3593

85.   Michele DE, Albayya FP, Metzger JM. Thin filament protein dynamics in fully differentiated adult cardiac myocytes: Toward a model of sarcomere maintenance. *The Journal of cell biology*. 1999;145:1483-1495

86.   Miyamoto CA, Fischman DA, Reinach FC. The interface between mybp-c and myosin: Site-directed mutagenesis of the cx myosin-binding domain of mybp-c. *Journal of muscle research and cell motility*. 1999;20:703-715

87.   Mohamed AS, Dignam JD, Schlender KK. Cardiac myosin-binding protein c (mybp-c): Identification of protein kinase a and protein kinase c phosphorylation sites. *Archives of biochemistry and biophysics*. 1998;358:313-319

88.   Monteiro da Rocha A, Guerrero-Serna G, Helms A, Luzod C, Mironov S, Russell M, Jalife J, Day SM, Smith GD, Herron TJ. Deficient cmybp-c protein expression during cardiomyocyte differentiation underlies human hypertrophic cardiomyopathy cellular phenotypes in disease specific human es cell derived cardiomyocytes. *Journal of molecular and cellular cardiology*. 2016;99:197-206

89.   Moolman-Smook J, Flashman E, de Lange W, Li Z, Corfield V, Redwood C, Watkins H. Identification of novel interactions between domains of myosin binding protein-c that are modulated by hypertrophic cardiomyopathy missense mutations. *Circulation research*. 2002;91:704-711

90.   Moos C, Mason CM, Besterman JM, Feng IN, Dubin JH. The binding of skeletal muscle c-protein to f-actin, and its relation to the interaction of actin with myosin subfragment-1. *Journal of molecular biology*. 1978;124:571-586

91.   Moos C, Offer G, Starr R, Bennett P. Interaction of c-protein with myosin, myosin rod and light meromyosin. *Journal of molecular biology*. 1975;97:1-9

92.   Morita H, Rehm HL, Menesses A, McDonough B, Roberts AE, Kucherlapati R, Towbin JA, Seidman JG, Seidman CE. Shared genetic causes of cardiac hypertrophy in children and adults. *The New England journal of medicine*. 2008;358:1899-1908

93.   Moss RL, Fitzsimons DP, Ralphe JC. Cardiac mybp-c regulates the rate and force of contraction in mammalian myocardium. *Circulation research*. 2015;116:183-192

94.   Nagayama T, Takimoto E, Sadayappan S, Mudd JO, Seidman JG, Robbins J, Kass DA. Control of in vivo left ventricular [correction] contraction/relaxation kinetics by myosin binding protein c: Protein kinase a phosphorylation dependent and independent regulation. *Circulation*. 2007;116:2399-2408

95. Offer G, Moos C, Starr R. A new protein of the thick filaments of vertebrate skeletal myofibrils. Extractions, purification and characterization. *Journal of molecular biology.* 1973;74:653-676

96. Okagaki T, Weber FE, Fischman DA, Vaughan KT, Mikawa T, Reinach FC. The major myosin-binding domain of skeletal muscle mybp-c (c protein) resides in the cooh-terminal, immunoglobulin c2 motif. *The Journal of cell biology.* 1993;123:619-626

97. Page SP, Kounas S, Syrris P, Christiansen M, Frank-Hansen R, Andersen PS, Elliott PM, McKenna WJ. Cardiac myosin binding protein-c mutations in families with hypertrophic cardiomyopathy: Disease expression in relation to age, gender, and long term outcome. *Circulation. Cardiovascular genetics.* 2012;5:156-166

98. Pare JA, Fraser RG, Pirozynski WJ, Shanks JA, Stubington D. Hereditary cardiovascular dysplasia. A form of familial cardiomyopathy. *The American journal of medicine.* 1961;31:37-62

99. Pepe FA, Drucker B. The myosin filament. Iii. C-protein. *Journal of molecular biology.* 1975;99:609-617

100. Pfuhl M, Gautel M. Structure, interactions and function of the n-terminus of cardiac myosin binding protein c (mybp-c): Who does what, with what, and to whom? *Journal of muscle research and cell motility.* 2012;33:83-94

101. Pohlmann L, Kroger I, Vignier N, Schlossarek S, Kramer E, Coirault C, Sultan KR, El-Armouche A, Winegrad S, Eschenhagen T, Carrier L. Cardiac myosin-binding protein c is required for complete relaxation in intact myocytes. *Circulation research.* 2007;101:928-938

102. Predmore JM, Wang P, Davis F, Bartolone S, Westfall MV, Dyke DB, Pagani F, Powell SR, Day SM. Ubiquitin proteasome dysfunction in human hypertrophic and dilated cardiomyopathies. *Circulation.* 2010;121:997-1004

103. Previs MJ, Beck Previs S, Gulick J, Robbins J, Warshaw DM. Molecular mechanics of cardiac myosin-binding protein c in native thick filaments. *Science (New York, N.Y.).* 2012;337:1215-1218

104. Previs MJ, Prosser BL, Mun JY, Previs SB, Gulick J, Lee K, Robbins J, Craig R, Lederer WJ, Warshaw DM. Myosin-binding protein c corrects an intrinsic inhomogeneity in cardiac excitation-contraction coupling. *Science advances.* 2015;1

105. Prondzynski M, Kramer E, Laufer SD, Shibamiya A, Pless O, Flenner F, Muller OJ, Munch J, Redwood C, Hansen A, Patten M, Eschenhagen T, Mearini G, Carrier L. Evaluation of mybpc3 trans-splicing and gene replacement as therapeutic options in human ipsc-derived cardiomyocytes. *Molecular therapy. Nucleic acids*. 2017;7:475-486

106. Razumova MV, Bezold KL, Tu AY, Regnier M, Harris SP. Contribution of the myosin binding protein c motif to functional effects in permeabilized rat trabeculae. *The Journal of general physiology*. 2008;132:575-585

107. Razumova MV, Shaffer JF, Tu AY, Flint GV, Regnier M, Harris SP. Effects of the n-terminal domains of myosin binding protein-c in an in vitro motility assay: Evidence for long-lived cross-bridges. *The Journal of biological chemistry*. 2006;281:35846-35854

108. Razzaque MA, Gupta M, Osinska H, Gulick J, Blaxall BC, Robbins J. An endogenously produced fragment of cardiac myosin-binding protein c is pathogenic and can lead to heart failure. *Circulation research*. 2013;113:553-561

109. Ribeiro AJS, Schwab O, Mandegar MA, Ang YS, Conklin BR, Srivastava D, Pruitt BL. Multi-imaging method to assay the contractile mechanical output of micropatterned human ipsc-derived cardiac myocytes. *Circulation research*. 2017;120:1572-1583

110. Rosas PC, Liu Y, Abdalla M, Thomas C, Kidwell D, Kumar R, Baker K, Patel B, Warrens C, Solaro R, Powers P, Moss R, Tong C. Phosphorylated cardiac myosin binding protein-c enhances lusitropy. *Journal of the American College of Cardiology*. 2014;63:A871

111. Rottbauer W, Gautel M, Zehelein J, Labeit S, Franz WM, Fischer C, Vollrath B, Mall G, Dietz R, Kubler W, Katus HA. Novel splice donor site mutation in the cardiac myosin-binding protein-c gene in familial hypertrophic cardiomyopathy. Characterization of cardiac transcript and protein. *The Journal of clinical investigation*. 1997;100:475-482

112. Rust EM, Albayya FP, Metzger JM. Identification of a contractile deficit in adult cardiac myocytes expressing hypertrophic cardiomyopathy-associated mutant troponin t proteins. *The Journal of clinical investigation*. 1999;103:1459-1467

113. Saber W, Begin KJ, Warshaw DM, VanBuren P. Cardiac myosin binding protein-c modulates actomyosin binding and kinetics in the in vitro motility assay. *Journal of molecular and cellular cardiology*. 2008;44:1053-1061

114. Sadayappan S, Finley N, Howarth JW, Osinska H, Klevitsky R, Lorenz JN, Rosevear PR, Robbins J. Role of the acidic n' region of cardiac troponin i in regulating myocardial function. *FASEB journal : official publication of the Federation of American Societies for Experimental Biology*. 2008;22:1246-1257

115. Sadayappan S, Gulick J, Osinska H, Barefield D, Cuello F, Avkiran M, Lasko VM, Lorenz JN, Maillet M, Martin JL, Brown JH, Bers DM, Molkentin JD, James J, Robbins J. A critical function for ser-282 in cardiac myosin binding protein-c phosphorylation and cardiac function. *Circulation research*. 2011;109:141-150

116. Sadayappan S, Gulick J, Osinska H, Martin LA, Hahn HS, Dorn GW, 2nd, Klevitsky R, Seidman CE, Seidman JG, Robbins J. Cardiac myosin-binding protein-c phosphorylation and cardiac function. *Circulation research*. 2005;97:1156-1163

117. Sadayappan S, Osinska H, Klevitsky R, Lorenz JN, Sargent M, Molkentin JD, Seidman CE, Seidman JG, Robbins J. Cardiac myosin binding protein c phosphorylation is cardioprotective. *Proceedings of the National Academy of Sciences of the United States of America*. 2006;103:16918-16923

118. Saez LJ, Gianola KM, McNally EM, Feghali R, Eddy R, Shows TB, Leinwand LA. Human cardiac myosin heavy chain genes and their linkage in the genome. *Nucleic acids research*. 1987;15:5443-5459

119. Saltzman AJ, Mancini-DiNardo D, Li C, Chung WK, Ho CY, Hurst S, Wynn J, Care M, Hamilton RM, Seidman GW, Gorham J, McDonough B, Sparks E, Seidman JG, Seidman CE, Rehm HL. Short communication: The cardiac myosin binding protein c arg502trp mutation: A common cause of hypertrophic cardiomyopathy. *Circulation research*. 2010;106:1549-1552

120. Sanbe A, Osinska H, Saffitz JE, Glabe CG, Kayed R, Maloyan A, Robbins J. Desmin-related cardiomyopathy in transgenic mice: A cardiac amyloidosis. *Proceedings of the National Academy of Sciences of the United States of America*. 2004;101:10132-10136

121. Sarikas A, Carrier L, Schenke C, Doll D, Flavigny J, Lindenberg KS, Eschenhagen T, Zolk O. Impairment of the ubiquitin-proteasome system by truncated cardiac myosin binding protein c mutants. *Cardiovascular research*. 2005;66:33-44

122. Schlossarek S, Englmann DR, Sultan KR, Sauer M, Eschenhagen T, Carrier L. Defective proteolytic systems in mybpc3-targeted mice with cardiac hypertrophy. *Basic research in cardiology*. 2012;107:235

123. Schlossarek S, Schuermann F, Geertz B, Mearini G, Eschenhagen T, Carrier L. Adrenergic stress reveals septal hypertrophy and proteasome impairment in

heterozygous mybpc3-targeted knock-in mice. *Journal of muscle research and cell motility*. 2012;33:5-15

124. Seeger T, Shrestha R, Lam CK, Chen C, McKeithan WL, Lau E, Wnorowski A, McMullen G, Greenhaw M, Lee J, Oikonomopoulos A, Lee S, Yang H, Mercola M, Wheeler M, Ashley EA, Yang F, Karakikes I, Wu JC. A premature termination codon mutation in mybpc3 causes hypertrophic cardiomyopathy via chronic activation of nonsense-mediated decay. *Circulation*.0

125. Sequeira V, Wijnker PJ, Nijenkamp LL, Kuster DW, Najafi A, Witjas-Paalberends ER, Regan JA, Boontje N, Ten Cate FJ, Germans T, Carrier L, Sadayappan S, van Slegtenhorst MA, Zaremba R, Foster DB, Murphy AM, Poggesi C, Dos Remedios C, Stienen GJ, Ho CY, Michels M, van der Velden J. Perturbed length-dependent activation in human hypertrophic cardiomyopathy with missense sarcomeric gene mutations. *Circulation research*. 2013;112:1491-1505

126. Shaffer JF, Kensler RW, Harris SP. The myosin-binding protein c motif binds to f-actin in a phosphorylation-sensitive manner. *The Journal of biological chemistry*. 2009;284:12318-12327

127. Shaffer JF, Razumova MV, Tu AY, Regnier M, Harris SP. Myosin s2 is not required for effects of myosin binding protein-c on motility. *FEBS letters*. 2007;581:1501-1504

128. Shah PM, Gramiak R, Kramer DH. Ultrasound localization of left ventricular outflow obstruction in hypertrophic obstructive cardiomyopathy. *Circulation*. 1969;40:3-11

129. Solomon SD, Geisterfer-Lowrance AA, Vosberg HP, Hiller G, Jarcho JA, Morton CC, McBride WO, Mitchell AL, Bale AE, McKenna WJ, et al. A locus for familial hypertrophic cardiomyopathy is closely linked to the cardiac myosin heavy chain genes, cri-l436, and cri-l329 on chromosome 14 at q11-q12. *American journal of human genetics*. 1990;47:389-394

130. Soteriou A, Gamage M, Trinick J. A survey of interactions made by the giant protein titin. *Journal of cell science*. 1993;104 (Pt 1):119-123

131. Squire JM, Luther PK, Knupp C. Structural evidence for the interaction of c-protein (mybp-c) with actin and sequence identification of a possible actin-binding domain. *Journal of molecular biology*. 2003;331:713-724

132. Starr R, Offer G. Polypeptide chains of intermediate molecular weight in myosin preparations. *FEBS letters*. 1971;15:40-44

133. Starr R, Offer G. The interaction of c-protein with heavy meromyosin and subfragment-2. *The Biochemical journal.* 1978;171:813-816

134. Stelzer JE, Fitzsimons DP, Moss RL. Ablation of myosin-binding protein-c accelerates force development in mouse myocardium. *Biophysical journal.* 2006;90:4119-4127

135. Tanaka A, Yuasa S, Mearini G, Egashira T, Seki T, Kodaira M, Kusumoto D, Kuroda Y, Okata S, Suzuki T, Inohara T, Arimura T, Makino S, Kimura K, Kimura A, Furukawa T, Carrier L, Node K, Fukuda K. Endothelin-1 induces myofibrillar disarray and contractile vector variability in hypertrophic cardiomyopathy-induced pluripotent stem cell-derived cardiomyocytes. *Journal of the American Heart Association.* 2014;3:e001263

136. Taylor EN, Hoffman MP, Barefield DY, Aninwene GE, 2nd, Abrishamchi AD, Lynch TLt, Govindan S, Osinska H, Robbins J, Sadayappan S, Gilbert RJ. Alterations in multi-scale cardiac architecture in association with phosphorylation of myosin binding protein-c. *Journal of the American Heart Association.* 2016;5:e002836

137. Teare D. Asymmetrical hypertrophy of the heart in young adults. *British heart journal.* 1958;20:1-8

138. Theis JL, Bos JM, Bartleson VB, Will ML, Binder J, Vatta M, Towbin JA, Gersh BJ, Ommen SR, Ackerman MJ. Echocardiographic-determined septal morphology in z-disc hypertrophic cardiomyopathy. *Biochemical and biophysical research communications.* 2006;351:896-902

139. Theis JL, Bos JM, Theis JD, Miller DV, Dearani JA, Schaff HV, Gersh BJ, Ommen SR, Moss RL, Ackerman MJ. Expression patterns of cardiac myofilament proteins: Genomic and protein analysis of surgical myectomy tissue from patients with obstructive hypertrophic cardiomyopathy. *Circulation. Heart failure.* 2009;2:325-333

140. Thierfelder L, Watkins H, MacRae C, Lamas R, McKenna W, Vosberg HP, Seidman JG, Seidman CE. Alpha-tropomyosin and cardiac troponin t mutations cause familial hypertrophic cardiomyopathy: A disease of the sarcomere. *Cell.* 1994;77:701-712

141. Thompson BR, Metzger JM. Cell biology of sarcomeric protein engineering: Disease modeling and therapeutic potential. *Anatomical record (Hoboken, N.J. : 2007).* 2014;297:1663-1669

142. Thottakara T, Friedrich FW, Reischmann S, Braumann S, Schlossarek S, Kramer E, Juhr D, Schluter H, van der Velden J, Munch J, Patten M, Eschenhagen T,

Moog-Lutz C, Carrier L. The e3 ubiquitin ligase asb2beta is downregulated in a mouse model of hypertrophic cardiomyopathy and targets desmin for proteasomal degradation. *Journal of molecular and cellular cardiology*. 2015;87:214-224

143.   Tong CW, Gaffin RD, Zawieja DC, Muthuchamy M. Roles of phosphorylation of myosin binding protein-c and troponin i in mouse cardiac muscle twitch dynamics. *The Journal of physiology*. 2004;558:927-941

144.   Tong CW, Stelzer JE, Greaser ML, Powers PA, Moss RL. Acceleration of crossbridge kinetics by protein kinase a phosphorylation of cardiac myosin binding protein c modulates cardiac function. *Circulation research*. 2008;103:974-982

145.   Tonino P, Kiss B, Strom J, Methawasin M, Smith JE, 3rd, Kolb J, Labeit S, Granzier H. The giant protein titin regulates the length of the striated muscle thick filament. *Nature communications*. 2017;8:1041

146.   van Dijk SJ, Bezold Kooiker K, Mazzalupo S, Yang Y, Kostyukova AS, Mustacich DJ, Hoye ER, Stern JA, Kittleson MD, Harris SP. The a31p missense mutation in cardiac myosin binding protein c alters protein structure but does not cause haploinsufficiency. *Archives of biochemistry and biophysics*. 2016;601:133-140

147.   van Dijk SJ, Boontje NM, Heymans MW, Ten Cate FJ, Michels M, Dos Remedios C, Dooijes D, van Slegtenhorst MA, van der Velden J, Stienen GJ. Preserved cross-bridge kinetics in human hypertrophic cardiomyopathy patients with mybpc3 mutations. *Pflugers Archiv : European journal of physiology*. 2014;466:1619-1633

148.   van Dijk SJ, Dooijes D, dos Remedios C, Michels M, Lamers JM, Winegrad S, Schlossarek S, Carrier L, ten Cate FJ, Stienen GJ, van der Velden J. Cardiac myosin-binding protein c mutations and hypertrophic cardiomyopathy: Haploinsufficiency, deranged phosphorylation, and cardiomyocyte dysfunction. *Circulation*. 2009;119:1473-1483

149.   van Dijk SJ, Paalberends ER, Najafi A, Michels M, Sadayappan S, Carrier L, Boontje NM, Kuster DW, van Slegtenhorst M, Dooijes D, dos Remedios C, ten Cate FJ, Stienen GJ, van der Velden J. Contractile dysfunction irrespective of the mutant protein in human hypertrophic cardiomyopathy with normal systolic function. *Circulation. Heart failure*. 2012;5:36-46

150.   Venema RC, Kuo JF. Protein kinase c-mediated phosphorylation of troponin i and c-protein in isolated myocardial cells is associated with inhibition of myofibrillar actomyosin mgatpase. *The Journal of biological chemistry*. 1993;268:2705-2711

151.   Vignier N, Schlossarek S, Fraysse B, Mearini G, Kramer E, Pointu H, Mougenot N, Guiard J, Reimer R, Hohenberg H, Schwartz K, Vernet M, Eschenhagen T,

Carrier L. Nonsense-mediated mrna decay and ubiquitin-proteasome system regulate cardiac myosin-binding protein c mutant levels in cardiomyopathic mice. *Circulation research*. 2009;105:239-248

152. Vikhorev PG, Vikhoreva NN. Cardiomyopathies and related changes in contractility of human heart muscle. *International journal of molecular sciences*. 2018;19

153. Walker LA, Walker JS, Glazier A, Brown DR, Stenmark KR, Buttrick PM. Biochemical and myofilament responses of the right ventricle to severe pulmonary hypertension. *American journal of physiology. Heart and circulatory physiology*. 2011;301:H832-840

154. Watkins H, Conner D, Thierfelder L, Jarcho JA, MacRae C, McKenna WJ, Maron BJ, Seidman JG, Seidman CE. Mutations in the cardiac myosin binding protein-c gene on chromosome 11 cause familial hypertrophic cardiomyopathy. *Nature genetics*. 1995;11:434-437

155. Weber FE, Vaughan KT, Reinach FC, Fischman DA. Complete sequence of human fast-type and slow-type muscle myosin-binding-protein c (mybp-c). Differential expression, conserved domain structure and chromosome assignment. *European journal of biochemistry*. 1993;216:661-669

156. Weisberg A, Winegrad S. Alteration of myosin cross bridges by phosphorylation of myosin-binding protein c in cardiac muscle. *Proceedings of the National Academy of Sciences of the United States of America*. 1996;93:8999-9003

157. Wessels MW, Herkert JC, Frohn-Mulder IM, Dalinghaus M, van den Wijngaard A, de Krijger RR, Michels M, de Coo IF, Hoedemaekers YM, Dooijes D. Compound heterozygous or homozygous truncating mybpc3 mutations cause lethal cardiomyopathy with features of noncompaction and septal defects. *European journal of human genetics : EJHG*. 2015;23:922-928

158. Whitten AE, Jeffries CM, Harris SP, Trewhella J. Cardiac myosin-binding protein c decorates f-actin: Implications for cardiac function. *Proceedings of the National Academy of Sciences of the United States of America*. 2008;105:18360-18365

159. Winegrad S. Cardiac myosin binding protein c. *Circulation research*. 1999;84:1117-1126

160. Witt CC, Gerull B, Davies MJ, Centner T, Linke WA, Thierfelder L. Hypercontractile properties of cardiac muscle fibers in a knock-in mouse model of cardiac myosin-binding protein-c. *The Journal of biological chemistry*. 2001;276:5353-5359

161. Xin B, Puffenberger E, Tumbush J, Bockoven JR, Wang H. Homozygosity for a novel splice site mutation in the cardiac myosin-binding protein c gene causes severe neonatal hypertrophic cardiomyopathy. *American journal of medical genetics. Part A*. 2007;143A:2662-2667

162. Yang Q, Sanbe A, Osinska H, Hewett TE, Klevitsky R, Robbins J. A mouse model of myosin binding protein c human familial hypertrophic cardiomyopathy. *The Journal of clinical investigation*. 1998;102:1292-1300

163. Yu B, French JA, Carrier L, Jeremy RW, McTaggart DR, Nicholson MR, Hambly B, Semsarian C, Richmond DR, Schwartz K, Trent RJ. Molecular pathology of familial hypertrophic cardiomyopathy caused by mutations in the cardiac myosin binding protein c gene. *Journal of medical genetics*. 1998;35:205-210

164. Yutani C, Imakita M, Ishibashi-Ueda H, Nagata S, Sakakibara H, Nimura Y. Histopathological study of hypertrophic cardiomyopathy with progression to left ventricular dilatation. *Acta pathologica japonica*. 1987;37:1041-1052

165. Zahka K, Kalidas K, Simpson MA, Cross H, Keller BB, Galambos C, Gurtz K, Patton MA, Crosby AH. Homozygous mutation of mybpc3 associated with severe infantile hypertrophic cardiomyopathy at high frequency among the amish. *Heart (British Cardiac Society)*. 2008;94:1326-1330

166. Zou Y, Song L, Wang Z, Ma A, Liu T, Gu H, Lu S, Wu P, Zhang dagger Y, Shen dagger L, Cai Y, Zhen double dagger Y, Liu Y, Hui R. Prevalence of idiopathic hypertrophic cardiomyopathy in china: A population-based echocardiographic analysis of 8080 adults. *The American journal of medicine*. 2004;116:14-18

CHAPTER 2

Heat Shock 70 kDa-family Molecular Chaperones Regulate
Degradation of Cardiac Myosin Binding Protein C

2.1 ABSTRACT

Cardiac myosin binding protein C (*MYBPC3*) is the most commonly mutated gene associated with hypertrophic cardiomyopathy (HCM). Haploinsufficiency of full-length MYBPC3 and disruption of proteostasis have both been proposed as central to HCM disease pathogenesis. Discriminating the relative contributions of these two mechanisms requires fundamental knowledge of how turnover of wild-type and mutant MYBPC3 proteins are regulated. While MYBPC3 is known to be degraded via the ubiquitin proteasome system, little is known of upstream protein quality control mechanisms involved in its routine turnover and maintenance of proper stoichiometry within the sarcomere. We expressed several disease-causing mutations in MYBPC3 in primary neonatal rat ventricular cardiomyocytes. In contrast to wild-type MYBPC3, mutant proteins showed reduced expression and failed to localize to the sarcomere. In an unbiased co-immunoprecipitation/mass spectrometry screen, we identified HSP70-family chaperones as novel interactors of both wild-type and mutant MYBPC3. Heat shock cognate 70kDa (HSC70) was the most abundant chaperone interactor. Knockdown of

HSC70 significantly slowed degradation of both WT and mutant MYBPC3, while pharmacologic activation of HSC70 and HSP70 accelerated degradation. HSC70 was expressed in discrete striations in the sarcomere. Together these data suggest that wild-type and mutant MYBPC3 proteins are clients for HSC70, and that the HSC70 chaperone system plays a major role in regulating MYBPC3 protein turnover.

2.2 INTRODUCTION

Hypertrophic cardiomyopathy (HCM), the most common inherited heart disease, is primarily caused by mutations in cardiac-specific sarcomere proteins, which make up the basic contractile unit of muscle. HCM typically presents with hypertrophy of the left ventricle and intraventricular septum, interstitial fibrosis, and diastolic dysfunction. Mutations linked to HCM occur in most major proteins of the contractile apparatus, including β-myosin heavy chain, regulatory and essential myosin light chain, α-cardiac actin, α-tropomyosin, cardiac isoforms of troponin T and I, and cardiac myosin binding protein C (*MYBPC3*)[Bonne, 1995, Geisterfer-Lowrance, 1990, Kimura, 1997, Olson, 2000, Poetter, 1996, Thierfelder, 1994, Watkins, 1995]. Uniquely among other sarcomere genes harboring HCM-linked mutations, most *MYBPC3* mutations are nonsense, frame-shifts or splice site-affecting, predicted to result in truncated proteins[Tardiff, 2005]. These truncating MYBPC3 mutations represent the most frequent cause of HCM[Alfares, 2015]. MYBPC3 is thick-filament associated protein with both structural and regulatory roles in the sarcomere. It is capable of modulating contraction by slowing the rate of cross-bridge cycling within the C-zone of the sarcomere, where it is exclusively localized[Craig, 1976, Previs, 2012].

An ongoing debate as to the primary pathogenic mechanism in MYBPC3-linked HCM has yielded evidence for both a loss-of-function mechanism: haploinsufficiency of

functional MYBPC3 in the sarcomere[Marston, 2009, McNamara, 2017, van Dijk, 2009, van Dijk, 2012]; and a gain-of-function mechanism: proteotoxicity of truncated MYBPC3 leading to loss of myocyte protein homeostasis (proteostasis)[Sarikas, 2005, Schlossarek, 2012, Schlossarek, 2012]. Proteostasis involves a complex array of cellular protein quality control systems which maintain balance between protein synthesis, folding, repair and degradation. Maintenance of proteostasis in the heart is critical to proper cardiac function, and quality control of MYBPC3 specifically is an important factor to consider in both putative pathogenic mechanisms. Cardiac hypertrophy, fundamentally caused by increased myocyte size as opposed to proliferation, is inherently an imbalance between protein synthesis and degradation [Willis, 2013]. The post-mitotic cardiomyocyte is particularly dependent on precise regulation of contractile protein stoichiometry, folding and repair, but mechanisms governing turnover of sarcomere proteins, including MYBPC3, are still largely unknown. Recent studies have underscored the importance of protein quality control pathways in various etiologies of cardiovascular disease [Li, 2011, Rodriguez, 2009, Sandri, 2014, Schlossarek, 2014, Yu, 2010]. Defects in proteostasis relating to mutations in genes encoding molecular chaperones, a class of proteins which assists in folding nascent or misfolded clients and preventing toxic aggregation of proteins, can cause pathological cardiac remodeling in human disease. Two notable examples are mutations in the small heat shock protein αB-crystallin and the co-chaperone BAG3 which cause dilated and myofibrillar cardiomyopathy, respectively [Inagaki, 2006, Li, 1999, Norton, 2011]. Therefore, we hypothesized that chaperone-client interactions may also play a role in the pathogenesis of hypertrophic cardiomyopathy.

Multiple chaperones involved in assembly and maintenance of myosin and actin monomers and filaments in striated muscle have been identified, whereas chaperones known to be associated with critical regulatory myofilament proteins are far fewer in number[Carlisle, 2017]. Identifying protein quality control factors specific to individual myofilament proteins would lead to a better understanding of their roles in general sarcomere maintenance as well as disease mechanisms. We therefore sought to identify potential MYBPC3 interactors related to chaperones and protein quality control. Through an unbiased co-immunoprecipitation mass spectrometry study, we identified HSP70-family chaperones as novel MYBPC3 interactors. The heat shock protein 70 kDa (HSP70) family, including but not limited to HSP70 and HSC70, is a group of highly ubiquitous chaperones with an ATP-dependent catalytic cycle which recognize exposed hydrophobic residues on client proteins [Zuiderweg, 2013]. In addition to promoting protein folding, the HSP70s participate in guiding proteins toward ubiquitin proteasome system (UPS)-mediated degradation through interactions with the E3 ligase carboxyl-terminus of HSP70 interacting protein (CHIP) [McDonough, 2003]. MYBPC3 is known to be degraded via the proteasome, and truncated MYBPC3 has been reported to cause UPS dysfunction[Sarikas, 2005]. This suggests that HSP70 chaperones may regulate proteasomal degradation of MYBPC3. Altered interactions with factors upstream of the proteasome, such as HSP70s, could contribute to dysfunction. Experimentally, *Hspa1a/b*-null mice and mice null for the HSP70 co-chaperone *Hspa4* developed left ventricular hypertrophy and fibrosis, suggesting loss of HSP70 chaperone function can lead to a phenotype similar to HCM [Kim, 2006, Mohamed, 2012].

While critical roles for HSC70 and its co-chaperones in myosin folding and Z-disk maintenance have been previously demonstrated, the role of molecular chaperones, including the ubiquitous and promiscuous HSP70 family, in handling sarcomeric regulatory proteins such as MYBPC3 is underexplored [Arndt, 2010, Hishiya, 2010, Srikakulam, 2004]. Given that MYBPC3 protein turnover and degradation are fundamental facets of both prevailing hypotheses regarding the primary pathogenic mechanism in MYBPC3-linked HCM, elucidating the chaperones and other protein quality control factors which handle MYBPC3 would greatly inform future research into targeted approaches for treating HCM. We hypothesized that MYBPC3 is a client of HSP70-family chaperones and these chaperones play a role in regulating MYBPC3 turnover. To test this, we expressed a panel of human MYBPC3 mutations in neonatal rat ventricular cardiomyocytes (NRVMs), and explored their physical and functional interactions with HSP70s. We present our findings that both WT and mutant MYBPC3 physically interact with the HSP70 family of molecular chaperones, and that modulation of HSC70 expression or activity specifically impacts MYBPC3 degradation. Moreover, we show that HSC70 localizes to the sarcomere adjacent to MYBPC3. These results represent the first identification of a chaperone for MYBPC3, and uncover a new role for HSC70 in sarcomere proteostasis in fully-differentiated myofibrils.

2.3 MATERIALS AND METHODS

2.3.1 Isolation and culture of neonatal rat ventricular cardiomyocytes.

NRVMs were isolated from excised ventricles of 1-3 day old Sprague-Dawley rats (Charles River) according to a modified version of the Worthington Neonatal

Cardiomyocyte Isolation System (Worthington Biochemical Corporation). Ventricles were minced in ice-cold HBSS and pre-digested in 1mg/mL trypsin (Worthington) at 4°C for 6 hours. Tissue was then digested in 30U/mL purified collagenase (Worthington), dissolved in Media 199 (Invitrogen) with Earle's salts, L-glutamine, 2.2g/L sodium bicarbonate, 2% penicillin/streptomycin, 25mM HEPES, and 15% heat inactivated qualified FBS (Invitrogen), in a Celstir® 50mL jacketed spinner flask (Wheaton) for 45 minutes at 37°C. Digested tissue was triturated and filtered through a 70μm strainer, then incubated for 20 minutes at room temperature to further digest partially degraded collagen. Cell suspension was pre-plated on untreated plastic dishes for 1 hour at 37°C to reduce adherent fibroblast contamination, then filtered through a 40μm strainer. NRVMs were seeded on plates coated with 5μg/mL bovine fibronectin (Sigma-Aldrich) or on fibronectin-micropatterned PDMS coverslips (see below) in maintenance media (Media 199 with Earle's salts, L-glutamine, 2.2g/L sodium bicarbonate, 2% penicillin/streptomycin, 25mM HEPES, and 5% FBS). Media was changed 24 hours after plating and every subsequent 48 hours unless otherwise noted. NRVMs undergoing heat shock treatment were incubated at 45°C for one hour immediately prior to collection or fixation.

2.3.2 Micropatterning of PDMS coverslips.

Micropatterned polydimethylsiloxane (PDMS) stamps with 20μm-wide rows spaced 3μm apart were fabricated as previously described with minor modifications (Figure 2.1) [Kuo, 2012]. To print fibronectin micropatterns onto 20mm-diameter coverslips cut from PDMS sheeting (Specialty Manufacturing, Inc), sterilized stamp surfaces were covered in a 1:40 dilution in PBS of fibronectin from human plasma, 0.1% solution (Sigma-Aldrich) and incubated at room temperature for 1 hour. Fibronectin solution was aspirated

and stamps were dried with compressed nitrogen gas. PDMS coverslips were cleaned by sonication in 70% ethanol, placed in 6-well cell culture plates and treated in a UV-ozone cleaner (Jelight Company) for 8 minutes prior to stamping. Stamps were inverted onto the PDMS circles and then removed. Stamped surfaces were then treated with 1% Pluronic F-127® (Sigma-Aldrich) for five minutes to render unstamped areas hydrophobic. Coverslips were washed 3 times in PBS and stored at 4°C until plating.

2.3.3 Expression of FLAG-tagged WT and truncated MYBPC3 constructs via recombinant adenovirus.

MYBPC3 mutants were generated by site-directed mutagenesis using the QuikChange II XL Kit (Agilent) from WT human MYBPC3 cDNA. Adenovirus was generated with the ViraPower™ Adenoviral Gateway® Expression Kit (Invitrogen) using the pAd/CMV/V5-DEST Gateway® vector, and amplified in HEK293A cells. MOI for NRVM transduction was optimized to levels at which no ectopic expression of WT MYBPC3 was detected by immunofluorescence (MOI 2-10).

2.3.4 Co-immunoprecipitation of MYBPC3-interacting proteins.

Un-patterned NRVMS were plated at a density of 1×10^7 cells per 100mm culture dish. Cells were transduced with WT or truncated MYBPC3 adenovirus at MOI 10 24 hours after plating. Cells were collected 48 hours later by scraping in ice cold PBS with Roche protease inhibitor cocktail; cell pellets were stored at -80°C. 2×10^7 cells were used per sample. Nontransduced cells were used as a negative control for the FLAG co-IP. Pellets were lysed in RIPA buffer (1% Triton X-100, 1% sodium deoxycholate, 0.1% SDS, 150mM NaCl, 10mM Na_2PO_4 pH 7.2, 1mM NaF, 1mM EDTA, 2.5mM EGTA, 20mM $(NH_4)_2MoO_4$, 100µM Na_3VO_4, Roche protease inhibitor cocktail) and incubated on ice for

15 minutes. Lysates were then sonicated for four 10 second bursts at 50% amplitude using a Branson digital sonifier with cup horn attachment, incubated on ice for a further 15 minutes, and centrifuged for 10 minutes at 13,000 rpm at 4°C to remove debris. Supernatants were recovered and protein concentration was determined by Bradford protein assay. This fraction was used as 'input' for Western blot analysis of co-IPs. 2mg of protein from supernatants was allocated to one FLAG co-IP tube and one normal mouse IgG control tube. All samples underwent initial pre-clearing of nonspecific interactors by adding 10µg of normal mouse IgG for one hour at 4°C followed by adding 20µL of a 1:1 mixture of protein A and protein G sepharose bead slurry (Sigma-Aldrich) for one hour at 4°C with gentle shaking. Pre-cleared supernatant was retained for IP. FLAG co-IP tubes received 20µL anti-FLAG M2-conjugated sepharose beads (Sigma-Aldrich) while normal mouse IgG control tubes received 10µg normal mouse IgG and 20µL 1:1 mix of protein A/protein G sepharose beads. Following overnight incubation at 4°C with gentle shaking, bead fractions were collected and immunoprecipitate was eluted by competitive binding in 100µL 100µg/mL 3X FLAG peptide (Sigma-Aldrich). Western blot analysis confirmed that FLAG-tagged MYPBC3 bait proteins were not non-specifically pulled down by normal mouse IgG controls.

2.3.5 Protein Identification by LC-Tandem Mass Spectrometry.

30µL of the FLAG immunoprecipitate was separated by SDS-PAGE. Gels were stained in Biosafe Coomassie (BioRad) for 1 hour at room temperature and destained in ddH$_2$O for 1 hour. Gel lanes were cut into 10-12 fragments and destained with 30% methanol for 4 hours. Upon reduction (10mM DDT) and alkylation (65 mM 2-chloroacetamide) of the cysteines, proteins were digested overnight with sequencing

grade modified trypsin (Promega). Resulting peptides were resolved on a nano-capillary reverse phase column (Acclaim PepMap C18, 2 micron, 50cm, ThermoScientific) using a 1% acetic acid/acetonitrile gradient at 300nL/min and directly introduced into Orbitrap Fusion Tribrid mass spectrometer (ThermoScientific). MS1 scans were acquired at 120K resolution. Data-dependent high-energy C-trap dissociation MS/MS spectra were acquired with top speed option (3 sec) following each MS1 scan (relative CE ~32%).

Data were collected for two independent IP-MS experiments. Peptide-to-spectrum assignments (PSMs) were statistically validated and protein lists were generated using PeptideProphet [Ma, 2012]. The ABACUS algorithm was used to extract adjusted spectral counts, making adjustments for shared peptides among closely homologous proteins [Fermin, 2011]. Criteria for identifying MYBPC3 interactors were the following: (i) proteins were detected in both experimental replicates, and (ii) proteins showed a calculated fold change score (FC-A) in adjusted spectral counts of ≥2 over the non-transduced sample in at least one replicate. FC-A was calculated as described previously [Mellacheruvu, 2013]. Spectral counts of interacting proteins were normalized to abundance of the FLAG-MYBPC3 bait protein by multiplying the adjusted spectral counts by a normalization factor equal to the ratio of adjusted spectral counts for FLAG-WT MYBPC3 to adjusted spectral counts for the respective FLAG-mutant MYBPC3 in each sample. ($S_{norm} = S_{adj} * \frac{S_{adj\_WT}}{S_{adj\_mutant}}$, where S_{adj} refers to the adjusted spectral counts retrieved from the Abacus algorithm and S_{norm} refers to the bait-normalized spectral counts.) When comparing spectral counts for interacting proteins between WT and mutant MYBPC3, we verified that the majority of MYBPC3 peptides detected in each sample could be attributed to the

human FLAG-MYBPC3 bait protein as opposed to any endogenous rat MYBPC3 that was pulled down non-specifically (Table 2.1).

2.3.6 Cycloheximide pulse-chase analysis of MYBPC3 degradation rates.

Un-patterned NRVMs were plated at a density of 2.25×10^5 cells/well in 24-well culture plates. Micropatterned NRVMs used for pulse-chase assays were plated at 1.5×10^5 cells/coverslip. Cells were transduced at MOI 2 with WT or truncated MYBPC3 adenovirus 24 hours after plating. 48 hours following MYBPC3 adenovirus, cells received one of the following treatments: 20nM scrambled siRNA (Silencer Select Negative Control #1, ThermoFisher Scientific), 20nM rat HSC70 siRNA (Silencer Select s127902, ThermoFisher Scientific), 1:1000 DMSO vehicle, or 10µM YM-1 small molecule Hsp70 activator in DMSO (1:1000 dilution). siRNA was delivered using Dharmafect 1 transfection reagent (DharmaCon) in antibiotic-free maintenance media. YM-1 or DMSO vehicle control was directly applied to NRVMs. Maintenance media containing 300µg/mL cycloheximide (Sigma-Aldrich) to inhibit *de novo* protein synthesis was added starting 24 hours after above treatments. Samples were collected in quadruplicate by scraping in 1X Laemmli buffer (BioRad) with protease inhibitor cocktail (EDTA-free, Sigma-Aldrich) at 0, 0.75, 1.5, 3, 6, 9 and 12 hours and stored at -80°C. Abundance of endogenous rat MYBPC3 and FLAG-tagged WT and truncated MYBPC3 protein over time was assessed by Western blotting. Data from three independent experiments were fit to a first-order exponential decay curve $[MYBPC3] = [MYBPC3]_0 e^{-kt}$ (with $[MYBPC3]_0$ normalized to 1), from which reaction constants k and half-lives $t_{1/2}$ (calculated as $t_{1/2} = \ln(2)/k$) were determined.

2.3.7 Western Blotting.

Prior to analysis, sample protein concentration was determined by Lowry (for samples collected in Laemmli buffer) or Bradford (for samples collected in RIPA buffer) protein assays. Final sample preparation was in 1X Laemmli buffer with 5% β-mercaptoethanol. Samples were boiled for 5 minutes at 95°C, separated on 18- or 26-well precast Tris-HCl 4-20% gradient gels (BioRad), and transferred to nitrocellulose membranes. Following transfer, gels were stained in Biosafe Coomassie for 1 hour at room temperature and destained in ddH$_2$O. Membranes were blocked in 5% non-fat dry milk in PBS for 1 hour at room temperature. Primary and secondary antibody solutions were made in 5% milk in PBS-T (0.03% Tween-20). Antibody conditions were as follows: MYBPC3, rabbit polyclonal 1:10000 (custom, provided by Samantha Harris, University of Arizona, Tucson, AZ)[Harris, 2002]; FLAG M2, mouse monoclonal 1:1000 (Sigma-Aldrich F1804); FLAG, rabbit polyclonal 1:500 (Sigma-Aldrich F7425) HSC70, mouse monoclonal 1:500 (Enzo Life Sciences ADI-SPA-815); Hsp70, mouse monoclonal 1:200 (Enzo Life Sciences ADI-SPA-810); α-actinin, mouse monoclonal 1:5000 (Sigma-Aldrich A7811); cardiac myosin heavy chain [BA-G5], mouse monoclonal 1:1000 (AbCam ab50967), GAPDH, rabbit polyclonal 1:1000 (Millipore ABS16); IRDye® 680RD goat anti-mouse IgG 1:5000 (LI-COR 926-68070); IRDye® 800CW goat anti-rabbit IgG 1:5000 (LI-COR 925-32211). Primary antibody incubations were either for 1 hour at room temperature or overnight at 4°C. Secondary antibodies were incubated for 1 hour at room temperature protected from light. For myosin heavy chain blots, blocking and antibody buffers were made using Odyssey blocking solution (LI-COR) with 0.2% Tween-20. Blots and gels were scanned on an Odyssey® CLx Imaging System (LI-COR) and analyzed

with LI-COR Image Studio™. For images of blots in figures, all lanes presented are from the same individual blot, but a solid line between adjacent lanes signifies the image is not contiguous. Omitted lanes were of additional experimental replicates.

2.3.8 Immunofluorescence of NRVMs.

NRVMs plated on glass or PDMS coverslips were washed in PBS, fixed for 15 minutes at room temperature in 4% paraformaldehyde (Sigma-Aldrich), and permeabilized in 0.2% Triton X-100 (Sigma-Aldrich) for 10 minutes. Cells were blocked in 5% normal goat serum (Vector Biolabs) in PBS for 30 minutes at room temperature. Primary and secondary antibody solutions were made in 5% normal goat serum in PBS. Antibody and staining conditions were as follows: MYBPC3, rabbit polyclonal 1:1000 (custom, Samantha Harris, University of Arizona, Tucson, AZ); FLAG M2, mouse monoclonal 1:500 (Sigma-Aldrich F1804); HSC70, mouse monoclonal, 1:200 (Enzo Life Sciences ADI-SPA-815); AlexaFluor 488 phalloidin, 1:1000 (ThermoFisher Scientific); goat anti-mouse IgG Alexa Fluor 594, 1:500 (ThermoFisher Scientific A11005); goat anti-rabbit IgG Alexa Fluor 488. 1:500 (ThermoFisher Scientific A11008). In samples dually stained for MYBPC3 and FLAG, primary antibodies were incubated sequentially for 1 hour each at room temperature; first with FLAG antibody, then with MYBPC3 antibody, to reduce antibody cross-reactivity. Secondary antibodies and phalloidin were incubated for 30 minutes at room temperature, protected from light. Following antibody incubations, cells were incubated with 200ng/mL DAPI in PBS for 10 minutes at room temperature, protected from light. Lastly, coverslips were mounted onto slides with ProLong Diamond Antifade (ThermoFisher Scientific) and cured overnight prior to imaging. PDMS coverslips were mounted face-up and topped with glass coverslips.

2.3.9 Assessment of HSC70 sarcomere periodicity.

Untreated patterned NRVMs plated at a density of 1.5×10^5 cells/coverslip were fixed and immunostained as described above for HSC70 and phalloidin. Images of three random fields per coverslip from three biological replicates were acquired with a 60X objective using a Nikon Eclipse Ti-E inverted fluorescence microscope. Using NIS-Elements software, fluorescence intensity profiles for HSC70 and phalloidin were obtained from longitudinal line-scans of 2-4 individual cells per field. Line-scans were set to 32 pixels wide (~20µm) to cover the entire width of the cardiomyocyte. Baseline correction, fast Fourier transforms and cross-correlation analysis of fluorescent intensity traces was done using MatLab software. Median periods of both HSC70 and phalloidin signals were determined.

2.3.10 Quantitative reverse transcription PCR.

qRT-PCR was used to validate knockdown of *Hspa8* transcript in NRVMs. RNA was isolated from cells using the standard Qiagen RNeasy Mini kit. The Qiagen Omniscript RT kit was used for generation of cDNA by reverse transcription. TaqMan™ gene expression assays for rat *Hspa8* and *GAPDH* were used in conjunction TaqMan® Fast Advanced Master Mix and samples were analyzed using an Applied Biosystems® 7500 Fast Real-Time PCR system. Data were analyzed as previously described [Pfaffl, 2001].

2.3.11 Statistics

Statistical analysis was done using GraphPad Prism software. Kruskal-Wallis nonparametric one-way ANOVA with Dunn's post hoc test for multiple comparisons were used for comparisons among control, WT MYBPC3 and mutant MYBPC3 groups. Outliers excluded from analysis were identified using GraphPad Prism's ROUT method with a Q

coefficient of 1%. Cycloheximide chase data analysis was performed by fitting data to a first-order exponential decay curve as described above and determining if control and treatment data could be explained by identical or differing fit parameters (i.e. reaction constant k). p-values of <0.05 were considered statistically significant. Data is reported as mean±SEM unless otherwise noted.

2.4 RESULTS

2.4.1 MYBPC3 mutants are unstably expressed and mislocalized.

We created WT and five mutant human MYBPC3 constructs with N-terminal FLAG epitope tags to express in NRVMs via adenoviral transduction. The mutations chosen have been identified as pathogenic in patients with HCM [Helms, 2014, Walsh, 2017] and occur at several loci along the MYBPC3 protein (Figure 2.2A). The Ile154Leufs*5, c.2905+1G>A, Asp1076Valfs*6, and Trp1098* mutations are nonsense, resulting in truncated proteins, while the Gly1248_Cys1253dup mutation contains an in-frame duplication near the C-terminus resulting in a full-length protein. Gly1248_Cys1253dup was included because unlike other MYBPC3 non-truncating mutations, the mutant protein appears to be unstable and is not detectable in human HCM tissue, similar to MYBPC3 truncating mutations [Helms, 2014]. We performed immunofluorescence of NRVMs on fibronectin-micropatterned PDMS coverslips to determine the subcellular localization of MYBPC3 mutants. This micropatterning technique constrains the NRVMs to 20µm-wide rows, inducing elongated rectangular morphologies more similar to adult cardiomyocyte geometry, and thus enabling precise analysis of sarcomere structure and protein localization (Figure 2.1). FLAG-WT MYBPC3 localized correctly to the C-zone, in the

characteristic doublet pattern flanking the M-line. In contrast, none of the MYBPC3 mutants exhibited sarcomere incorporation, instead localizing diffusely to the cytosol and in the case of Ile154Leufs*5, to the nucleus (Figure 2.3A, B). Select MYBPC3 mutants also showed significantly decreased expression compared to WT as assessed by Western blot of NRVM whole lysate (Figure 2.2B, D). However, total MYBPC3 protein levels (sum of endogenous rat and adenovirally-expressed protein) were unchanged, indicating that overall sarcomere stoichiometry of MYBPC3 was maintained (Figure 2.2C, E, F).

2.4.2 MYBPC3 associates with HSP70 chaperone proteins.

In order to identify MYBPC3 interacting proteins, we purified WT, Ile154Leufs*5, and Trp1098* FLAG-MYBPC3 and binding partners from NRVM lysates by co-immunoprecipitation (Figure 2.4A) and analyzed them by LC-MS/MS. Two independent IP-MS experiments were performed. Interactors were defined as those proteins with ≥2 assigned peptides detected in both experiments, and with a calculated fold-change in spectral counts (FC-A score) of ≥2 compared to the non-transduced NRVM sample in at least one of the two experiments. Gene ontology enrichment analysis of 37 proteins identified as WT interactors (Figure 2.4B) analyzed against a background list of all 515 proteins detected in the samples transduced with WT FLAG-MYBPC3 identified an annotation cluster for chaperones, unfolded protein binding, and protein folding as the most enriched category of proteins (For full results and analysis of interactors, see Table 2.2). Among these, members of the HSP70 family of molecular chaperones were the most abundant chaperones identified, with heat shock cognate 70kDa (HSC70/*Hspa8*) exhibiting the highest spectral counts among chaperones in both experiments. The

stress-inducible cytosolic HSP70 (*Hspa1a)*, endoplasmic reticulum-specific binding immunoglobulin protein (BiP/*Hspa5*), and mitochondrial HSP70 (*Hspa9*), were also identified as interacting proteins. The abundance of peptides corresponding to each HSP70 chaperone was mutation-specific: the Ile154Leufs*5 mutant had the lowest spectral counts for HSP70 and HSC70, while Trp1098* had the highest spectral counts relative to WT MYBPC3 (Figure 2.4D). Sarcomere proteins known to bind to MYBPC3 (i.e. α- and β- myosin heavy chains) were identified in WT immunoprecipitates, and were less abundant or absent in mutant MYBPC3 samples, reflecting loss of binding domains and lack of sarcomere incorporation (Figure 2.4F). While α-cardiac actin (*Actc1)*, a known major binding partner of MYBPC3, was detected in both IP-MS replicates, it did not meet the requisite threshold for an interacting protein due to the presence of high spectral counts in the non-transduced samples. This was likely due to non-specific binding of *Actc1* to the sepharose beads or IgG, as actin isoforms are known common contaminants in affinity purification assays[Mellacheruvu, 2013]. Additionally, *Acta1* (α-skeletal muscle), *Acta2* (aortic smooth muscle), *Actb* and *Actg1* (cytoplasmic) were also detected. Due to the high sequence homology among different actin isoforms, it is also possible that some peptides assigned to cardiac actin originated from the other forms of actin, and vice-versa. Other potentially novel interacting proteins associated with the myofilament and cytoskeleton were also identified (e.g. FLNA, FLNC, CSRP3, LDB3 and SORBS2) as were several proteins involved in other cellular functions, including metabolism and translation (Figure 2.4B, Table 2.2). 5 proteins retained interaction with WT, Trp1098* and Ile154Leufs*5 MYBPC3: polyubiquitin-C, *Hspa1a, Hspa5, Hspa8, and Hspa9* (Figure 2.4C)*.* Both mutants showed an overall loss of interaction with non-HSP70 chaperones and other

protein quality control related factors compared to WT. For example, we identified a loss of interaction with the small heat shock proteins αB-crystallin (*Cryab*) and HSP27 (*Hspb1*) for both MYBPC3 mutants (Figure 2.4E).

2.4.3 HSC70 knockdown slows degradation rate of WT and mutant MYBPC3.

Both HSC70 and HSP70 act upstream of proteasomal degradation by interacting with UPS substrates and the E3 ubiquitin ligase CHIP, thereby facilitating ubiquitination [McDonough, 2003]. Because the affinity-purification mass spectrometry experiment demonstrated the strongest evidence for an MYBPC3-HSC70 interaction, we focused initially on HSC70. We hypothesized that if MYBPC3 is a client for HSC70, modulating expression or activity of HSC70 would affect its degradation. To investigate this, we measured the degradation rates of WT and mutant MYBPC3 by cycloheximide (CHX) pulse-chase assay. First, NRVMs were treated with either non-specific scrambled control siRNA or siRNA directed against the gene encoding HSC70 (*Hspa8*). 24 hours of siRNA treatment produced significant (>50%) knock-down of both HSC70 transcript and protein compared to scrambled control (Figure 2.5*A-C*). NRVMs were then incubated in media containing CHX to block *de novo* protein synthesis and allow measurement of the rates of degradation for individual proteins by Western blot. Scrambled siRNA treatment did not significantly affect the endogenous rat MYBPC3 degradation rate compared with the untreated condition (Figure 2.7F). For endogenous rat MYBPC3, FLAG-WT, and Trp1098*, $t_{1/2}$ was significantly longer in cells treated with HSC70 siRNA versus scrambled siRNA, while the effect of HSC70 knockdown on Ile154Leufs*5 and Gly1248_Cys1253dup MYBPC3 was not significant (Figure 2.7*A-E,* Table 2.3, representative Western blots can be found in Figure 2.8). The Gly1248_Cys1253dup

mutant exhibited a very rapid rate of degradation, and earlier time points post CHX treatment (45 and 90 minutes) were added to better capture its degradation kinetics. The Z-disk protein α-actinin and myosin heavy chain (Figure 2.7G) did not degrade at the same rate as MYBPC3, demonstrating that the degradation kinetics we observed are specific to MYBPC3 and do not simply reflect general turnover of all sarcomere proteins. Lastly, we demonstrated that FLAG-MYBPC3(WT) is primarily degraded through the proteasome rather than autophagy by treating NRVMs with CHX in conjunction with either the proteasome inhibitor lactacystin or the autophagy inhibitor bafilomycin. At 12 hours post CHX, MYBPC3 expression in lactacystin treated cells was not significantly different from levels in untreated cells, while levels in bafilomycin treated cells were reduced to a similar extent as cells treated with CHX alone (Figure 2.6).

2.4.4 HSP70 activator YM-1 accelerates degradation of WT and mutant MYBPC3.

YM-1 is a small-molecule activator which stabilizes the ADP-bound conformation of HSP70 chaperones including but not limited to HSC70, resulting in tighter substrate binding. YM-1 has previously been shown to promote degradation and clearance of misfolded clients [Wang, 2013]. Addition of YM-1 did not affect HSP70 or HSC70 protein levels (Figure 2.5D-F). DMSO itself prolonged the half-lives of WT and mutant MYBPC3 relative to scrambled siRNA control in the previous experiment (Table 2.3, Figure 2.7F). This is likely because DMSO can non-specifically disrupt protein-protein interactions. However, the addition of DMSO was necessary to maintain the solubility of YM-1 and therefore was used in the control buffer for this set of experiments. YM-1 significantly accelerated degradation of both endogenous rat WT and FLAG-WT MYBPC3 as well as Trp1098* and Ile154Leufs*5, compared to DMSO vehicle control (Figure 2.7A-D).

Gly1248_Cys1253dup was not significantly affected (Figure 2.7E). Representative Western blots can be found in Figure 2.8.

2.4.5 HSC70 localizes to the sarcomere M-line and Z-disk in NRVMs.

HSC70 is expressed in both the cytosol and nucleus in most cell types, but the precise localization of HSC70 in cardiac myocytes has not been previously reported to our knowledge. We observed HSC70 signal localizing to prominent striations within the sarcomere of NVRMs. To precisely assess localization patterns of HSC70 in the sarcomere, we analyzed aligned micropatterned NRVMs by immunofluorescence. In untreated cells, fluorescence intensity traces from line-scans of individual NRVMs showed that sarcomere HSC70 signal appeared in an alternating pattern compared to phalloidin (actin) staining (Figure 2.9A,B) The center of the area of phalloidin signal demarks the Z-disk, indicating that HSC70 peaks occur at the M-line. A weaker HSC70 band which colocalized with phalloidin was also visible. Fast Fourier transform analysis of HSC70 intensity traces, which quantitatively determined the period of HSC70 signal, confirmed that local HSC70 maxima occurred once every ~1µm, in comparison to phalloidin, with maxima once every ~1.75µm (Figure 2.9C). The fact that the periodicity of HSC70 is slightly greater than twice the periodicity of phalloidin may be explained by the relative weakness of the Z-disk signal compared to the more prominent M-line signal. This places HSC70 in immediate proximity to the C-zone.

2.5 DISCUSSION

The major findings of this study are the following: (i) MYBPC3 interacts with the molecular chaperones HSP70 and HSC70; (ii) decreasing the pool of HSC70 prolonged

the half-life of both WT and mutant MYBPC3, while pharmacological activation of HSP70/HSC70 shortened half-life; and (iii) a fraction of the HSC70 pool is positioned within the sarcomere adjacent to the C-zone. These data provide evidence that proteasomal degradation of MYBPC3 is mediated by HSC70. To our knowledge, our study is the first to identify a chaperone for which MYBPC3 is a client. HSC70 has previously been shown to be involved in assembly of myosin intermediates in skeletal muscle myoblasts, regulation of actin capping machinery, and turnover of filamin C at the Z-disk in response to mechanical stress [Arndt, 2010, Hishiya, 2010, Srikakulam, 2004]. However, the role of HSC70 in routine sarcomere protein turnover in fully differentiated cardiac myofibrils has not been explored previously. By showing that HSC70 regulates degradation of MYBPC3, we reveal an essential role for this chaperone family in cardiac sarcomere protein homeostasis, and provide a proof of concept for therapeutic manipulation of chaperone-client interactions to regulate sarcomere protein turnover in HCM.

The extent to which MYBPC3 nonsense mutations produce loss of functional protein is governed by regulation of MYBPC3 expression and degradation. Exploration of MYBPC3's binding partners has previously been focused almost exclusively on its sarcomeric interactors. Yet, in an unbiased screen, we found that the most enriched category of interactors for WT MYBPC3 were chaperones and protein quality control-related partners. Most abundant among these were HSP70 molecular chaperones, supporting a role in the degradation pathway of MYBPC3. Furthermore, HCM-related mutations may affect the specificity of MYBPC3-HSP70/HSC70 interactions. HSC70 and HSP70 co-immunoprecipitated with WT, Ile154Leufs*5, and Trp1098* MYBPC3.

However, normalized spectral counts for both chaperones were substantially reduced for Ile154Leufs*5 compared to WT, suggesting decreased interaction for that particular mutant. Consistent with these findings, HSC70 knockdown had no significant effect on degradation of the Ile154Leufs*5 mutant, although YM-1 did accelerate degradation of Ile154Leufs*5. The effect of YM-1 on Ile154Leufs*5 could be explained by activation of other HSP70 isoforms in addition to HSC70. Conversely, spectral counts for HSP70 and HSC70 were increased for the Trp1098* mutant compared to WT. Since expression of Trp1098* did not upregulate HSP70 or HSC70, we speculate that either a larger pool of the mutant protein is associated with HSP70 chaperones or that the binding is more avid for the mutant than for the wild-type protein. However, the effects of HSC70 knockdown and YM-1 on the $t_{\frac{1}{2}}$ of the Trp1098* mutant were similar to the effects on FLAG-WT MYBPC3. Interestingly, neither the Ile154Leufs*5 nor Trp1098* truncated mutants showed a significantly shorter $t_{\frac{1}{2}}$ at baseline than that of FLAG-WT MYBPC3. In fact, Ile154Leufs*5 had a longer $t_{\frac{1}{2}}$, which could be explained by its aberrant nuclear localization. On the other hand, degradation of the Gly1248_Cys1253dup mutant was significantly accelerated, despite exhibiting similar cytosolic localization to Trp1098*. While the Gly1248_Cys1253dup mutation encodes for a full-length protein, the protein has not been detected in myocardium from HCM patients, suggesting that this mutation renders it highly unstable. Although it was degraded via the UPS in the same manner as WT and Trp1098* MYBPC3, neither HSC70 knockdown nor YM-1 affected the $t_{\frac{1}{2}}$ of Gly1248_Cys1253dup. This could imply that this particular mutation disrupts interaction with HSP70 chaperones, but does not affect its ability to be targeted for proteasomal degradation. Together, these results imply differential effects on MYBPC3-HSP70

chaperone interactions based on mutation locus within MYBPC3. Specificity of a given MYBPC3 mutant's interaction with HSP70 chaperones could potentially be dictated by its subcellular localization, presence or absence of binding domains, protein length, or folding state.

Because the HSP70 family interacts with a very broad range of clients and because HSC70 participates in many critical cellular functions, it is unknown whether direct targeting of these chaperones would be possible without adversely affecting turnover of other proteins or other cellular processes. Therefore, further elucidation of the mechanism by which HSC70 facilitates degradation of MYBPC3 and identification of potential co-chaperones involved is warranted as it could open new therapeutic avenues to address haploinsufficiency of MYBPC3 in HCM. HSC70 interacts with the E3 ubiquitin ligase CHIP, which links it to UPS-mediated degradation. A recent study identified a potential interaction between MYBPC3 and the HSC70 co-chaperone BAG3 [Judge, 2017]. BAG3 localizes to the Z-disk and participates in both proteasomal and chaperone-assisted autophagic degradation pathways, most notably in a complex with HSC70, CHIP, and HSPB8 [Arndt, 2010, Minoia, 2014, Norton, 2011, Ulbricht, 2013]. However, clients of this complex undergo chaperone assisted selective autophagy, while MYBPC3 seems primarily to be degraded by the proteasome. BAG3 and HSC70 have also been found to form a complex with the actin capping protein CapZ at the Z-disk in NRVMs, which is consistent with the sarcomeric localization of HSC70 we observed [Hishiya, 2010]. We found that HSC70 also localized prominently to the M-line in NRVMs. This localization pattern is consistent with a regulatory role of HSC70 in the turnover of MYBPC3, which is localized as a doublet within the A-band of the sarcomere, adjacent to the M-line on either

side. We speculate that this juxtapositioning of HSC70 relative to MYBPC3 within the sarcomere facilitates its mobilization to degrade MYBPC3 as the protein is being released from the sarcomere. It is also possible that a pool of non-sarcomere-bound MYBPC3 interacts with HSC70 prior to sarcomere incorporation or after it has been fully disengaged from the sarcomere. It is notable that FLAG-WT MYBPC3 had a shorter $t_{1/2}$, and higher expression after addition of lactacystin compared to endogenous MYBPC3. A higher rate of proteasome-mediated degradation is consistent with the existence of a larger pool of newly synthesized FLAG-WT MYBPC3 that is not yet incorporated into the sarcomere. This could also explain why HSC70 knockdown elicited a lesser magnitude change in protein $t_{1/2}$ for the FLAG-WT MYBPC3 compared to endogenous MYBPC3 (~2 fold vs ~12 fold, Table 1). Conversely, YM-1 accelerated degradation of FLAG-WT MYBPC3 to a greater extent than endogenous MYBPC3 (~4.5 fold vs ~2.5 fold, Table 1) which could be explained by a greater contribution of HSP70 cytosolic chaperones to its degradation.

Several other chaperones and protein quality control-related proteins were identified in the co-immunoprecipitation experiments as interacting with WT MYBPC3, including the small heat shock proteins (sHSPs) αB-crystallin and HSP27 (*Hspb1*). A subset of sHSP family members are highly expressed in striated muscle and some have been found to be cardioprotective against ischemia/reperfusion injury [Golenhofen, 2004, Hollander, 2004, Martin, 1997]. Mutations in αB-crystallin, which are hypothesized to alter its interactions with its client protein desmin, result in a dilated cardiomyopathy characterized by the presence of desmin aggregates [Inagaki, 2006, McLendon, 2011, Perng, 1999]. Both αB-crystallin and HSP27 may also act to prevent aggregation of unfolded titin domains [Kotter, 2014]. In

this study, we observed a substantial loss of interaction between these sHSPs and truncated MYBPC3 mutants in co-IP/MS experiments. Given the importance of these sHSPs in maintaining cardiomyocyte proteostasis by preventing aggregation of intermediate filament and myofilament proteins, further studies are warranted to define the potential role they play in the folding and turnover of MYBPC3.

Our model system of expressing mutant MYBPC3 proteins in NRVMs has some limitations. Because truncated MYBPC3 protein has not been detected in human myocardium samples from patients with nonsense *MYBPC3* mutations, the levels at which FLAG-MYBPC3 mutant proteins are expressed are supra-physiological. However, in our model the total expression levels of mutant MYBPC3 are relatively low compared to the endogenous protein without affecting total MYBPC3 stoichiometry. Furthermore, this expression system enabled quantification and modulation of the degradation kinetics of each individual mutant protein relative to WT MYBPC3.

Most existing therapeutic interventions for HCM address symptoms but do not modify the progression of the underlying disease substrate. Recent clinical and preclinical trials targeting calcium flux and contractility have shown promise [Coppini, 2013, Ho, 2015, Nag, 2015], but it is not apparent whether such therapies will be effective for all genetic subtypes of HCM. If haploinsufficiency is the major underlying mechanism in MYBPC3-linked HCM, restoring normal sarcomere levels of MYBPC3 would be attractive as a targeted therapy. In demonstrating interactions between HSP70/HSC70 and MYBPC3, we have identified a new mechanism by which MYBPC3 degradation, and thereby turnover, could be modulated. These findings further our understanding of disease mechanisms in the most

common genetic form of HCM, and contribute a piece to the longstanding puzzle of sarcomere protein turnover and maintenance of stoichiometry.

2.6 ACKNOWLEDGEMENTS

FIGURE 2.1

Figure 2.1. Fibronectin micropatterning technique constrains immature NRVMs to a rod-like morphology. *(A)* Micropatterned stamps with 20μm-wide rows spaced 3μm apart were used to print fibronectin onto PDMS coverslips prior to plating of NRVMs. NRVMs adhered only within the 20μm-wide rows. *(B)* Representative immunofluorescent micrographs of NRVMs stained for MYBPC3 showing an example of amorphous morphology and non-parallel sarcomeres of an unpatterned cell (left) versus rod-like morphology and aligned Z-disks of a patterned cell (right). 60X magnification.

FIGURE 2.2
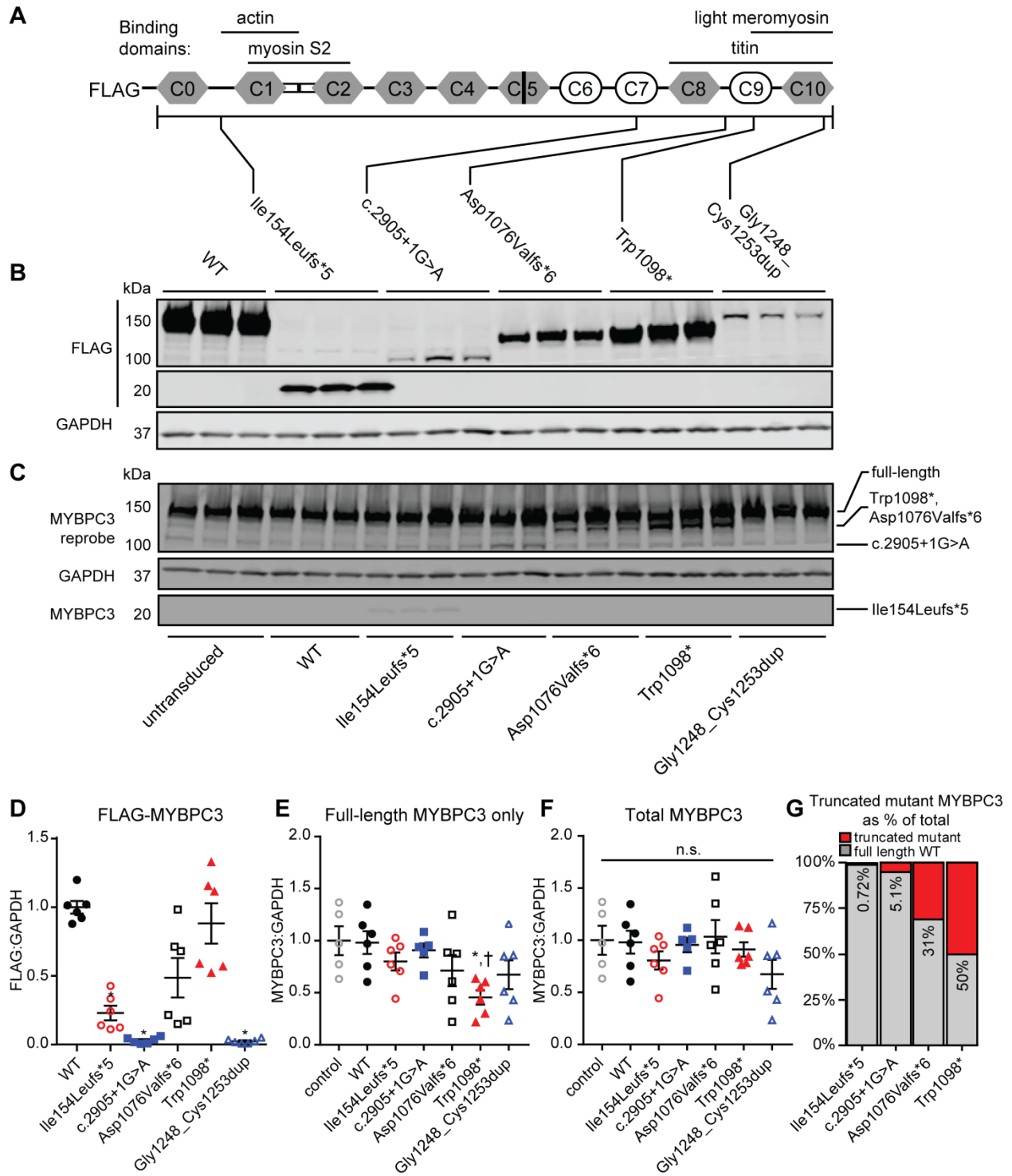
Figure 2.2. FLAG-tagged WT and mutant MYBPC3 constructs were expressed in NRVMs via adenovirus. *(A)* FLAG-MYBPC3 protein schematic showing the 11 domains and locations of mutations. *(B,C)* Representative Western blots of FLAG-MYBPC3 and total MYBPC3, respectively, from NRVMs expressing WT or truncated FLAG-MYBPC3. Shorter truncated mutants and Gly1248_Cys1253dup are more unstably expressed compared to WT MYBPC3 or longer truncated mutants. *(D)* Quantification of FLAG-MYBPC3 expression for WT and mutants. n=6, Kruskal-Wallis one-way ANOVA p<0.0001. *p<0.05 vs WT, Dunn's multiple comparisons test. Mean±SEM. *(E)* Effect of truncated FLAG-MYBPC3 on full-length MYBPC3 levels. Higher expression of truncated mutants tended to suppress expression of endogenous MYBPC3. Note that FLAG-WT and FLAG-Gly1248_Cys1253dup were not sufficiently separated from endogenous MYBPC3 by SDS-PAGE, and therefore quantification for these conditions includes both endogenous and FLAG-MYBPC3. n≥5, Kruskal Wallis one-way ANOVA p=0.0282. *p<0.05 vs WT, Dunn's multiple comparisons test. Mean±SEM. *(F)* Quantification of total MYBPC3 (endogenous and FLAG-MYBPC3) demonstrated that overall stoichiometry of MYBPC3 was maintained when FLAG-MYBPC3 mutants were expressed. n≥5, Kruskal Wallis one-way ANOVA p=0.565. *p<0.05 vs WT, Dunn's multiple comparisons test. Mean±SEM. *(G)* Comparison of abundance of FLAG-MYBPC3 mutants as a percent of total MYBPC3 shows a potential relationship between fragment size and expression stability.

FIGURE 2.3
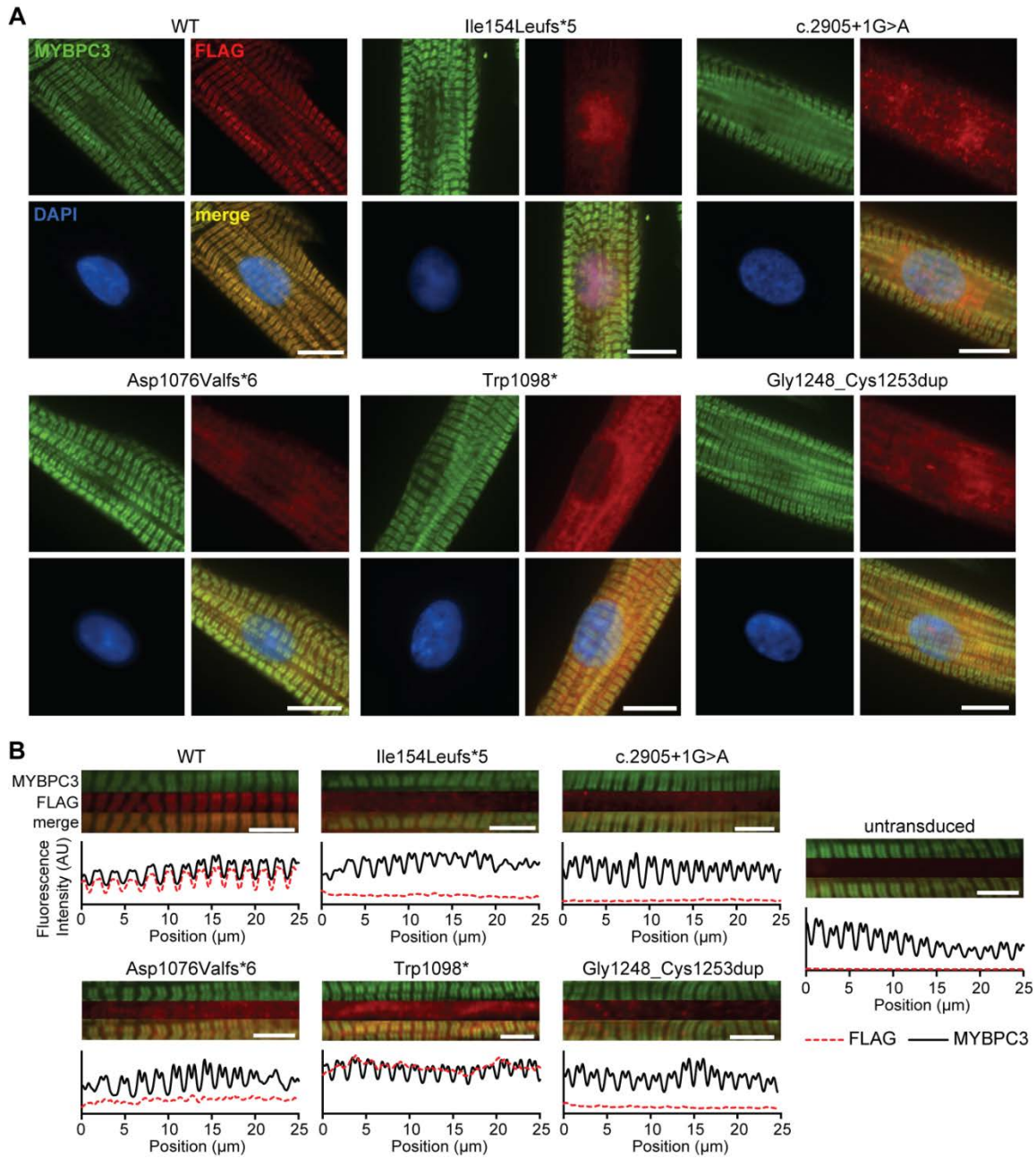
Figure 2.3. Localization of truncated MYBPC3 mutants. *(A)* FLAG-WT MYBPC3 is correctly expressed in the sarcomere C-zone in patterned NRVMs, while MYBPC3 mutants show diffuse aberrant signal in the cytosol or nucleus (Ile154Leufs*5) with little to no sarcomere localization. Immunofluorescence micrographs, 60X magnification. Scale bar=10µm. *(B)* Immunofluorescence micrographs and corresponding intensity traces sarcomeres from patterned NRVMs treated with FLAG-MYBPC3 adenovirus. FLAG-WT shows proper C-zone periodicity, while FLAG-mutants show no significant sarcomere periodicity. Scale bar = 20µm.
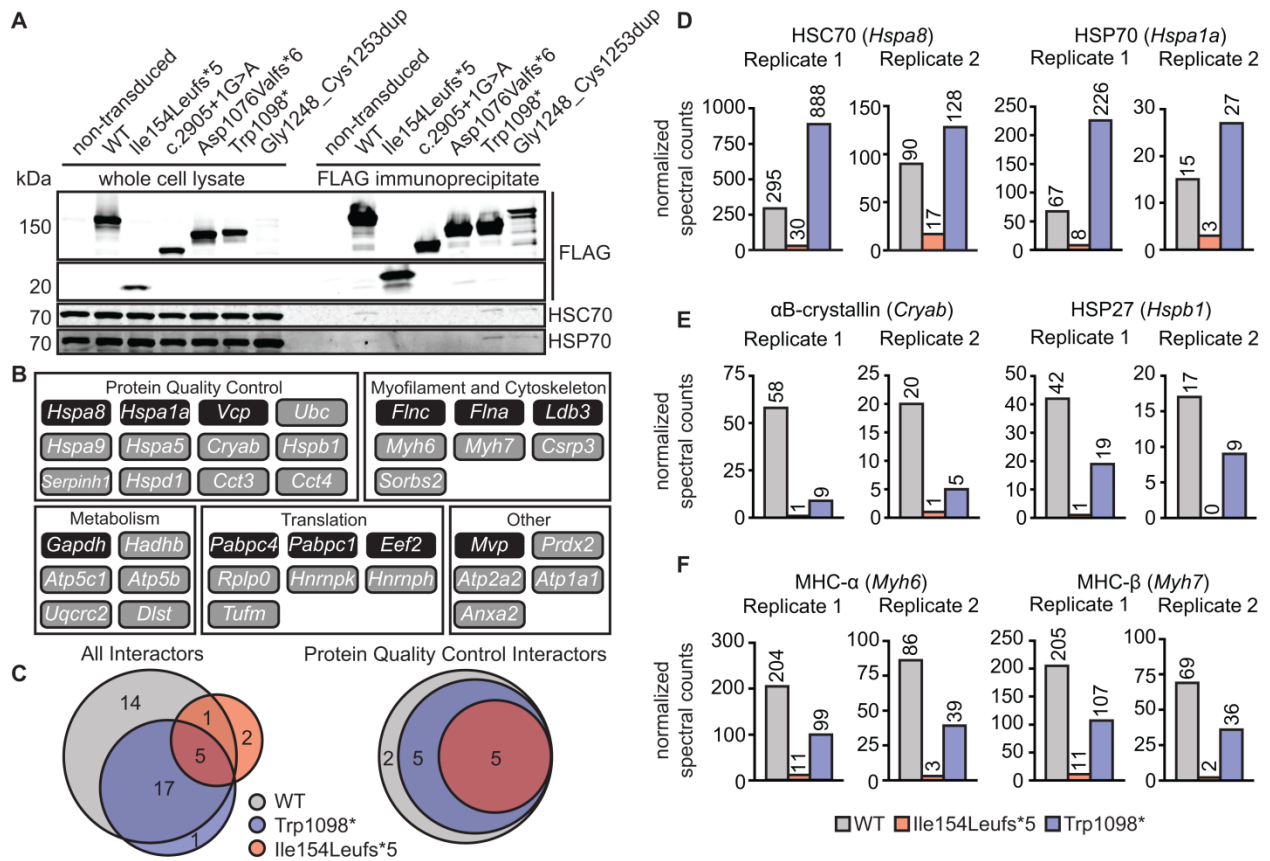
FIGURE 2.4

Figure 2.4. Interactions between MYBPC3 and molecular chaperones. *(A)* Western blot showing co-IP of HSC70 and HSP70 with FLAG-tagged WT and mutant MYBPC3. Shorter MYBPC3 truncated proteins show loss of this interaction. *(B)* Summary of WT MYBPC3-interacting proteins manually categorized by function. All interactors were detected in both IP-MS experiments and showed a calculated fold change (FC-A) in spectral counts ≥ 2 over non-transduced myocytes in at least one independent experiment. Interactors within dark boxes showed an FC-A ≥ 2 over background in both experiments. *(C)* Venn diagrams showing overlap of interacting proteins (left: all interactors; right: protein quality control interactors) identified in immunoprecipitates for WT, Ile154Leufs*5, and Trp1098* MYBPC3. MYBPC3 mutants show loss of interaction with protein quality control-related proteins. *(D-F)* Normalized spectral counts for a subset of MYBPC3 interacting proteins from two independent IP-MS experiments. Adjusted spectral counts were normalized to abundance of FLAG-MYBPC3 bait protein. *(D)* HSC70 and HSP70 were more abundant in FLAG-Trp1098* samples, but less abundant in FLAG-Ile154Leufs*5 samples compared to FLAG-WT; while small heat shock proteins *(E)* showed loss of interaction with both mutants. *(F)* MYBPC3 mutants also showed reduced association with known binding partners myosin heavy chains α and β.
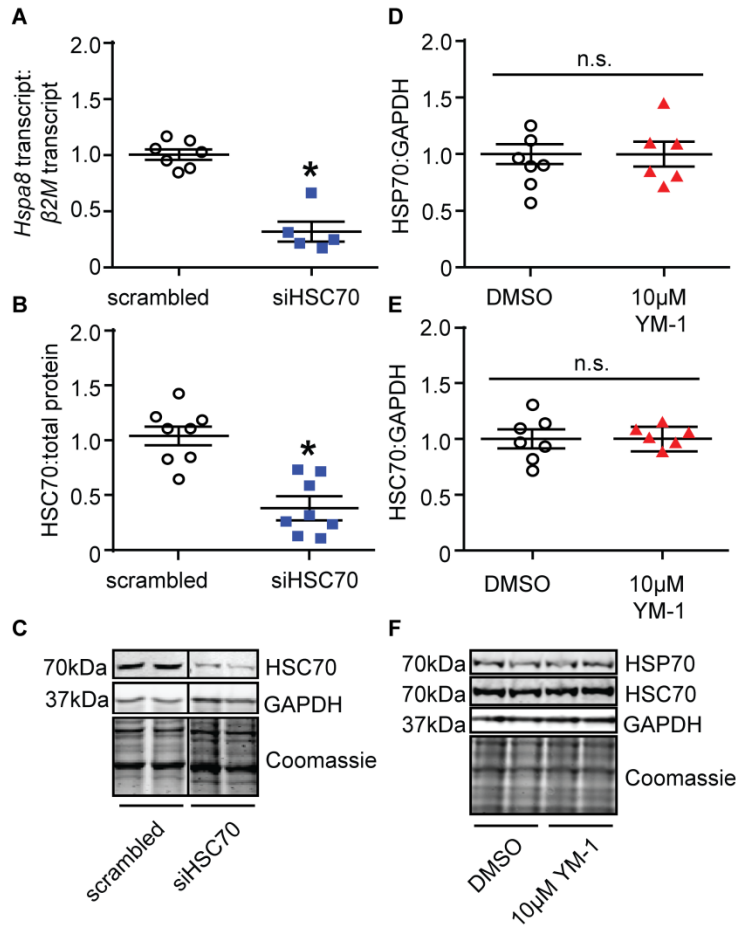
FIGURE 2.5

Figure 2.5. Validation of HSC70 siRNA efficacy and effect of YM-1 on HSP70/HSC70 expression. *(A)* NRVMs treated with 20µM siRNA directed against the rat *Hspa8* gene for 24hr show reduced HSC70 transcript compared to treatment with 20µM non-specific scrambled siRNA. (*B*) HSC70 protein is also reduced 24hr after siRNA treatment. Mean±SEM, *p<0.05 vs scrambled, student's t test. *(C)* Representative Western blot and total protein from siRNA-treated cells. Black line between lanes indicates noncontiguous samples from the same blot. *(D and E)* YM-1 treatment does not affect protein levels of HSP70 or HSC70, respectively. Mean±SEM. *(F)* Representative Western blot and total protein from YM-1 and DMSO vehicle-treated cells.

FIGURE 2.6
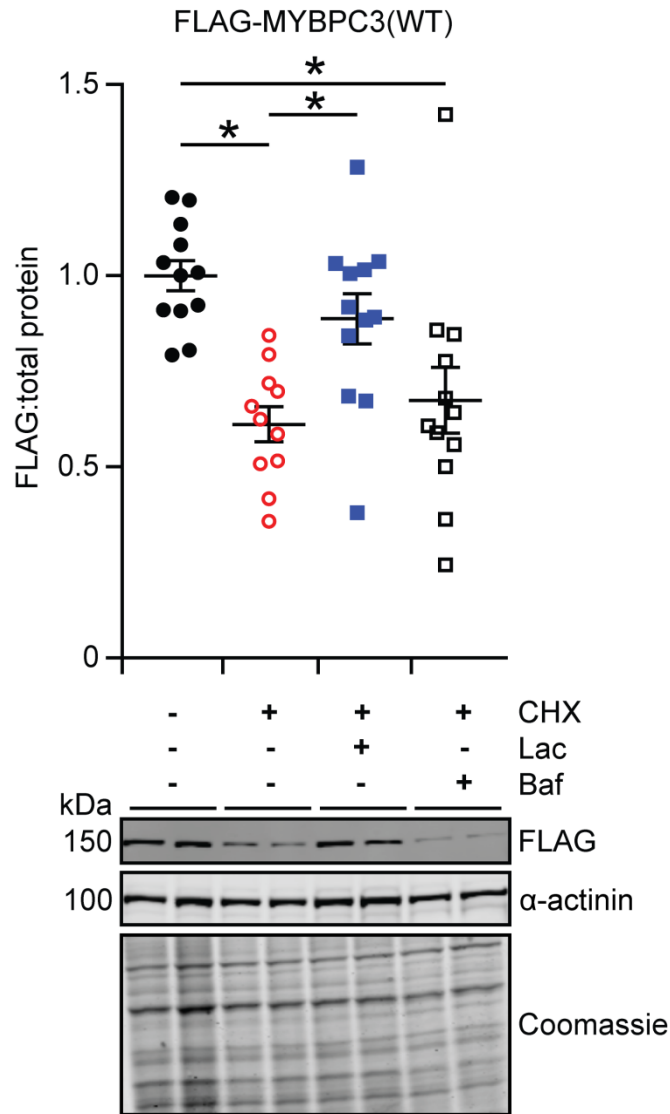
Figure 2.6. MYBPC3 is primarily degraded through the proteasome rather than autophagy. Quantification of MYBPC3 and representative Western blot from NRVMs treated with 300μg/mL CHX for 12 hr. Addition of 25μM of the proteasome inhibitor lactacystin (Lac) along with CHX prevented degradation of MYBPC3, while addition of 50nM of the autophagy inhibitor bafilomycin (Baf) along with CHX did not. Kruskal-Wallis one-way ANOVA p=0.0001, *p<0.05 Dunn's test for multiple comparisons. Mean±SEM. n=12.

FIGURE 2.7
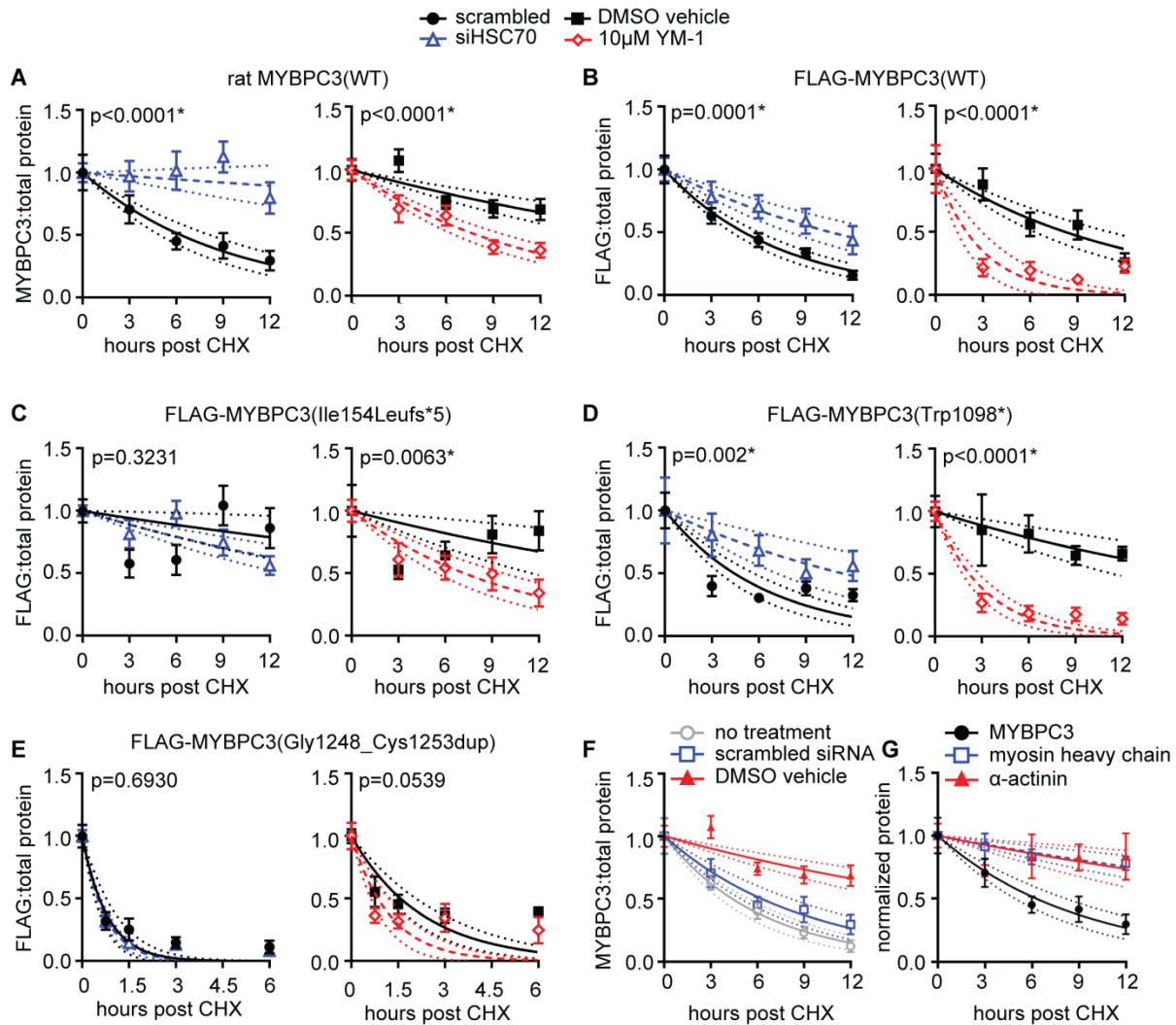
Figure 2.7. Degradation rates of WT and mutant MYBPC3 are affected by HSC70 knockdown and small molecule HSP70 activator YM-1. *(A-E, left panel)* MYBPC3 degradation was slowed in NRVMs treated with HSC70 siRNA (open triangles, dashed line) compared to scrambled control siRNA treatment (closed circles, solid line). *(A-E, right panel)* MYBPC3 degradation was accelerated in NRVMs treated with 10μM YM-1 (open diamonds, dashed line) compared to DMSO vehicle control (closed circles, solid line). n≥7, Mean±SEM, p values represent significance of comparison of reaction constant *k* between conditions. Dotted lines show 95% confidence intervals for *k*. *(F)* Scrambled siRNA and DMSO vehicle control degradation curves (as in *A*) for endogenous MYBPC3 compared to degradation of endogenous MYBPC3 in untreated NRVMs. While scrambled siRNA has no effect on the normal degradation rate, DMSO treatment significantly slowed degradation, p<0.05 vs. no treatment. *(G)* Degradation of endogenous MYBPC3 in untreated NRVMs (as in *F*) as compared to degradation of myosin heavy chain and α-actinin. MYBPC3 degrades at a rate independent of other thick filament or Z-disk components, p<0.05 vs myosin heavy chain and α-actinin.
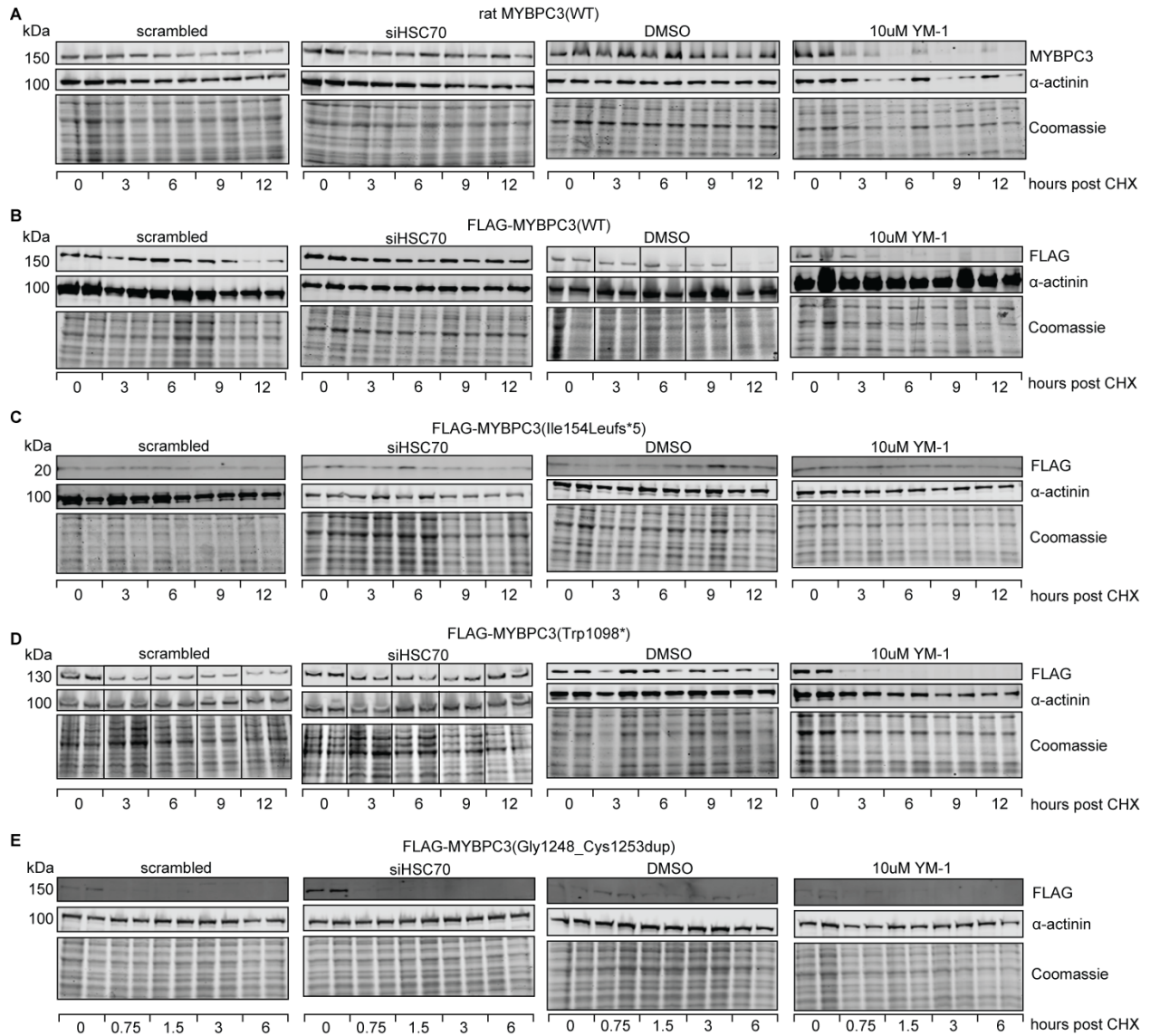
FIGURE 2.8

Figure 2.8. Representative Western blots for MYBPC3 cycloheximide experiments shown in Figure 2.5. *(A)* Endogenous rat WT MYBPC3, *(B)* FLAG-WT MYBPC3, *(C)* FLAG-Ile154Leufs*5 MYBPC3, *(D)* FLAG-Trp1098* MYBPC3, *(E)* FLAG-Gly1248_Cys1253dup MYBPC3. MYBPC3 or FLAG band strength was normalized to Coomassie-stained total protein signal from the corresponding gel. α-actinin is shown to verify MYBPC3 band is reflective of its own intrinsic degradation rate and not general sarcomere degradation. Blots are representative of three independent experiments per condition. Black line between lanes indicates noncontiguous samples from the same blot. Lanes omitted were additional replicates of conditions shown.

FIGURE 2.9
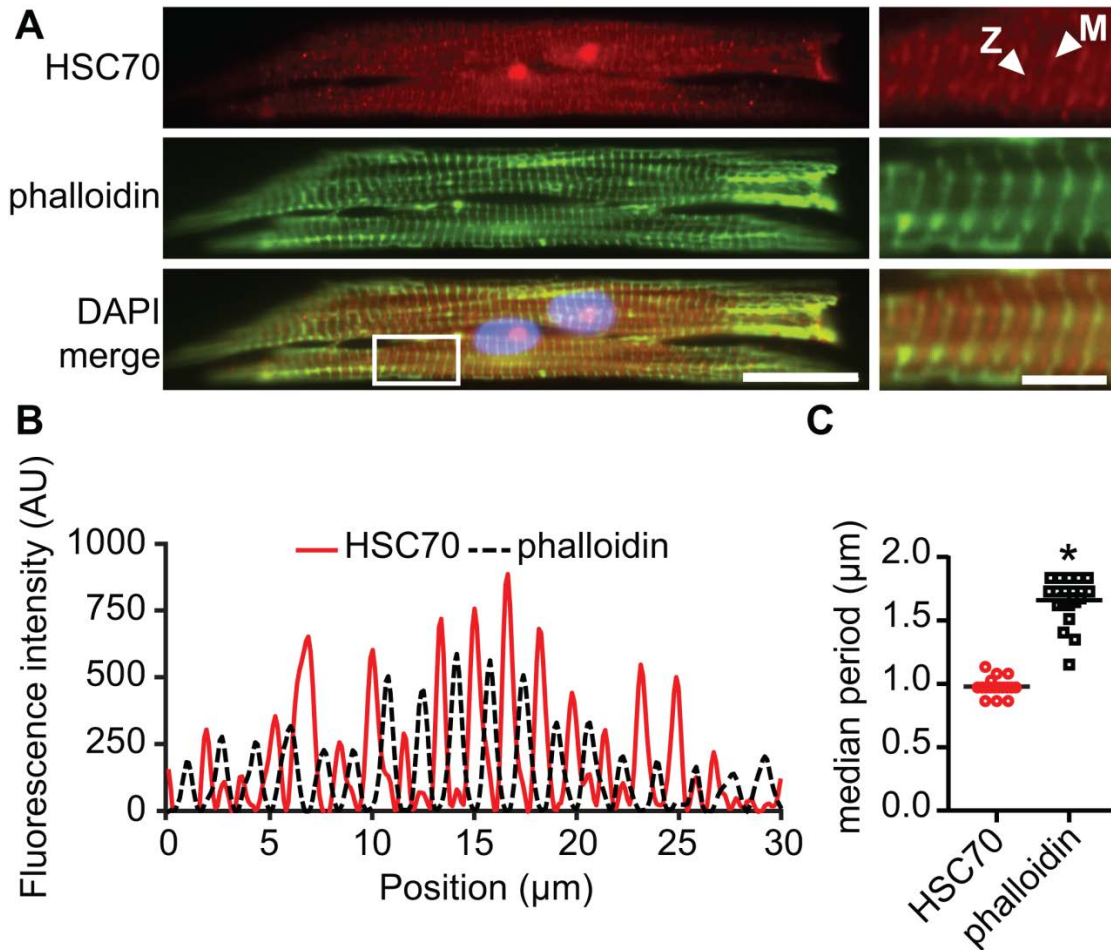
Figure 2.9. HSC70 is expressed in the sarcomere in NRVMs. *(A)* Representative immunofluorescence micrograph of untransduced NRVM. HSC70 localizes in sarcomeric striations in row-patterned NRVMs, occurring in a prominent band at the M-line and a weak band at the Z-disk (arrowheads). M-line signal exhibits an alternating pattern with phalloidin (actin) staining. Scale bar = 20µm. Scale bar in insert = 5µm. 60X magnification. *(B)* Representative baseline-corrected fluorescence intensity profiles for HSC70 and phalloidin taken from a line-scan of the cell pictured in *(A)*. Strong HSC70 peaks coincide with phalloidin (Z-disk) troughs; weak HSC70 peaks coincide with phalloidin peaks. *(C)* Median frequency of HSC70 and phalloidin peaks as determined by fast Fourier transform analysis of intensity profiles from n=18 cells. HSC70 signal repeats every 1µm, approximately twice as often as phalloidin, reflecting both M-line and Z-disk localization. Mean±SEM, *p<0.0001, Wilcoxon signed-rank test.

TABLE 2.1. Overlap in matching peptides for bait vs. endogenous MYBPC3.

IP-MS Set 1	Bait-unique MYBPC3 peptides	common peptides	Endogenous-unique MYBPC3 peptides	Total peptides
Control	86	57	0	143
WT	1709	949	24	2682
Ile154Leufs*5	409	0	58	467
Trp1098*	1350	808	17	2175

IP-MS Set 2	Bait-unique MYBPC3 peptides	common peptides	Endogenous-unique MYBPC3 peptides	Total peptides
Control	38	41	3	82
WT	333	263	9	605
Ile154Leufs*5	85	0	52	137
Trp1098*	188	146	20	354

TABLE 2.2. MYBPC3 interacting proteins for WT, Trp1098*, and Ile154Leufs*5.

Co-immunoprecipitated proteins with FC-A ≥ 2 in one or both replicates				
Uniprot ID *(rattus norvegicus)*	Gene Name	WT	Trp1098*	Ile154Leufs*5
P63039	Hspd1	✓	✓	
P19945	Rplp0	✓		
P06761	Hspa5	✓	✓	✓
P23928	Cryab	✓	✓	
Q07936	Anxa2	✓	✓	
G3V6D3	Atp5b	✓		✓
P35435	Atp5c1	✓	✓	
G3V936	Cs			✓
G3V7U0	Csrp3	✓		
P32551	Uqcrc2	✓	✓	
G3V6P2	Dlst	✓		
P05197	Eef2	✓	✓	
P85834	Tufm	✓		
C0JPT7	Flna	✓	✓	
A0A0H2UHR7	Flnc	✓	✓	
P04797	Gapdh	✓	✓	
G3V913	Hspb1	✓	✓	
P0DMW0	Hspa1a	✓	✓	✓
P63018	Hspa8	✓	✓	✓
A0A0G2JTG7	Hnrnph1	✓		
P61980	Hnrnpk	✓	✓	
B5DEN4	Ldha		✓	
Q62667	Mvp	✓		
G3V885	Myh6	✓	✓	
G3V8B0	Myh7	✓	✓	
A0A0G2JSH9	Prdx2	✓		
Q9EPH8	Pabpc1	✓		
G3V9N0	Pabpc4	✓		
F1LML2	Ubc	✓	✓	✓
Q6IFU9	Krt16			✓
A0A096MJ01	Ldb3	✓		
P11507	Atp2a2	✓	✓	
P29457	Serpinh1	✓	✓	
P06685	Atp1a1	✓	✓	
F1LPM3	Sorbs2	✓		
F1M953	Hspa9	✓	✓	✓
Q7TPB1	Cct4	✓		
Q6P502	Cct3	✓		
P46462	Vcp	✓	✓	
Q60587	Hadhb	✓		

TABLE 2.3. Kinetic fit parameters for cycloheximide pulse-chase data.

	treatment	$t_{1/2}$ (hr)	$t_{1/2}$ 95% CI (hr)	k (hr^{-1}) ± SE	R^2	p value for k comparison
rat MYBPC3(WT)	scrambled siRNA	6.29	4.81 to 9.06	0.110±0.017	0.34	<0.0001*
	HSC70 siRNA	75.6	18.5 to 460	0.0179±0.0089	0.02	
	DMSO vehicle	20.2	14.6 to 32.8	0.0343±0.0067	0.13	<0.0001*
	10µM YM-1	7.59	8.83 to 14.4	0.0913±0.011	0.33	
FLAG-MYBPC3(WT)	scrambled siRNA	5.04	4.21 to 6.37	0.137±0.014	0.57	0.0001*
	HSC70 siRNA	10.7	7.80 to 16.8	0.0651±0.012	0.26	
	DMSO vehicle	13.6	9.71 to 22.8	0.0508±0.010	0.24	<0.0001*
	10µM YM-1	3.04	1.45 to 3.88	0.329±0.057	0.44	
FLAG-MYBPC3 (Ile154Leufs*5)	scrambled siRNA	23.7	12.3 to 87.6	0.0293±0.011	0.06	0.323
	HSC70 siRNA	17.9	12.6 to 31.1	0.0388±0.0083	0.15	
	DMSO vehicle	21.1	10.2 to 99.0	0.0328±0.014	0.05	0.0063*
	10µM YM-1	7.21	5.33 to 11.1	0.0961±0.017	0.23	
FLAG-MYBPC3 (Trp1098*)	scrambled siRNA	4.43	3.43 to 6.24	0.157±0.023	0.35	0.002*
	HSC70 siRNA	11.4	6.38 to 24.5	0.0611±0.019	0.10	
	DMSO vehicle	17.6	11.1 to 42.0	0.0394±0.011	0.09	<0.0001*
	10µM YM-1	2.20	1.70 to 3.09	0.316±0.046	0.72	
FLAG-MYBPC3 (Glu1248_Cys1253dup)	scrambled siRNA	0.548	0.334 to 0.854	1.27±0.25	0.57	0.693
	HSC70 siRNA	0.498	0.396 to 0.619	1.39±0.14	0.81	
	DMSO vehicle	1.58	1.07 to 2.33	0.439±0.070	0.33	0.0539
	10µM YM-1	0.849	0.485 to 1.41	1.23±0.16	0.32	

Abbreviations. $t_{1/2}$: half-life; k: reaction constant; CI: confidence interval; SE: standard error

*p<0.05 for parameter k in first-order decay reaction fit for scrambled vs. HSC70 siRNA or DMSO vehicle vs. 10µM YM-1

2.7 REFERENCES

1. Alfares AA, Kelly MA, McDermott G, Funke BH, Lebo MS, Baxter SB, Shen J, McLaughlin HM, Clark EH, Babb LJ, Cox SW, DePalma SR, Ho CY, Seidman JG, Seidman CE, Rehm HL. Results of clinical genetic testing of 2,912 probands with hypertrophic cardiomyopathy: Expanded panels offer limited additional sensitivity. *Genetics in medicine : official journal of the American College of Medical Genetics*. 2015

2. Arndt V, Dick N, Tawo R, Dreiseidler M, Wenzel D, Hesse M, Furst DO, Saftig P, Saint R, Fleischmann BK, Hoch M, Hohfeld J. Chaperone-assisted selective autophagy is essential for muscle maintenance. *Current biology : CB*. 2010;20:143-148

3. Bonne G, Carrier L, Bercovici J, Cruaud C, Richard P, Hainque B, Gautel M, Labeit S, James M, Beckmann J, Weissenbach J, Vosberg HP, Fiszman M, Komajda M, Schwartz K. Cardiac myosin binding protein-c gene splice acceptor site mutation is associated with familial hypertrophic cardiomyopathy. *Nature genetics*. 1995;11:438-440

4. Carlisle C, Prill K, Pilgrim D. Chaperones and the proteasome system: Regulating the construction and demolition of striated muscle. *International journal of molecular sciences*. 2017;19

5. Coppini R, Ferrantini C, Yao L, Fan P, Del Lungo M, Stillitano F, Sartiani L, Tosi B, Suffredini S, Tesi C, Yacoub M, Olivotto I, Belardinelli L, Poggesi C, Cerbai E, Mugelli A. Late sodium current inhibition reverses electromechanical dysfunction in human hypertrophic cardiomyopathy. *Circulation*. 2013;127:575-584

6. Craig R, Offer G. The location of c-protein in rabbit skeletal muscle. *Proceedings of the Royal Society of London. Series B, Biological sciences*. 1976;192:451-461

7. Fermin D, Basrur V, Yocum AK, Nesvizhskii AI. Abacus: A computational tool for extracting and pre-processing spectral count data for label-free quantitative proteomic analysis. *Proteomics*. 2011;11:1340-1345

8. Geisterfer-Lowrance AA, Kass S, Tanigawa G, Vosberg HP, McKenna W, Seidman CE, Seidman JG. A molecular basis for familial hypertrophic cardiomyopathy: A beta cardiac myosin heavy chain gene missense mutation. *Cell*. 1990;62:999-1006

9. Golenhofen N, Perng MD, Quinlan RA, Drenckhahn D. Comparison of the small heat shock proteins alphab-crystallin, mkbp, hsp25, hsp20, and cvhsp in heart and skeletal muscle. *Histochemistry and cell biology*. 2004;122:415-425

10. Harris SP, Bartley CR, Hacker TA, McDonald KS, Douglas PS, Greaser ML, Powers PA, Moss RL. Hypertrophic cardiomyopathy in cardiac myosin binding protein-c knockout mice. *Circulation research*. 2002;90:594-601

11. Helms AS, Davis FM, Coleman D, Bartolone SN, Glazier AA, Pagani F, Yob JM, Sadayappan S, Pedersen E, Lyons R, Westfall MV, Jones R, Russell MW, Day SM. Sarcomere mutation-specific expression patterns in human hypertrophic cardiomyopathy. *Circulation. Cardiovascular genetics*. 2014;7:434-443

12. Hishiya A, Kitazawa T, Takayama S. Bag3 and hsc70 interact with actin capping protein capz to maintain myofibrillar integrity under mechanical stress. *Circulation research*. 2010;107:1220-1231

13. Ho CY, Lakdawala NK, Cirino AL, Lipshultz SE, Sparks E, Abbasi SA, Kwong RY, Antman EM, Semsarian C, Gonzalez A, Lopez B, Diez J, Orav EJ, Colan SD, Seidman CE. Diltiazem treatment for pre-clinical hypertrophic cardiomyopathy sarcomere mutation carriers: A pilot randomized trial to modify disease expression. *JACC. Heart failure*. 2015;3:180-188

14. Hollander JM, Martin JL, Belke DD, Scott BT, Swanson E, Krishnamoorthy V, Dillmann WH. Overexpression of wild-type heat shock protein 27 and a nonphosphorylatable heat shock protein 27 mutant protects against ischemia/reperfusion injury in a transgenic mouse model. *Circulation*. 2004;110:3544-3552

15. Inagaki N, Hayashi T, Arimura T, Koga Y, Takahashi M, Shibata H, Teraoka K, Chikamori T, Yamashina A, Kimura A. Alpha b-crystallin mutation in dilated cardiomyopathy. *Biochemical and biophysical research communications*. 2006;342:379-386

16. Judge LM, Perez-Bermejo JA, Truong A, Ribeiro AJ, Yoo JC, Jensen CL, Mandegar MA, Huebsch N, Kaake RM, So PL, Srivastava D, Pruitt BL, Krogan NJ, Conklin BR. A bag3 chaperone complex maintains cardiomyocyte function during proteotoxic stress. *JCI insight*. 2017;2

17. Kim YK, Suarez J, Hu Y, McDonough PM, Boer C, Dix DJ, Dillmann WH. Deletion of the inducible 70-kda heat shock protein genes in mice impairs cardiac contractile function and calcium handling associated with hypertrophy. *Circulation*. 2006;113:2589-2597

18. Kimura A, Harada H, Park JE, Nishi H, Satoh M, Takahashi M, Hiroi S, Sasaoka T, Ohbuchi N, Nakamura T, Koyanagi T, Hwang TH, Choo JA, Chung KS, Hasegawa A, Nagai R, Okazaki O, Nakamura H, Matsuzaki M, Sakamoto T,

Toshima H, Koga Y, Imaizumi T, Sasazuki T. Mutations in the cardiac troponin i gene associated with hypertrophic cardiomyopathy. *Nature genetics.* 1997;16:379-382

19. Kotter S, Unger A, Hamdani N, Lang P, Vorgerd M, Nagel-Steger L, Linke WA. Human myocytes are protected from titin aggregation-induced stiffening by small heat shock proteins. *The Journal of cell biology.* 2014;204:187-202

20. Kuo PL, Lee H, Bray MA, Geisse NA, Huang YT, Adams WJ, Sheehy SP, Parker KK. Myocyte shape regulates lateral registry of sarcomeres and contractility. *The American journal of pathology.* 2012;181:2030-2037

21. Li D, Tapscoft T, Gonzalez O, Burch PE, Quinones MA, Zoghbi WA, Hill R, Bachinski LL, Mann DL, Roberts R. Desmin mutation responsible for idiopathic dilated cardiomyopathy. *Circulation.* 1999;100:461-464

22. Li J, Horak KM, Su H, Sanbe A, Robbins J, Wang X. Enhancement of proteasomal function protects against cardiac proteinopathy and ischemia/reperfusion injury in mice. *The Journal of clinical investigation.* 2011;121:3689-3700

23. Ma K, Vitek O, Nesvizhskii AI. A statistical model-building perspective to identification of ms/ms spectra with peptideprophet. *BMC bioinformatics.* 2012;13 Suppl 16:S1

24. Marston S, Copeland O, Jacques A, Livesey K, Tsang V, McKenna WJ, Jalilzadeh S, Carballo S, Redwood C, Watkins H. Evidence from human myectomy samples that mybpc3 mutations cause hypertrophic cardiomyopathy through haploinsufficiency. *Circulation research.* 2009;105:219-222

25. Martin JL, Mestril R, Hilal-Dandan R, Brunton LL, Dillmann WH. Small heat shock proteins and protection against ischemic injury in cardiac myocytes. *Circulation.* 1997;96:4343-4348

26. McDonough H, Patterson C. Chip: A link between the chaperone and proteasome systems. *Cell stress & chaperones.* 2003;8:303-308

27. McLendon PM, Robbins J. Desmin-related cardiomyopathy: An unfolding story. *American journal of physiology. Heart and circulatory physiology.* 2011;301:H1220-1228

28. McNamara JW, Li A, Lal S, Bos JM, Harris SP, van der Velden J, Ackerman MJ, Cooke R, Dos Remedios CG. Mybpc3 mutations are associated with a reduced

super-relaxed state in patients with hypertrophic cardiomyopathy. *PloS one*. 2017;12:e0180064

29.   Mellacheruvu D, Wright Z, Couzens AL, Lambert JP, St-Denis NA, Li T, Miteva YV, Hauri S, Sardiu ME, Low TY, Halim VA, Bagshaw RD, Hubner NC, Al-Hakim A, Bouchard A, Faubert D, Fermin D, Dunham WH, Goudreault M, Lin ZY, Badillo BG, Pawson T, Durocher D, Coulombe B, Aebersold R, Superti-Furga G, Colinge J, Heck AJ, Choi H, Gstaiger M, Mohammed S, Cristea IM, Bennett KL, Washburn MP, Raught B, Ewing RM, Gingras AC, Nesvizhskii AI. The crapome: A contaminant repository for affinity purification-mass spectrometry data. *Nature methods*. 2013;10:730-736

30.   Minoia M, Boncoraglio A, Vinet J, Morelli FF, Brunsting JF, Poletti A, Krom S, Reits E, Kampinga HH, Carra S. Bag3 induces the sequestration of proteasomal clients into cytoplasmic puncta: Implications for a proteasome-to-autophagy switch. *Autophagy*. 2014;10:1603-1621

31.   Mohamed BA, Barakat AZ, Zimmermann WH, Bittner RE, Muhlfeld C, Hunlich M, Engel W, Maier LS, Adham IM. Targeted disruption of hspa4 gene leads to cardiac hypertrophy and fibrosis. *Journal of molecular and cellular cardiology*. 2012;53:459-468

32.   Nag S, Sommese RF, Ujfalusi Z, Combs A, Langer S, Sutton S, Leinwand LA, Geeves MA, Ruppel KM, Spudich JA. Contractility parameters of human beta-cardiac myosin with the hypertrophic cardiomyopathy mutation r403q show loss of motor function. *Science advances*. 2015;1:e1500511

33.   Norton N, Li D, Rieder MJ, Siegfried JD, Rampersaud E, Zuchner S, Mangos S, Gonzalez-Quintana J, Wang L, McGee S, Reiser J, Martin E, Nickerson DA, Hershberger RE. Genome-wide studies of copy number variation and exome sequencing identify rare variants in bag3 as a cause of dilated cardiomyopathy. *American journal of human genetics*. 2011;88:273-282

34.   Olson TM, Doan TP, Kishimoto NY, Whitby FG, Ackerman MJ, Fananapazir L. Inherited and de novo mutations in the cardiac actin gene cause hypertrophic cardiomyopathy. *Journal of molecular and cellular cardiology*. 2000;32:1687-1694

35.   Perng MD, Muchowski PJ, van Den IP, Wu GJ, Hutcheson AM, Clark JI, Quinlan RA. The cardiomyopathy and lens cataract mutation in alphab-crystallin alters its protein structure, chaperone activity, and interaction with intermediate filaments in vitro. *The Journal of biological chemistry*. 1999;274:33235-33243

36.   Pfaffl MW. A new mathematical model for relative quantification in real-time rt-pcr. *Nucleic acids research*. 2001;29:e45

37.   Poetter K, Jiang H, Hassanzadeh S, Master SR, Chang A, Dalakas MC, Rayment I, Sellers JR, Fananapazir L, Epstein ND. Mutations in either the essential or regulatory light chains of myosin are associated with a rare myopathy in human heart and skeletal muscle. *Nature genetics*. 1996;13:63-69

38.   Previs MJ, Beck Previs S, Gulick J, Robbins J, Warshaw DM. Molecular mechanics of cardiac myosin-binding protein c in native thick filaments. *Science (New York, N.Y.)*. 2012;337:1215-1218

39.   Rodriguez JE, Schisler JC, Patterson C, Willis MS. Seek and destroy: The ubiquitin----proteasome system in cardiac disease. *Current hypertension reports*. 2009;11:396-405

40.   Sandri M, Robbins J. Proteotoxicity: An underappreciated pathology in cardiac disease. *Journal of molecular and cellular cardiology*. 2014;71:3-10

41.   Sarikas A, Carrier L, Schenke C, Doll D, Flavigny J, Lindenberg KS, Eschenhagen T, Zolk O. Impairment of the ubiquitin-proteasome system by truncated cardiac myosin binding protein c mutants. *Cardiovascular research*. 2005;66:33-44

42.   Schlossarek S, Englmann DR, Sultan KR, Sauer M, Eschenhagen T, Carrier L. Defective proteolytic systems in mybpc3-targeted mice with cardiac hypertrophy. *Basic research in cardiology*. 2012;107:235

43.   Schlossarek S, Frey N, Carrier L. Ubiquitin-proteasome system and hereditary cardiomyopathies. *Journal of molecular and cellular cardiology*. 2014;71:25-31

44.   Schlossarek S, Schuermann F, Geertz B, Mearini G, Eschenhagen T, Carrier L. Adrenergic stress reveals septal hypertrophy and proteasome impairment in heterozygous mybpc3-targeted knock-in mice. *Journal of muscle research and cell motility*. 2012;33:5-15

45.   Srikakulam R, Winkelmann DA. Chaperone-mediated folding and assembly of myosin in striated muscle. *Journal of cell science*. 2004;117:641-652

46.   Tardiff JC. Sarcomeric proteins and familial hypertrophic cardiomyopathy: Linking mutations in structural proteins to complex cardiovascular phenotypes. *Heart failure reviews*. 2005;10:237-248

47.   Thierfelder L, Watkins H, MacRae C, Lamas R, McKenna W, Vosberg HP, Seidman JG, Seidman CE. Alpha-tropomyosin and cardiac troponin t mutations

cause familial hypertrophic cardiomyopathy: A disease of the sarcomere. *Cell*. 1994;77:701-712

48.   Ulbricht A, Arndt V, Hohfeld J. Chaperone-assisted proteostasis is essential for mechanotransduction in mammalian cells. *Communicative & integrative biology*. 2013;6:e24925

49.   van Dijk SJ, Dooijes D, dos Remedios C, Michels M, Lamers JM, Winegrad S, Schlossarek S, Carrier L, ten Cate FJ, Stienen GJ, van der Velden J. Cardiac myosin-binding protein c mutations and hypertrophic cardiomyopathy: Haploinsufficiency, deranged phosphorylation, and cardiomyocyte dysfunction. *Circulation*. 2009;119:1473-1483

50.   van Dijk SJ, Paalberends ER, Najafi A, Michels M, Sadayappan S, Carrier L, Boontje NM, Kuster DW, van Slegtenhorst M, Dooijes D, dos Remedios C, ten Cate FJ, Stienen GJ, van der Velden J. Contractile dysfunction irrespective of the mutant protein in human hypertrophic cardiomyopathy with normal systolic function. *Circulation. Heart failure*. 2012;5:36-46

51.   Walsh R, Thomson KL, Ware JS, Funke BH, Woodley J, McGuire KJ, Mazzarotto F, Blair E, Seller A, Taylor JC, Minikel EV, Exome Aggregation C, MacArthur DG, Farrall M, Cook SA, Watkins H. Reassessment of mendelian gene pathogenicity using 7,855 cardiomyopathy cases and 60,706 reference samples. *Genetics in medicine : official journal of the American College of Medical Genetics*. 2017;19:192-203

52.   Wang AM, Miyata Y, Klinedinst S, Peng HM, Chua JP, Komiyama T, Li X, Morishima Y, Merry DE, Pratt WB, Osawa Y, Collins CA, Gestwicki JE, Lieberman AP. Activation of hsp70 reduces neurotoxicity by promoting polyglutamine protein degradation. *Nature chemical biology*. 2013;9:112-118

53.   Watkins H, Conner D, Thierfelder L, Jarcho JA, MacRae C, McKenna WJ, Maron BJ, Seidman JG, Seidman CE. Mutations in the cardiac myosin binding protein-c gene on chromosome 11 cause familial hypertrophic cardiomyopathy. *Nature genetics*. 1995;11:434-437

54.   Willis MS, Patterson C. Proteotoxicity and cardiac dysfunction--alzheimer's disease of the heart? *The New England journal of medicine*. 2013;368:455-464

55.   Yu X, Kem DC. Proteasome inhibition during myocardial infarction. *Cardiovascular research*. 2010;85:312-320

56.   Zuiderweg ER, Bertelsen EB, Rousaki A, Mayer MP, Gestwicki JE, Ahmad A. Allostery in the hsp70 chaperone proteins. *Topics in current chemistry*. 2013;328:99-153

CHAPTER 3

Expression of truncated MYBPC3 mutants in the context of normal WT MYBPC3 stoichiometry is not associated with proteotoxicity or hypertrophic remodeling

3.1 ABSTRACT

Although mutations in cardiac myosin binding protein C (MYBPC3) have been known to cause familial hypertrophic cardiomyopathy (HCM) for two decades, debate over the primary pathogenic mechanism in MYBPC3-linked HCM continues. Evidence exists in support of two non-mutually exclusive hypotheses: haploinsufficiency of functional MYBPC3 within the sarcomere, and a "poison peptide" effect of truncated mutant MYBPC3 proteins associated with impaired ubiquitin proteasome system (UPS) function. While haploinsufficient knock-out animal models with no expression of truncated proteins have demonstrated that haploinsufficiency of MYBPC3 is sufficient to cause HCM, few studies have evaluated the "poison peptide" effect in isolation from haploinsufficiency or its consequences on cardiomyocyte protein homeostasis (proteostasis) beyond the proteasome. To determine whether truncated MYBPC3 expression alone directly affects proteostasis and induces hypertrophic left ventricular remodeling, we utilized a neonatal rat ventricular cardiomyocyte (NRVM) culture model and a MYBPC3 transgenic mouse model to identify effects of acute and chronic lifelong

expression of truncated MYBPC3, respectively. We expressed disease-associated truncating MYBPC3 mutations of varying lengths in NRVMs but observed no changes in UPS function or HSP70-family chaperone stress responses associated with any of the five mutants. Further, expression of a ~75kDa truncated protein in transgenic mice was not associated with proteasome dysfunction or deranged proteostasis, and was not sufficient in the context of normal MYBPC3 stoichiometry to produce a hypertrophic cardiac phenotype. Therefore, neither acute nor chronic expression of truncated MYBPC3 protein were capable of disrupting cardiomyocyte proteostasis. These results challenge evidence for the "poison peptide" hypothesis and support the necessity of MYBPC3 haploinsufficiency in HCM pathogenesis.

3.2 Introduction

Hypertrophic cardiomyopathy (HCM), characterized by left ventricular hypertrophy and fibrosis, is the most common monogenetic form of inherited heart disease affecting ~1 in 500 individuals. Patients with HCM are predisposed to heart failure, outflow tract obstruction, arrhythmias, and sudden cardiac death. The most frequently mutated gene in HCM is cardiac myosin binding protein C (*MYBPC3*), accounting for >50% of cases in which the causative gene has been identified [Alfares, 2015]. MYBPC3 is a 150kDa myofilament protein found in the C-zone of the thick filament that interacts with both myosin and actin, acting as a molecular 'brake' on cross-bridge cycling [Previs, 2012]. In contrast to other sarcomere genes which primarily harbor missense mutations, over 90% of MYBPC3 mutations are nonsense, resulting in premature termination and predicted to yield truncated proteins [Alfares, 2015, Tardiff, 2005]. Yet, multiple studies have failed to identify the presence of mutant truncated MYBPC3 in myocardium

92

from HCM patients [Jacques, 2008, Marston, 2009, van Dijk, 2009]. Consequently, the most widely accepted hypothesis regarding the primary pathogenic mechanism in MYBPC3-linked HCM is haploinsufficiency. Nonsense mutant MYBPC3 transcript has been shown to undergo nonsense-mediated decay (NMD), suggesting the majority of mutant transcript is degraded [Vignier, 2009]. However, we have previously shown that in myocardium from patients with MYBPC3-linked HCM, transcript originating from the mutant allele of MYBPC3 is still detectable in sufficient quantities to provide a template for mutant protein synthesis [Helms, 2014]. While the absence of truncated proteins supports a disease mechanism arising from insufficient full-length MYBPC3 within the sarcomere, a contribution from mutant protein expression has not been conclusively excluded.

In several studies using both cell and animal models, expression of truncated mutant MYBPC3 protein was associated with impairment of the ubiquitin proteasome system (UPS), one of the major cellular protein degradation pathways [Sarikas, 2005, Schlossarek, 2012, Schlossarek, 2012]. Deficits in the ubiquitin proteasome system (UPS) have been previously linked to human HCM particularly when caused by truncating mutations in MYBPC3 [Predmore, 2010, Thottakara, 2015]. UPS dysfunction is one indicator that protein homeostasis, or proteostasis, is disrupted. Proteostasis is maintained by several intersecting protein quality control (PQC) networks, and is essential to maintenance of the sarcomere, whose function relies on conservation of the appropriate protein stoichiometry; therefore, proteostasis is critical to cardiac function overall. Where UPS dysfunction and loss of proteostasis fit into the molecular progression of disease in HCM – whether they are a cause or effect of remodeling - is unknown. *In vitro* studies suggest mutant MYBPC3 is sufficient to disrupt UPS function[Bahrudin, 2008, Sarikas, 2005]; additionally,

some *in vivo* models show that it is necessary for development of UPS dysfunction alongside cardiac hypertrophy in heterozygous MYBPC3-mutant mice (but importantly, not necessary for hypertrophy alone)[Schlossarek, 2012, Schlossarek, 2012]. Impaired proteasome activity preceded structural changes in the hearts of these mice, which would indicate that it may be an active contributor to pathogenesis rather than a downstream effect. However, several studies have found that proteasome inhibition intervention is beneficial in mouse models of left ventricular hypertrophy, including pressure overload-induced (transaortic constriction and hypertension), sympathetic stimulation-induced (isoproterenol treatment), and genetic (MYBPC3 mutation), ameliorating structural and functional deficits[Hedhli, 2008, Meiners, 2008, Schlossarek, 2014, Stansfield, 2008]. These findings argue more towards UPS dysfunction being a compensatory effect of hypertrophic remodeling.

The extent to which, if at all, loss of proteostasis acts as a driving mechanism in HCM is an important unanswered question highly pertinent to development of targeted therapeutics for patients with truncating MYBPC3 mutations. Limited work has been done to identify the effects of truncated MYBPC3 protein expression in a non-haploinsufficient model system. Therefore, we sought to determine whether truncated MYBPC3 protein expression is deleterious when WT MYBPC3 is present at normal stoichiometric levels. We hypothesized that expression of truncated MYBPC3 is sufficient to induce stress responses associated with HSP70 chaperones, contributing to UPS impairment and defective proteostasis in cardiomyocytes. To test this hypothesis, we expressed a panel of human MYBPC3 mutations in neonatal rat ventricular cardiomyocytes (NRVMs), and determined effects on HSC70/HSC70 chaperone stress responses and UPS function. Further, we hypothesized that expression of truncated MYBPC3 protein is sufficient to

cause hypertrophic cardiac remodeling *in vitro,* in the absence of haploinsufficiency. To do this, we observed cardiac phenotype over the course of 12 months in transgenic mice expressing a 75kDa truncated MYBPC3 protein on a background with two functional WT MYBPC3 alleles.

We found that expression of truncated MYBPC3 was not associated with proteasome dysfunction, induction of HSP70 expression, or stress-induced translocation of cytosolic HSC70 to the nucleus. Further, transgenic expression of a truncated MYBPC3 protein alongside normal MYBPC3 stoichiometry was not sufficient to cause UPS dysfunction or hypertrophic remodeling in mice up to 12 months of age. These results challenge the hypothesis that HCM-associated truncated MYBPC3 directly disrupts proteostasis, and suggest that UPS dysfunction is not a primary pathogenic mechanism in MYBPC3-linked HCM, but arises secondarily to haploinsufficiency or hypertrophic cardiac remodeling.

3.3 METHODS

3.3.1 Isolation and culture of neonatal rat ventricular cardiomyocytes.

See section 2.3.1

3.3.2 Micropatterning of PDMS coverslips.

See section 2.3.2

3.3.3 Expression of FLAG-tagged WT and truncated MYBPC3 constructs via recombinant adenovirus.

See section 2.3.3

3.3.4 Western Blotting.

Sample preparation, SDS-PAGE, transfer, blocking, and analysis were performed as in section 2.3.7. Primary and secondary antibody solutions were made in 5% milk in PBS-T (0.03% Tween-20). Antibody conditions were as follows: MYBPC3, rabbit polyclonal 1:10000 (custom, provided by Samantha Harris, University of Arizona, Tucson, AZ)[Harris, 2002]; FLAG M2, mouse monoclonal 1:1000 (Sigma-Aldrich F1804); FLAG, rabbit polyclonal 1:500 (Sigma-Aldrich F7425) HSC70, mouse monoclonal 1:500 (Enzo Life Sciences ADI-SPA-815); Hsp70, mouse monoclonal 1:200 (Enzo Life Sciences ADI-SPA-810); GAPDH, rabbit polyclonal 1:1000 (Millipore ABS16); IRDye® 680RD goat anti-mouse IgG 1:5000 (LI-COR 926-68070); IRDye® 800CW goat anti-rabbit IgG 1:5000 (LI-COR 925-32211). Primary antibody incubations were either for 1 hour at room temperature or overnight at 4°C. Secondary antibodies were incubated for 1 hour at room temperature protected from light. For images of blots in figures, all lanes presented are from the same individual blot, but a solid line between adjacent lanes signifies the image is not contiguous. Omitted lanes were of additional experimental replicates.

3.3.5 Immunofluorescence of NRVMs.

Plating, blocking, and mounting were performed as in section 2.3.8. Primary and secondary antibody solutions were made in 5% normal goat serum in PBS. Antibody and staining conditions were as follows: HSC70, mouse monoclonal, 1:200 (Enzo Life Sciences ADI-SPA-815); AlexaFluor 488 phalloidin, 1:1000 (ThermoFisher Scientific); goat anti-mouse IgG Alexa Fluor 594, 1:500 (ThermoFisher Scientific A11005). Primary antibody was incubated for 1 hour at room temperature. Secondary antibody and phalloidin were incubated for 30 minutes at room temperature, protected from light.

Following antibody incubations, cells were incubated with 200ng/mL DAPI in PBS for 10 minutes at room temperature, protected from light.

3.3.6 Flow cytometry analysis of ubiquitin proteasome function.

Un-patterned NRVMs were plated at a density of 4.5×10^5 cells/well in 12-well culture plates. Cells were transduced with WT or truncated MYBPC3 adenovirus at MOI 10, 24 hours after plating. 48 hours following MYBPC3 adenovirus, cells were transduced with GFPu degron adenovirus (provided by XJ Wang, University of South Dakota, Vermillion, SD) at MOI 7.5. GFPu is a fusion protein of the yeast CL1 degron to GFP which acts as a UPS substrate and is constitutively degraded under normal physiological conditions, but accumulates when the UPS is impaired (26). Positive control wells were treated with 25µM proteasome inhibitor lactacystin (Enzo Life Sciences). 24 hours later, NRVMs were dissociated in 0.05% trypsin EDTA (Invitrogen) for 10 minutes at 37°C, washed twice in ice cold PBS with 5% FBS, fixed in 4% paraformaldehyde, and stored at 4°C. Cells were analyzed using an LSRFortessa Cell Analyzer (BD Biosciences). Debris and events larger than single cells were gated out. GFPu signal was detected using a 488nm laser (530/30 filter), and data was processed using FlowJo® software.

3.3.7 Assessment of HSC70 nuclear colocalization.

To determine if mutant MYBPC3 expression affects compartmental localization of HSC70, we performed colocalization analysis of HSC70 and DAPI signals in confocal Z-stack images of nuclei from patterned immunostained NRVMs. NRVMs were plated at a density of 1.5×10^5 cells/coverslip, fixed and immunostained as described above for HSC70 and phalloidin. Z-stack images with a step size of 0.6µm were acquired with a 60X objective using a Nikon A1 confocal laser microscope system. 5-6 individual nuclei

from three random fields per coverslip per condition were subjected to colocalization analysis using NIS Elements Confocal imaging software.

3.3.8 Assessment of HSC70 sarcomere periodicity.

Untreated patterned NRVMs were prepared as described in section 2.3.9. Images of three random fields per coverslip from three biological replicates per condition were acquired with a 60X objective using a Nikon Eclipse Ti-E inverted fluorescence microscope. Image and data analysis were performed as described in section 2.3.9. Image acquisition and data analysis were done under single-blind conditions. Median periods of both HSC70 and phalloidin signals were determined.

3.3.9 Procurement of human heart tissue.

Intraventricular septum samples from HCM patients were collected from tissue excised during septal myectomy, and control tissue was collected from the intraventricular septum of unmatched donor hearts, as described previously [Helms, 2016]. Tissue was snap frozen in liquid N_2 and stored at -80°C. Patient demographic data were recorded at the time of tissue collection, including genotype status determined by clinical genetic testing performed in CLIA approved laboratories. All MYBPC3 HCM samples came from patients with truncating mutations.

3.3.10 Quantitative reverse transcription PCR.

qRT-PCR was used to assess transcript abundance of *HSPA8*/HSC70 and *HSPA1A*/HSP70 in human myocardial tissue. RNA was isolated from tissue using the Qiagen RNeasy Fibrous Tissue Mini kit. The Qiagen Omniscript RT kit was used for generation of cDNA by reverse transcription. TaqMan™ gene expression assays for

human *HSPA8*, *HSPA1A*, *B2M* (β2-microglobulin), and *RPL32* (60S ribosomal protein L32) were used in conjunction TaqMan® Fast Advanced Master Mix and samples were analyzed using an Applied Biosystems® 7500 Fast Real-Time PCR system. β2-microglobulin and RPL32 were used as internal reference genes; data was analyzed as previously described [Pfaffl, 2001].

3.3.11 MYBPC3 transgenic mouse model.

A mouse line expressing a ~75kDa prematurely truncating MYBPC3 transgene on the FVB background was acquired as frozen embryos from Dr. Jeffrey Robbins of Cincinnati Children's Hospital Heart Institute. Transgenic males were bred to wild-type FVB females to produce both wild-type and transgenic littermates. Animals were sacrificed at 3, 6, 9, 12, and 15 months of age, and equivalent numbers of male and female mice were used in experiments. Hearts were collected by perfusing sterile PBS through the left ventricle to flush out blood, and then excised. Tissue allocated for Western blotting and proteasome activity assays was snap frozen in liquid N_2 and stored at -80°. Tissue allocated for other applications was prepared as stated below.

3.3.12 Transgene genotyping.

Forward primer 5'-TGTCAGCCTTCAACAAGAAGCCAAG-3' and reverse primer 5'-CTTCAGGACTTGAGACACTTTCTTC-3' were used to generate PCR products from genomic DNA isolated from tail snips. With electrophoresis using 1% agarose gel, WT (Ntg) DNA produced an 800bp product, while MYBPC transgenic (Tg) DNA produced a 366bp product.

3.3.13 Echocardiography.

Cardiac function in a cohort of wild-type and transgenic animals was assessed by echocardiography at 3, 6, 9 ,12, and 15 months of age by the University of Michigan Physiology Phenotyping core.

3.3.14 Histology.

PBS-perfused murine hearts were preserved in Tissue-Tek™ O.C.T.embedding medium (Sakura Finetek USA) at -80°. Heart tissue was sectioned at a thickness of 5µm and mounted on glass slides. Haematoxylin & Eosin staining was used to determine myocyte cross-sectional area, and Masson Trichrome staining was used to mark areas of interstitial fibrosis. Level of fibrosis was determined in ImageJ using a binary mask with a set background threshold to detect blue-stained depositions of collagen. Extent of fibrosis was defined as the percent area of the field of view above the set threshold for detection. Images were acquired using a Nikon Ti-E Inverted microscope with color camera and taken at 20X magnification. For fibrosis quantification, ImageJ software was used to generate a binary mask over blue-stained fibrotic regions, from which the masked area as a percent of the total image was calculated.

3.3.15 Electron Microscopy.

To prepare tissue for EM, mice were first perfused with PBS and then with a solution of 2% glutaraldehyde (EM grade, Sigma-Aldrich) and 2% paraformaldehyde (EM grade, Sigma-Aldrich) in 0.1M Sorensen's phosphate buffer, pH7.4. Fixed hearts were excised and submerged in glutaraldehyde/paraformaldehyde fixative solution. 1mm^3 pieces of tissue were dissected from the left ventricular free wall and intraventricular septum and stored in fixative solution at 4°C prior to further processing. Samples were

rinsed three times in 0.1M Sorensen's phosphate buffer for 15 minutes each, followed by post fixation in 1% osmium tetroxide in 0.1M Sorensen's buffer for one hour at room temperature. After three additional 15-minute rinses in 0.1M Sorensen's buffer, samples were dehydrated in increasingly concentrated acetone solutions for 5 minutes (1x25, 1x50, 1x70, 1x95, 2x100% acetone). Tissue was embedded using Embed 812 resin (Thermo Fisher) and polymerized at 60°C for 24 hours. 70nm sections were cut using an ultra-microtome, placed on 200 mesh fine bar hex grids and stained with uranyl acetate and lead citrate. Tissue was imaged using a Jeol JEM-1400 transmission electron microscope.

3.3.16 Proteasome chymotrypsin-like activity assay.

Mouse myocardial tissue (50-60mg) was homogenized in proteasome assay buffer (50mM HEPES pH7.5, 20mM KCl, 5mM $MgCl_2$, 1mM Dithiothreitol), on ice. Homogenate was centrifuged for 10 minutes at 10,000g at 4°C. Supernatant was retained and used to determine protein concentration using the Bradford assay (Bio-Rad). Serial dilutions of ATP were prepared in 25mM HEPES pH7.5 (50, 28, 14, 7 and 3.5μM). Each sample was analyzed in triplicate in an opaque black 96-well plate with 200μL assay buffer, 10uL ATP dilution, and 20μL protein sample. 10μL 0.45mM lactacystin proteasome inhibitor (Enzo LifeSciences) was used to determine background non-proteasomal signal. 10μL of 0.45mM Suc-LLVY-AMC substrate (Enzo LifeSciences) was mixed with each reaction well and plate was protected from light until analysis. A SpectraMax® multi-mode microplate reader programmed to read 380nm excitation/440nm emission data every minute for 45 minutes at 37°C was used to collect results. Background signal was

101

subtracted from the averaged signal from triplicate wells. Data is reported as relative fluorescence vs. [ATP].

3.3.17 Statistics

Statistical analysis was done using GraphPad Prism software. Kruskal-Wallis nonparametric one-way ANOVA with Dunn's post hoc test for multiple comparisons were used for data with ≥3 groups. Student's t test was used for data with 2 groups. Outliers excluded from analysis were identified using GraphPad Prism's ROUT method with a Q coefficient of 1%. p-values of <0.05 were considered statistically significant. Data is reported as mean±SEM unless otherwise noted.

3.4 RESULTS

3.4.1 Expression of mutant MYBPC3 in NRVMs does not disrupt ubiquitin proteasome system function.

Expression of truncated mutant MYBPC3 in vitro has been previously shown to impair UPS function[Sarikas, 2005]. We used the fluorescent degron reporter GFPu to assay the effect of mutant MYBPC3 expression on UPS function. GFPu accumulates when the UPS is impaired[Kumarapeli, 2005]. The proteasome inhibitor lactacystin was used as a positive control. While some MYBPC3 mutants showed increased GFPu signal compared to untransduced NRVMs, none of the MYBPC3 mutants significantly induced GFPu accumulation compared to cells expressing WT MYBPC3 (Figure 3.1A,B). Lactacystin treatment clearly blocked degradation of adenovirally-expressed MYBPC3 proteins (Figure 3.1C), but there was no apparent direct effect of mutant MYBPC3 on UPS function.

3.4.2 Mutant MYBPC3 expression is not associated with stress-induced HSP70 expression or HSC70 nuclear translocation.

HSP70 chaperones have well-characterized roles in cellular stress responses, most notably in the cytoplasmic heat shock response [Kregel, 2002]. In order to determine whether mutant MYBPC3 expression affected established signs of protein folding stress associated with HSP70 chaperones, we assessed HSP70 and HSC70 expression levels and localization following WT and mutant MYBPC3 expression. Elevation of HSP70 mRNA and protein levels occurs as part of the heat shock response pathway and during other challenges to proteostasis [Kregel, 2002]. We found no significant differences in HSP70 protein in NRVMs expressing mutant MYBPC3. HSP70 exhibited very low expression levels in NRVMs and was only significantly elevated in cells heat shocked for 1 hour at 45°C (Figure 3.2A). HSC70 protein was not significantly affected by either mutant MYBPC3 expression or heat shock (Figure 3.2B). While HSC70 is constitutively expressed under both baseline and stress conditions, it is known to undergo nuclear translocation in response to heat stress [Adhikari, 2004, Kodiha, 2005]. HSC70 has been shown to translocate in complex with heat shock factor 1 (HSF-1) and regulates HSF-1 mediated transcriptional activity [Ahn, 2005]. We performed colocalization analysis of HSC70 and DAPI signals using confocal microscopy to determine if mutant MYBPC3 expression affected compartmental localization of HSC70. In both control and mutant MYBPC3-expressing cells, HSC70 was present in concentrated areas within nuclei, likely nucleoli (Figure 3.3). However, nuclear localization of HSC70 significantly increased only in heat shocked NRVMs (Figure 3.2C,D). Overall, mutant MYBPC3 was not associated with the typical responses of HSP70 and HSC70 to protein folding stress.

3.4.3 Sarcomere localization of HSC70 in NRVMs expressing truncated MYBPC3

We previously determined that HSC70 is expressed in the sarcomere in NRVMs and occurs at approximately 1μM intervals, corresponding to the M-line and Z-disk (see section 2.4.5). and HSC70 was not disrupted by expression of mutant MYBPC3, suggesting no effect on the periodicity of HSC70 localization in the sarcomere (Figure 3.4).

3.4.4 Transcript and protein abundance for HSP70 and HSC70 are not upregulated in human HCM.

Our *in vitro* studies did not indicate a direct effect of acute truncated MYBPC3 expression on levels of HSP70 chaperone proteins. However, because HCM is a chronic disease, expression of these chaperones could be altered over time as a secondary effect of the primary pathogenic mechanism. To determine whether HSP70 chaperones may be upregulated in HCM patients with MYBPC3 mutations, we measured transcript and protein abundance of HSP70 and HSC70 in patient myocardial tissue samples collected following surgical myectomy of portions of the intraventricular septum. MYBPC3 mutation samples, which all came from patients with truncating mutation genotypes, to tissue from healthy donors, were compared to MYH7 mutation samples and samples with undetermined mutations not in any sarcomere protein. Transcript levels were normalized two separate housekeeping genes: β-2 microglobulin (*B2M*) and 60S ribosomal protein L32 (*RPL32*). No change in *HSPA1A* transcript was observed among the experimental groups when normalized to either housekeeping gene (Figure 3.5A). HSPA8 transcript also showed no change when normalized to *B2M*; however, when normalized to *RPL32*,

transcript abundance in all three HCM groups was significantly reduced to approximately 50% of donor controls (Figure 3.5B). Protein expression of neither HSP70 nor HSC70 was significantly affected in any HCM group as measured by Western blot (Figure 3.5C-E) and mass spectrometry (Figure 3.5F).

3.4.5 Stable expression of a truncated MYBPC3 protein does not induce a hypertrophic cardiac phenotype in mice.

Previous animal studies have explored the effect of MYBPC3 mutations on whole heart physiology in a context of haploinsufficiency or complete absence of WT MYBPC3. This has made it difficult to tease out which effects, if any, may result from the potential presence of truncated protein rather than pure MYBPC3 haploinsufficiency. To explore whether the presence of truncated MYBPC3 is sufficient to cause hypertrophic remodeling, we utilized a murine model expressing a mutant MYBPC3 transgene under control of the αMyHC promoter on a background of full WT MYBPC3 expression. The transgene produces stable cardiac-specific expression of a 75kDa truncated MYBPC3 protein which is readily detectable by Western blot and is not rapidly cleared as in human HCM. Cardiac performance in a cohort of both male and female transgenic (MYBPC3 Tg) and nontransgenic (Ntg) mice was assessed by echocardiography at three-month intervals, starting at 3 months and ending at 12 months of age. A complete summary of the echocardiogram data can be found in Table 3.1. Parameters indicative of ventricular hypertrophy such as intraventricular septum thickness, LV posterior wall thickness, and LV mass showed no statistically significant differences between Ntg and MYBPC3 Tg mice at any age, demonstrating absence of hypertrophic remodeling (Figure 3.6A-F). In fact, LV posterior wall thickness was slightly but significantly lower in MYBPC3 Tg mice

versus Ntg mice. The ratio of heart weight to body weight determined at time of sacrifice (12 months) was also unchanged. Additionally, functional measures including ejection fraction and fractional shortening were not significantly affected at any age, although both parameters showed a trend toward decreasing in MYBPC3 Tg mice at 12 months (p≈0.07) (Figure 3.6G,H). Finally, the left atrium showed a slight trend toward increased size in 12-month old MYBPC3 Tg mice (p≈0.085) (Figure 3.6I). Although not statistically significant, these three parameters may be indicative of the beginnings of diastolic dysfunction, a key symptom in HCM. Nevertheless, these findings overall suggest expression of truncated MYBPC3 protein is insufficient on its own to be a primary pathogenic mechanism in hypertrophic cardiomyopathy.

3.4.6 Transgenic expression of truncated MYBPC3 in mice is not associated with tissue- or ultrastructural-level disarray.

We sought to ascertain whether hallmarks of HCM could be present at the tissue and subcellular level despite the absence of a whole-organ phenotype in MYBPC Tg mice. Pursuant to this goal we assessed cardiomyocyte size, myocardial disarray, and interstitial fibrosis in histological sections of myocardium from MYBPC3 Tg and Ntg mice at 9. Cardiomyocyte size and disarray were observed from hæmatoxylin & eosin-stained sections, while fibrosis was quantified using Masson trichrome-stained sections. We found no differences in any of these aspects between MYBPC3 Tg and Ntg mice from ages 3 to 12 months (Figure 3.7A). Next, ultrastructural sarcomere organization was observed using transmission electron microscopy. Myofibrillar disorganization and misalignment of Z-disks has been observed previously in HCM[Maron, 1979, Razzaque, 2013]. Images were collected from myocardium of two male and two female mice of each

genotype aged 9 months (Figure 3.7B). Both MYBPC3 Tg and Ntg mice had neatly packed sarcomeres and few out-of-register Z-disks. Furthermore, no conspicuous granular or filamentous cytosolic aggregates were seen in MYBPC3 Tg myocardium, as are observed in desmin- or α-B crystallin-associated cardiomyopathy[Inagaki, 2006, McLendon, 2011, Perng, 1999]. The tissue and ultrastructural findings indicate that expression of the truncated MYBPC3 protein is also insufficient to cause pathological tissue or myofibrillar disorganization consistent with hypertrophic remodeling or loss of sarcomere proteostasis.

3.4.7 Ubiquitin proteasome function is not impaired in truncated MYBPC3 transgenic mice.

Lastly, we aimed to determine whether expression of the truncated MYBPC3 transgene was associated with impaired proteasome activity similar to that observed in previous studies of human HCM myocardium[Predmore, 2010, Thottakara, 2015]. We utilized an optimized assay to measure proteasome activity in tissue homogenate by detecting cleavage of a fluorophore from a short peptide substrate by the chymotrypsin-like catalytic proteasome subunit (PSMB5/β5)[Powell, 2007]. Ventricular myocardium of n=18 MYBPC3 Tg mice and n=14 Ntg mice aged 9-12 months was homogenized. Proteasome activity in MYBPC3 Tg ventricular myocardium was not significantly different from activity in Ntg myocardium (Figure 3.7). Therefore, chronic expression of a substantial amount of truncated MYBPC3 protein *in vivo* does not reproduce the proteasome dysfunction found in HCM patients.

3.5 DISCUSSION

The major findings of this study are the following: (i) expression of truncated mutant MYBPC3 in NRVMs did not induce UPS dysfunction, heat-shock response-associated HSP70 expression, or HSC70 nuclear translocation; (ii) stable expression of a truncated MYBPC3 mutant without accompanying haploinsufficiency *in vivo* is not sufficient to elicit cardiac hypertrophy in mice; and (iii) expression of HSP70 chaperones is not altered in myocardium from HCM patients. These results challenge previous findings that truncated MYBPC3 protein is sufficient to disrupt proteostasis in cardiomyocytes, and that truncated MYBPC3 may be directly responsible for UPS dysfunction observed in HCM patients[Bahrudin, 2008, Sarikas, 2005, Schlossarek, 2012, Schlossarek, 2012]. Instead, they suggest that defective proteostasis and proteasome impairment in HCM are downstream consequences of cardiac remodeling, most likely induced by haploinsufficiency of WT MYBPC3.

Two non-mutually exclusive hypotheses to explain pathogenesis in HCM caused by nonsense mutations in MYBPC3 have been proposed: haploinsufficiency of functional MYBPC3[Marston, 2012], and a "poison peptide" effect associated with truncated MYBPC3[Schlossarek, 2014]. Evidence supporting the existence of MYBPC3 haploinsufficiency in patients is strong, but a precise mechanism tying haploinsufficiency to activation of hypertrophic signaling and remodeling is less so. To date, truncated MYBPC3 mutant protein has not been identified in myocardial tissue from HCM patients [Jacques, 2008, Marston, 2009, van Dijk, 2009]. Furthermore, several studies have identified reduced expression of WT MYBPC3 in patients with nonsense mutations in *MYBPC3* [Marston, 2009, van Dijk, 2009, van Dijk, 2012]. Functionally, ablation of MYBPC3 in cardiac muscle fibers causes destabilization of

the myosin super-relaxed conformation[McNamara, 2017, McNamara, 2016], and increased myofilament calcium sensitivity [Stelzer, 2006], which has been linked to diastolic dysfunction both in patient studies and mouse models of HCM [Fraysse, 2012, van Dijk, 2012]. These findings suggest that in patients with MYBPC3 nonsense mutations, truncated MYBPC3 is absent and WT MYBPC3 levels may be insufficient to maintain normal contractile function, energy balance, and calcium sensitivity, leading to diastolic dysfunction, a defining feature of HCM. It is known that nonsense mutant transcript is removed by via nonsense-mediated decay (NMD) [van Dijk, 2009, Vignier, 2009]. However, we have previously found that some nonsense MYBPC3 transcripts escape NMD to varying degrees across individual patients [Helms, 2014]. Therefore, any truncated protein that is translated is likely degraded soon after. Consistent with prior studies [Sarikas, 2005, Vignier, 2009], we observed that truncated MYBPC3 is degraded by the UPS, and that several mutants maintained significantly lower steady-state expression compared to WT MYBPC3.

Evidence for truncated MYBPC3 exhibiting a "poison peptide" effect has been suggested based on observations of UPS dysfunction in human HCM [Predmore, 2010, Thottakara, 2015], mutant MYBPC3 mouse models [Schlossarek, 2012, Schlossarek, 2012], and in vitro expression of truncated MYBPC3 [Sarikas, 2005]. Whether UPS dysfunction is directly associated with a burden imposed on protein quality control by truncated MYBPC3 or indirectly due to adverse remodeling in HCM is unresolved. Our *in vitro* experimental system allowed us to study the acute effect of mutant MYBPC3 on UPS function in a context of normal total MYBPC3 expression and intact sarcomere structure, in the absence of remodeling. We found that expression of mutant MYBPC3 did not induce UPS dysfunction when compared to expression of FLAG-WT MYBPC3 in NRVMs. This is in contrast with a

previous finding which observed accumulation of a Ub^{G76V}-DSRed degron reporter associated with expression of a 40kDa truncated MYBPC3 protein in NRVMs, despite similar experimental conditions [Sarikas, 2005]. Several differences between this and the present study may explain the divergent results. First, of the two mutants tested in the prior study, which both localized to the cytosol, only the shorter one (truncation in C1) caused degron accumulation as measured by flow cytometry. The mutant we tested which was most similar (truncation in the C0-C1 linker) showed primarily nuclear localization, and may not be degraded by cytosolic UPS machinery. Additionally, the prior study showed formation of ubiquitin-positive cytosolic MYBPC3 aggregates in some NRVMs expressing the shorter mutant, while we did not observe aggregates associated with any of the five mutants tested. Therefore, proteasomal burden of mutant MYBPC3 may be dependent on the severity of truncation and subcellular localization.

HSP70 expression can be induced in myocytes by hypertrophic stimuli, and can in turn regulate hypertrophic signaling, for example by activating histone deacetylase-2[Kee, 2008, Osaki, 1998]. Therefore, elevated HSP70 as a result of protein folding stress associated with truncated MYBPC3 could contribute to remodeling. However, we also found no correlation between expression of mutant MYBPC3 and changes in expression or subcellular localization of HSP70 and HSC70. These findings indicate that expression of truncated MYBPC3 by itself, even well above the sub-threshold expression in human HCM, likely does not represent an acute challenge to proteostasis, at least in the presence of WT MYBPC3. It is notable that even the highest expression levels of WT or mutant MYBPC3 did not induce UPS dysfunction, HSP70 induction or HSC70 nuclear translocation, suggesting that the source of proteasome insufficiency in HCM is not direct

effect of mutant MYBPC3 expression. Additionally, the absence of any marked protein folding stress response suggests that the interaction between MYBPC3 and HSC70 explored in Chapter 2 is important for normal physiologic regulation of MYBPC3 expression. Nevertheless, it is possible that proteotoxic effects may arise from long-term expression over the course of a patient's lifetime. Indeed, UPS impairment in mutant MYBPC3 knock-in mice was not observed until one year of age [Schlossarek, 2012]. However, these heterozygous knock-in mice expressed MYBPC3 at ~80% of WT control levels, and thus did not allow differentiation between effects associated with reduced MYBPC3 expression versus presence of a truncated protein.

To further dissect the possible contribution of a "poison peptide" mechanism in MYBPC3-linked HCM over a longer period of time, we utilized a mouse model carrying a truncating MYBPC3 mutant transgene along with two functioning endogenous WT MYBPC3 alleles. This model was previously characterized and the ~75kDa transgene product was found to be stable and expressed at levels similar to endogenous MYBPC3, with poor sarcomere incorporation[Yang, 1998]. We initially hypothesized that high expression of the truncated protein without a decrease in WT MYBPC3 would be associated with left ventricular remodeling, preceded by UPS dysfunction, implying that loss of proteostasis is an instigating mechanism in HCM. However, after comprehensive echocardiographic, histological and ultrastructural analysis, we observed neither cardiac remodeling nor UPS dysfunction in this mouse model at 9-12 months of age. Only non-significant trends in ejection fraction, fractional shortening, and left atrial diameter at 12 months hinted at any phenotype. As such, while this data reinforces the findings from our *in vitro* model system, we can make no conclusions from this study about whether impaired myocyte

111

proteostasis is a cause or effect of cardiac hypertrophy. The study by Schlossarek et. al. reported reduced chymotrypsin-like proteasome activity in heterozygous knock-in mice at 1 year, while HW/BW ratio was already significantly larger compared to WT mice at 9 weeks. Interestingly, also at 9 weeks steady-state levels of ubiquitinated protein were elevated and chymotrypsin-, trypsin- and caspase-like proteasome activities were increased. Additionally, proteasome activity showed positive correlation with HW/BW ratio. One explanation put forward for increased proteasome activity occurring early in disease development suggests that proteasome subunits are upregulated in order to facilitate increased protein turnover during hypertrophy as well as routine maintenance of proteostasis[Su, 2010]. This hypothesis suggests initiation of hypertrophic remodeling places an additional burden on the UPS and other PQC pathways, which ultimately disrupts proteostasis and overloads the proteasome as HCM progresses over many years. It also leaves open the possibility that the necessity to degrade any translated truncated MYBPC3 proteins could exacerbate this burden and contribute to pathogenesis, though likely only subsequent to haploinsufficiency-induced hypertrophy. Overall, our *in vivo* data are more supportive of the idea that UPS dysfunction in HCM is an indirect consequence of pathological cardiac remodeling as has been observed for other forms of cardiomyopathy and heart failure[Day, 2013, Fessart, 2014, Gilda, 2017].

Finally, we investigated transcript and protein expression of HSP70 and HSC70 in myocardium from HCM patients with truncating MYBPC3 mutations. Our lab has previously observed significant UPS impairment in patients with similar genotypes[Predmore, 2010]. Nonetheless, expression of upstream chaperones was unchanged compared to healthy donor hearts or myocardium from HCM patients with non-sarcomere gene

112

mutations. This may indicate that in cardiomyocytes, the UPS is particularly vulnerable to functional insufficiency compared to other branches of PQC pathways such as the chaperone network, because the proteasome is responsible for degradation of most major sarcomere proteins[Mitch, 1996, Solomon, 1996]. However, the HSP70-family represents only one class of chaperones involved in cardiomyocyte proteostasis, and other groups, such as the small heat shock proteins, may be more significantly affected.

In conclusion, the results of this study challenge the viability of the "poison peptide" hypothesis of HCM pathogenesis. In contrast to previously reported findings, expression of truncated MYBPC3 did not compromise proteostasis *in vitro* or *in vivo.* Furthermore, we found that truncated MYBPC3 expression alone is not sufficient to provoke a hypertrophic cardiac phenotype in mice and is likely not a key root of pathogenesis. The mechanistic origin of UPS dysfunction in HCM remains unknown, and further studies are required to understand the role of proteostasis in this enigmatic disease.

3.6 ACKNOWLEDGEMENTS

FIGURE 3.1

Figure 3.1. Expression of MYBPC3 mutants does not significantly affect ubiquitin proteasome function as assessed by the degron reporter GFPu. *(A)* Representative flow cytometry density plots. x-axis: GFPu fluorescence; y-axis: side scatter area (SSC-A). Data in the boxed area indicates GFP-positive cells. *(B)* Quantification of GFPu expression. Data is normalized to % GFPu-positive cells for control (untransduced) NRVMs. Mean±SEM, n≥11. Kruskal-Wallis one-way ANOVA p<0.0001. *p<0.05 vs control, Dunn's test for multiple comparisons. *(C)* Representative Western blot of NRVMs expressing MYBPC3 constructs ± treatment with 25µM proteasome inhibitor lactacystin. Black line between lanes indicates noncontiguous samples from the same blot. Lactacystin treatment resulted in significant accumulation of FLAG-MYBPC3, while endogenous rat WT MYBPC3 levels were not significantly affected. This indicates that the ubiquitin proteasome system is able to handle a high rate of truncated FLAG-MYBPC3 turnover without being impaired.

FIGURE 3.2
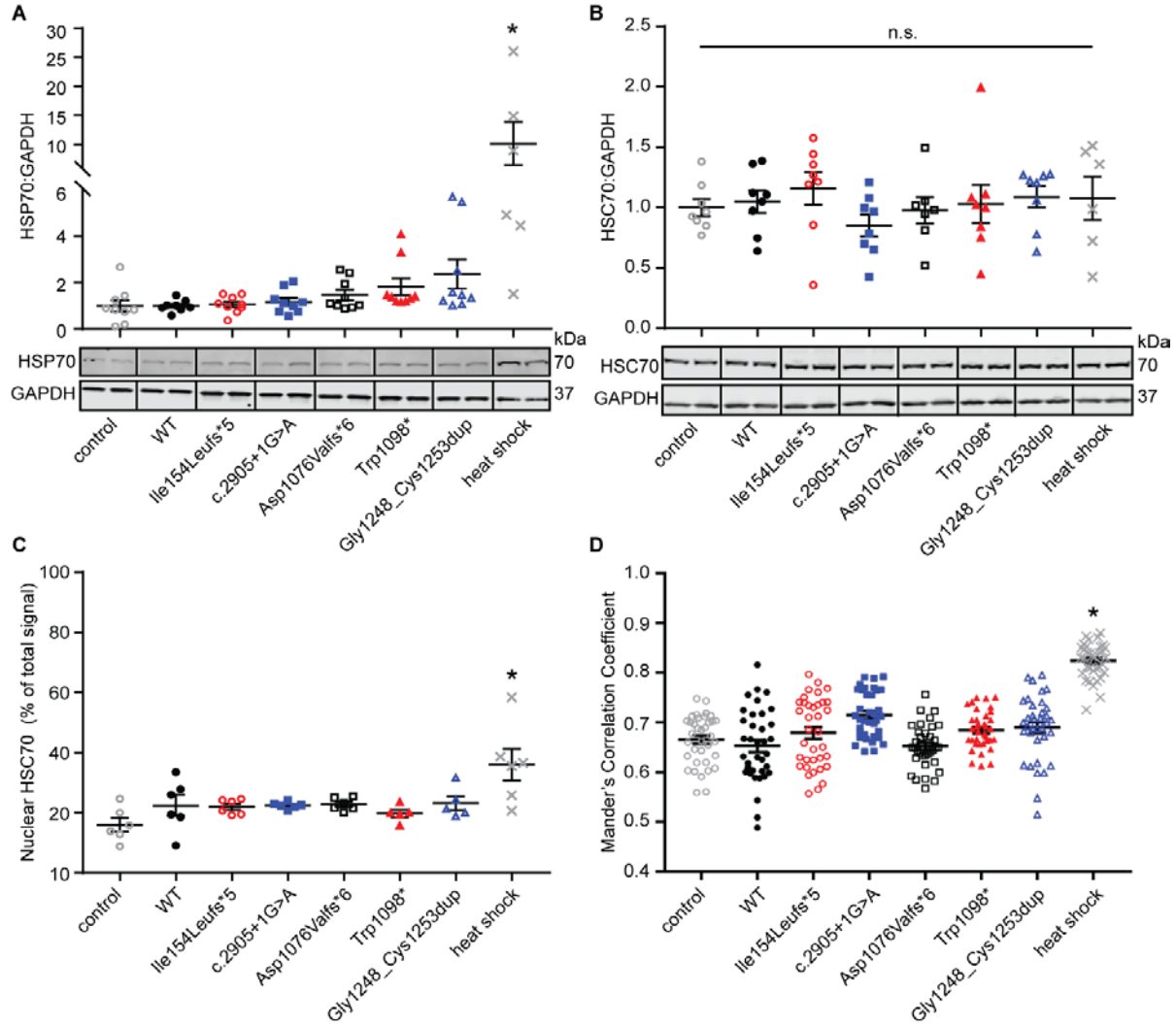
Figure 3.2. Mutant MYBPC3 expression in NRVMs does not induce HSP70 upregulation or HSC70 nuclear translocation. *(A)* Quantification and representative Western blot for HSP70 (stress-inducible). HSP70 protein levels were only significantly elevated in NRVMs heat shocked for 1 hour at 45°C. n≥6, Kruskal-Wallis one way ANOVA p=0.003. *p<0.05 vs control, Dunn's test for multiple comparisons. Mean±SEM. *(B)* Quantification and representative Western blot for HSC70. HSC70 protein levels were consistent across all conditions. n≥6, Kruskal-Wallis one-way ANOVA p=0.48. Mean±SEM. *(C)* Immunofluorescence-based Quantification of HSC70 signal localized to DAPI-positive areas as a percent of total signal. Only heat shocked cells showed significantly increased nuclear localization of HSC70. n≥5 fields of view, Kruskal-Wallis one way ANOVA p=0.021. *p<0.05 vs control, Dunn's test for multiple comparisons. Mean±SEM. *(D)* Mander's correlation coefficient between DAPI and HSC70 signals for n=36 nuclei per condition. Kruskal-Wallis one-way ANOVA p<0.0001. *p<0.05 vs control, Dunn's Dunn's test for multiple comparisons. Mean±SEM. Black line between lanes indicates noncontiguous samples from the same blot.

FIGURE 3.3
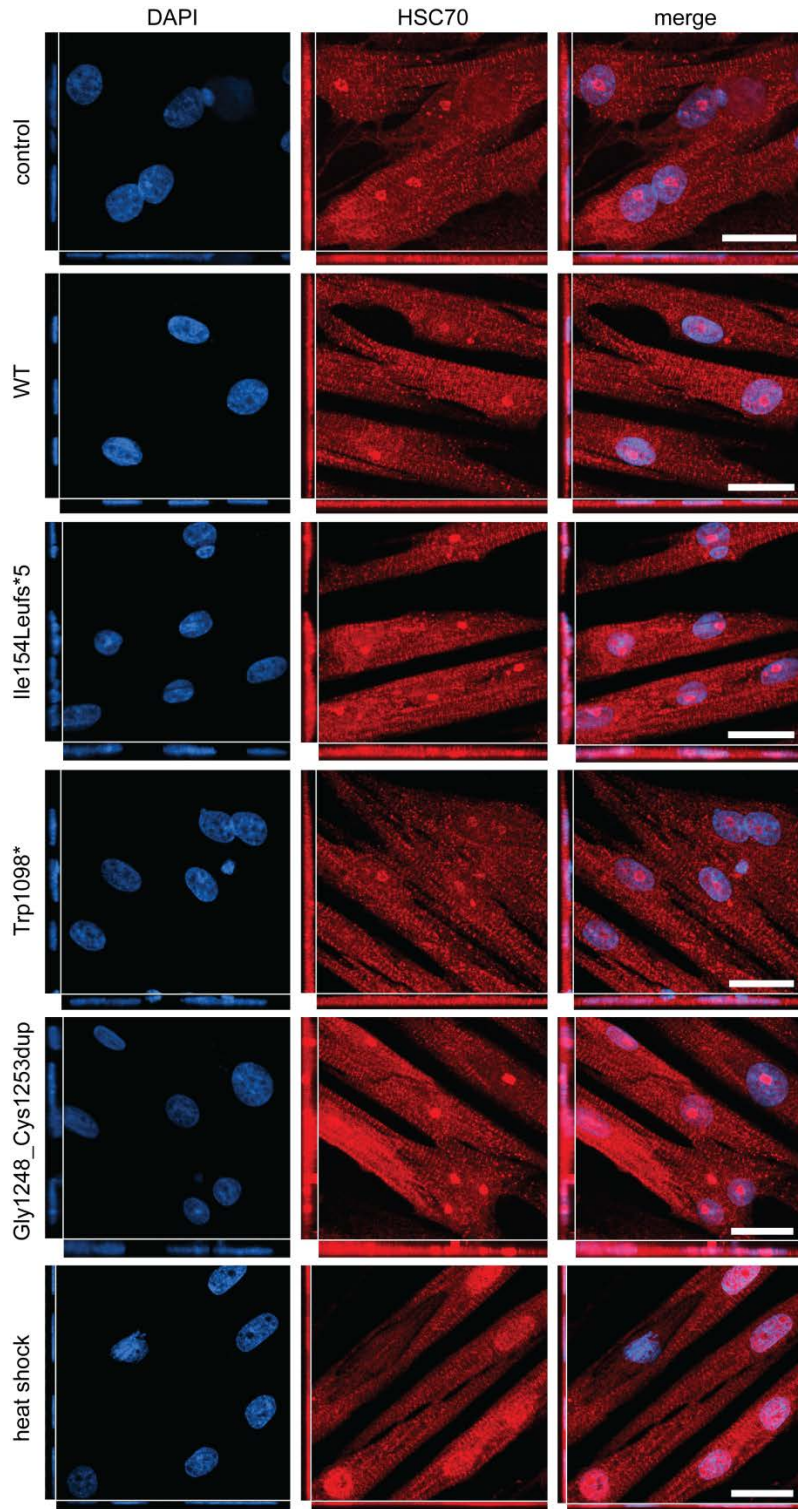
Figure 3.3. Representative confocal images with Z-projections of patterned NRVMs immunostained for HSC70. Z-plane step size of 0.6µm. Scale bar = 20µm, 60X magnification. Only heat shock caused marked nuclear translocation of HSC70.

FIGURE 3.4
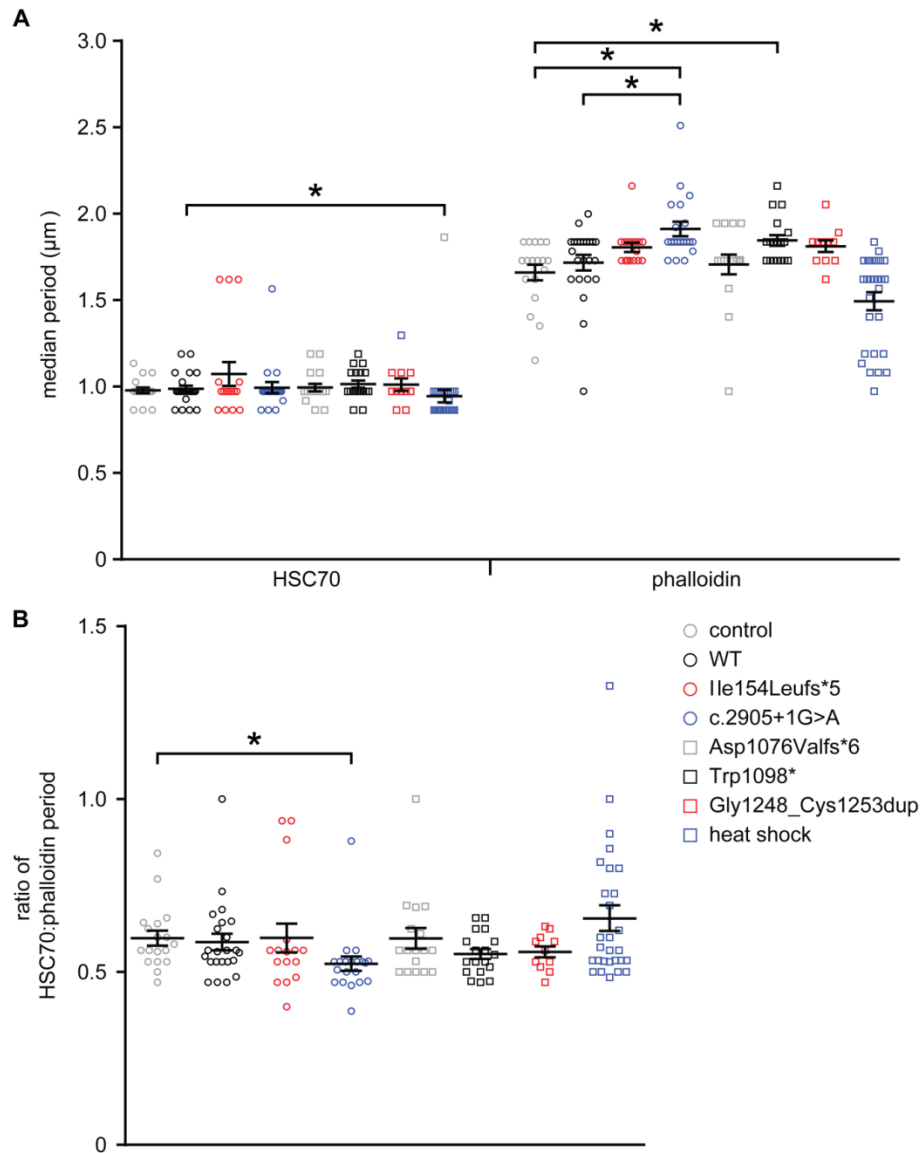
Figure 3.4. Mutant MYBPC3 protein expression does not alter HSC70 sarcomere periodicity. *(A)* Frequency of HSC70 and phalloidin peaks in untreated control vs. FLAG-MYBPC3 adenovirus treated and heat shocked NRVMs, determined by fast Fourier transform analyses on fluorescent intensity profiles. HSC70 frequency was not significantly affected by mutant MYBPC3 protein expression or heat shock. *(B)* Only cells expressing the c.2905+1G>A mutant showed a significantly altered ratio of HSC70 frequency to phalloidin frequency when compared to untreated cells, but not FLAG-WT treated cells. Kruskal-Wallis one-way ANOVA with Dunn's test for multiple comparisons, *p<0.05. Mean±SEM. n≥16 cells per condition.

FIGURE 3.5
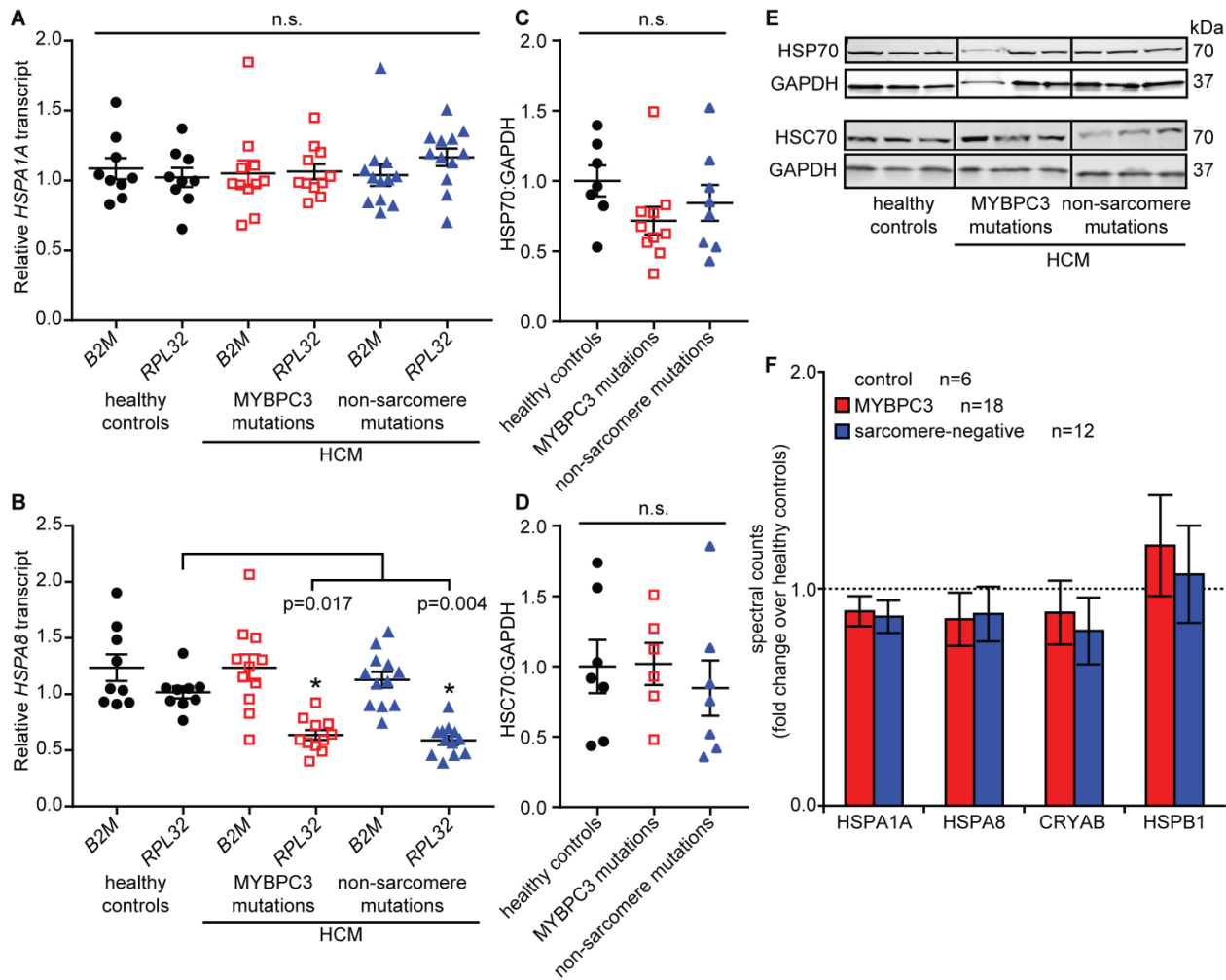
Figure 3.5. HSP70 and HSC70 transcript and protein are not upregulated in human MYBPC3-linked HCM. *(A)* HSP70 (*HSPA1A*) transcript and *(C)* protein abundance in human myocardial tissue from donor controls and HCM patients (septal myectomy samples). *HSPA1A* mRNA abundance was normalized to two different internal reference genes (β2-microglobulin/*B2M* and 60S ribosomal protein L32/*RPL32*). No significant differences in HSP70 mRNA or protein were observed in tissue samples from HCM patients with *MYBPC3* mutations compared to controls or HCM patients with no identified sarcomere gene mutations. Mean±SEM, Kruskal Wallis one-way ANOVA p>0.05. *(B)* HSC70 (*HSPA8*) mRNA and *(D)* protein abundance. No differences in HSC70 protein expression were observed. *HSPA8* mRNA was significantly reduced in both MYBPC3 and sarcomere-mutation negative HCM samples when normalized to *RPL32*, but not *B2M*. Mean±SEM, Kruskal Wallis one-way ANOVA; *p<0.0001, Dunn's test for multiple comparisons. (*E*) Representative Western blots for HSP70 and HSC70. Black line between lanes indicates noncontiguous samples from the same blot. For transcripts, healthy control n=11, MYBPC3 mutations n=11, non-sarcomere mutations n=12. For HSP70 protein, healthy control n=7, MYBPC3 mutations n=10, non-sarcomere mutations n=18. For HSC70 protein, healthy control n=7, MYBPC3 mutations n=6, non-sarcomere mutations n=7. *(F)* Quantitative mass spectrometry of key chaperones from MYBPC3-linked and sarcomere gene mutation-negative HCM myectomy samples. Bars represent fold change in spectral counts over mean abundance in healthy control samples, indicated by dotted line.

FIGURE 3.6
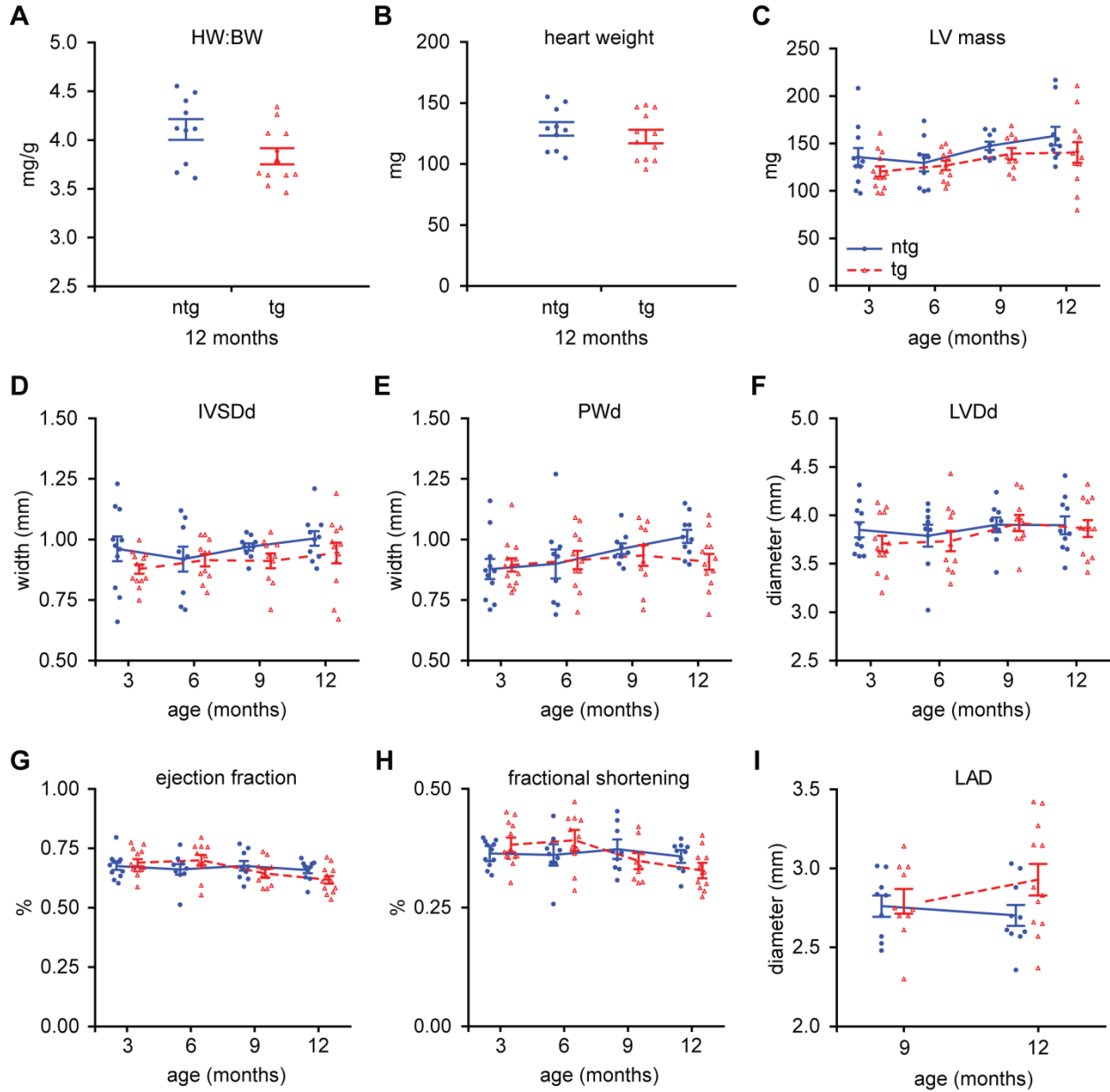
Figure 3.6. Echocardiograms show absence of hypertrophic phenotype in truncated MYBPC3 transgenic mice compared to non-transgenic mice. *(A)* Heart weight to body weight ratios and *(B)* uncorrected heart weight as determined upon sacrifice at 12 months. *(C)* Left ventricular mass as determined by echocardiogram at three-month intervals over a total of 12 months. Salient structural parameters *(D)* intraventricular septum width during diastole, *(E)* left ventricle posterior wall width during diastole, and *(F)* left ventricular diameter during diastole showed no significant differences between MYBPC3 tg and ntg mice. Functional parameters *(G)* ejection fraction and *(H)* fractional shortening were also unaffected. *(I)* Left atrial diameter was mildly but non-significantly (p=0.086) increased in mutant MYBPC3 tg mice at 12 months. Mean±SEM, Ntg n=10, Tg n=12.

FIGURE 3.7
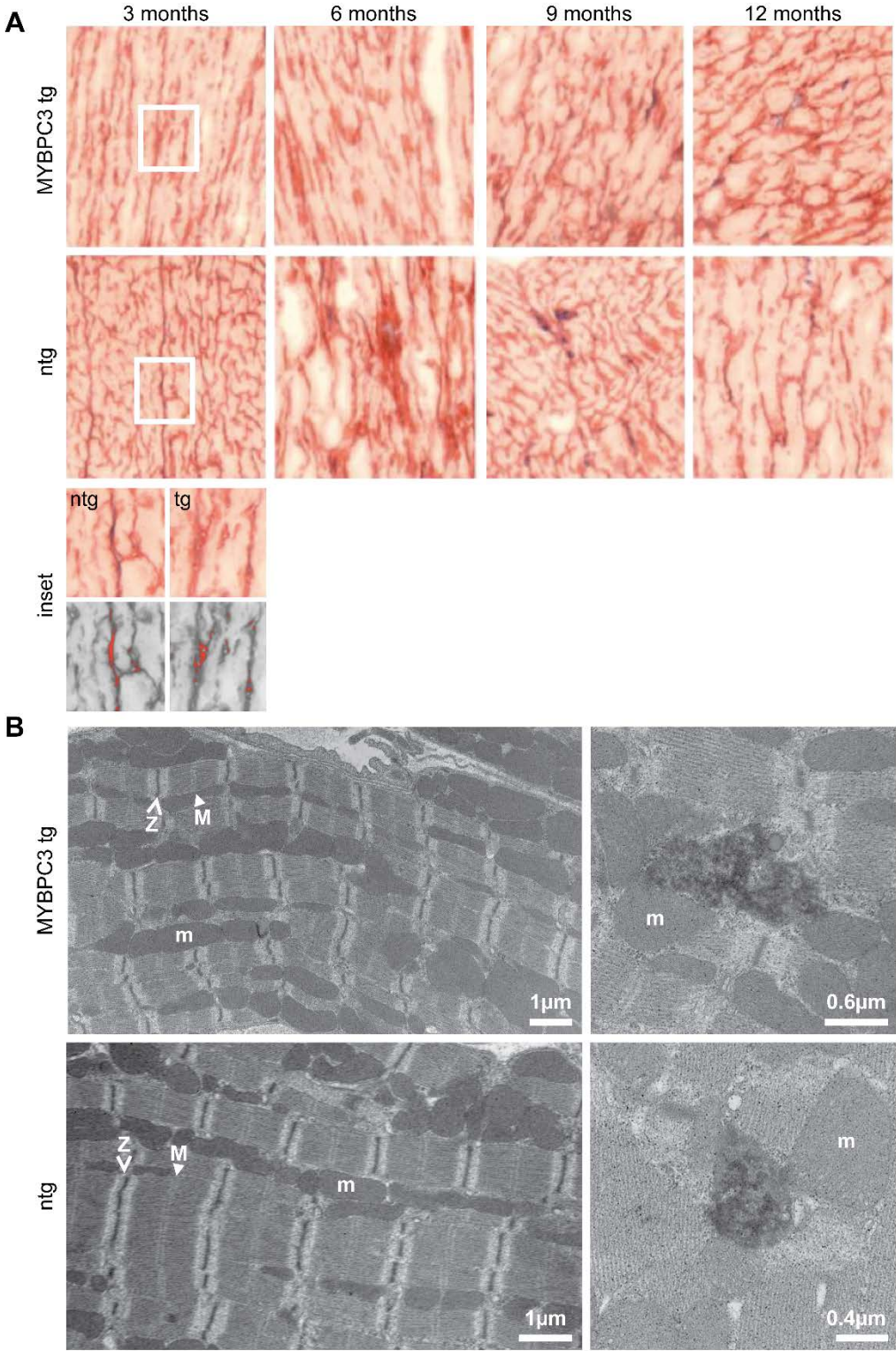
Figure 3.7. 9 month-old MYBPC3 transgenic mice do not develop interstitial fibrosis or myofibrillar disarray. (A) Masson-Trichrome stained myocardial tissue sections from 9 month-old Ntg and MYBPC3 Tg mice. Collagen appears as blue while cytoplasm appears pink. Inset shows magnified fibrotic regions with an example of the binary mask used to quantify fibrosis; red areas were counted toward % area fibrosis. 20X Magnification. (B) Electron micrographs from myocardium (LV free wall) of 9 month-old Ntg and MYBPC3 Tg mice. No significant myofibrillar disorganization or misalignment of Z-disks was observed in either line (left). Both lines had infrequent occurrence of amorphous, non-membrane-bound structures but no distinct granular or fibrous protein aggregates (right). m=mitochondrion; M=sarcomere M-line, arrowhead; Z=sarcomere Z-disk, arrow.

FIGURE 3.8
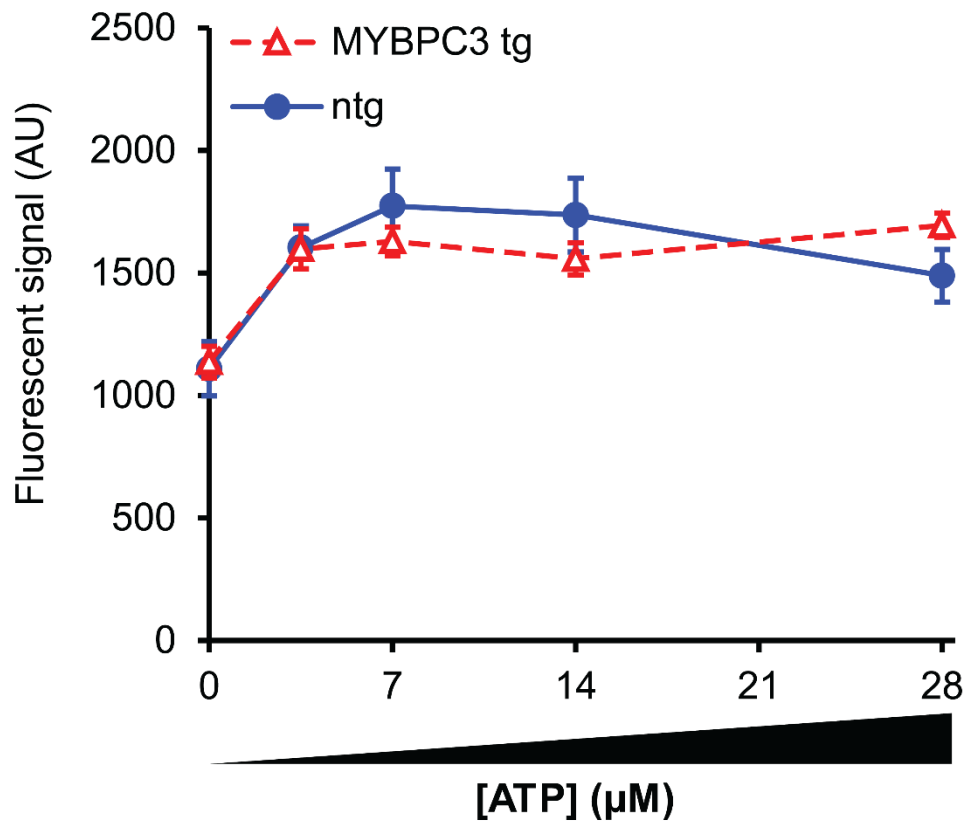
Figure 3.8. 9 month-old MYBPC3 transgenic mice do not exhibit proteasome dysfunction in ventricular myocardium. A fluorogenic substrate-cleavage assay specific for chymotrypsin-like proteasome activity was performed using murine myocardial tissue homogenate. Signal from activity not inhibited by lactacystin (non-proteasomal) was subtracted from total. No significant difference in chymotrypsin-like activity was observed between hearts from non-transgenic mice (closed circles, solid line) and MYBPC3 transgenic mice (open triangles, dashed line). Mean±SEM; Ntg n=14, MYBPC3 Tg n=18; p>0.05 for all concentrations of ATP, student's T test.

TABLE 3.1. Echocardiographic assessment of heart structure and function in 12 month-old non-transgenic vs. MYBPC3 mutant transgenic mice.

	12 months			
sex	**M**		**F**	
genotype	**ntg**	**MYBPC3 tg**	**ntg**	**MYBPC3 tg**
n	5	6	5	6
BW (g)	33.16 ± 1.20	35.49 ± 0.709	29.40 ± 0.300	28.33 ± 0.918*
HR (bpm)	490.7 ± 28.6	525.4 ± 12.2	465.3 ± 39.0	420.7 ± 24.1
HW:BW (mg/g)	4.291 ± 0.0855	3.917 ± 0.143	3.927 ± 0.166	3.750 ± 0.0877
LV mass (mg)	176.3 ± 15.2	163.1 ± 13.4	139.4 ± 4.792	117.8 ± 11.6
IVSd (mm)	1.018 ± 0.0589	1.008 ± 0.0405	0.9900 ± 0.0230	0.8810 ± 0.0695
IVSs (mm)	1.564 ± 0.0464	1.547 ± 0.0730	1.500 ± 0.0303	1.238 ± 0.0865*
IVSth (%)	0.5475 ± 0.0566	0.5350 ± 0.0359	0.5171 ± 0.0345	0.4161 ± 0.0643
LVDd (mm)	4.118 ± 0.0644	4.038 ± 0.116	3.675 ± 0.0969	3.688 ± 0.0823
LVDs (mm)	2.650 ± 0.124	2.712 ± 0.0890	2.354 ± 0.0393	2.484 ± 0.115
PWd (mm)	1.036 ± 0.0247	0.9562 ± 0.0464	0.9900 ± 0.0493	0.8592 ± 0.0415*
PWs (mm)	1.454 ± 0.0369	1.238 ± 0.0783*	1.327 ± 0.0444	1.216 ± 0.0761
PWth (%)	0.4130 ± 0.0578	0.2895 ± 0.0278	0.3429 ± 0.0513	0.4198 ± 0.0657
LVVd (uL)	75.43 ± 4.17	72.00 ± 3.50	57.49 ± 2.39	58.31 ± 4.50
LVVs (uL)	26.27 ± 3.20	27.62 ± 2.24	19.39 ± 0.804	22.44 ± 2.67
LA (mm)	2.733 ± 0.127	3.080 ± 0.118	2.672 ± 0.0563	2.778 ± 0.1437
EF (%)	0.6559 ± 0.0227	0.6157 ± 0.0259	0.6609 ± 0.0169	0.6189 ± 0.0223
FS (%)	0.3575 ± 0.0159	0.3282 ± 0.0188	0.3578 ± 0.0132	0.3276 ± 0.0157

Abbreviations. BW: body weight; HR: heart rate; HW:BW heart weight to body weight ratio; LV: left ventricle; IVSd: diastolic intraventricular septum width; IVSs: systolic intraventricular septum width; IVSth: % change in intraventricular septum thickness from systole to diastole; LVDd: diastolic left ventricle diameter; LVDs: systolic left ventricle diameter; PWd: diastolic posterior wall width; PWs: systolic posterior wall width; PWth: % change in posterior wall thickness from systole to diastole; LVVd: diastolic left ventricle volume; LVVs: systolic left ventricle volume; LA: left atrial diameter; EF: ejection fraction; FS: fractional shortening.
*$p < 0.05$ vs. nontransgenic mice of same sex
Mean ± SEM

3.7 REFERENCES

1.   Adhikari AS, Sridhar Rao K, Rangaraj N, Parnaik VK, Mohan Rao C. Heat stress-induced localization of small heat shock proteins in mouse myoblasts: Intranuclear lamin a/c speckles as target for alphab-crystallin and hsp25. *Experimental cell research*. 2004;299:393-403

2.   Ahn SG, Kim SA, Yoon JH, Vacratsis P. Heat-shock cognate 70 is required for the activation of heat-shock factor 1 in mammalian cells. *The Biochemical journal*. 2005;392:145-152

3.   Alfares AA, Kelly MA, McDermott G, Funke BH, Lebo MS, Baxter SB, Shen J, McLaughlin HM, Clark EH, Babb LJ, Cox SW, DePalma SR, Ho CY, Seidman JG, Seidman CE, Rehm HL. Results of clinical genetic testing of 2,912 probands with hypertrophic cardiomyopathy: Expanded panels offer limited additional sensitivity. *Genetics in medicine : official journal of the American College of Medical Genetics*. 2015

4.   Bahrudin U, Morisaki H, Morisaki T, Ninomiya H, Higaki K, Nanba E, Igawa O, Takashima S, Mizuta E, Miake J, Yamamoto Y, Shirayoshi Y, Kitakaze M, Carrier L, Hisatome I. Ubiquitin-proteasome system impairment caused by a missense cardiac myosin-binding protein c mutation and associated with cardiac dysfunction in hypertrophic cardiomyopathy. *Journal of molecular biology*. 2008;384:896-907

5.   Day SM. The ubiquitin proteasome system in human cardiomyopathies and heart failure. *American journal of physiology. Heart and circulatory physiology*. 2013;304:H1283-1293

6.   Fessart D, Martin-Negrier ML, Claverol S, Thiolat ML, Crevel H, Toussaint C, Bonneu M, Muller B, Savineau JP, Delom F. Proteomic remodeling of proteasome in right heart failure. *Journal of molecular and cellular cardiology*. 2014;66:41-52

7.   Fraysse B, Weinberger F, Bardswell SC, Cuello F, Vignier N, Geertz B, Starbatty J, Kramer E, Coirault C, Eschenhagen T, Kentish JC, Avkiran M, Carrier L. Increased myofilament ca2+ sensitivity and diastolic dysfunction as early consequences of mybpc3 mutation in heterozygous knock-in mice. *Journal of molecular and cellular cardiology*. 2012;52:1299-1307

8.   Gilda JE, Gomes AV. Proteasome dysfunction in cardiomyopathies. *The Journal of physiology*. 2017;595:4051-4071

9.   Harris SP, Bartley CR, Hacker TA, McDonald KS, Douglas PS, Greaser ML, Powers PA, Moss RL. Hypertrophic cardiomyopathy in cardiac myosin binding protein-c knockout mice. *Circulation research*. 2002;90:594-601

10.   Hedhli N, Lizano P, Hong C, Fritzky LF, Dhar SK, Liu H, Tian Y, Gao S, Madura K, Vatner SF, Depre C. Proteasome inhibition decreases cardiac remodeling after initiation of pressure overload. *American journal of physiology. Heart and circulatory physiology*. 2008;295:H1385-1393

11.   Helms AS, Alvarado FJ, Yob J, Tang VT, Pagani F, Russell MW, Valdivia HH, Day SM. Genotype-dependent and -independent calcium signaling dysregulation in human hypertrophic cardiomyopathy. *Circulation*. 2016;134:1738-1748

12.   Helms AS, Davis FM, Coleman D, Bartolone SN, Glazier AA, Pagani F, Yob JM, Sadayappan S, Pedersen E, Lyons R, Westfall MV, Jones R, Russell MW, Day SM. Sarcomere mutation-specific expression patterns in human hypertrophic cardiomyopathy. *Circulation. Cardiovascular genetics*. 2014;7:434-443

13.   Inagaki N, Hayashi T, Arimura T, Koga Y, Takahashi M, Shibata H, Teraoka K, Chikamori T, Yamashina A, Kimura A. Alpha b-crystallin mutation in dilated cardiomyopathy. *Biochemical and biophysical research communications*. 2006;342:379-386

14.   Jacques A, Hoskins AC, Kentish JC, Marston SB. From genotype to phenotype: A longitudinal study of a patient with hypertrophic cardiomyopathy due to a mutation in the mybpc3 gene. *Journal of muscle research and cell motility*. 2008;29:239-246

15.   Kee HJ, Eom GH, Joung H, Shin S, Kim JR, Cho YK, Choe N, Sim BW, Jo D, Jeong MH, Kim KK, Seo JS, Kook H. Activation of histone deacetylase 2 by inducible heat shock protein 70 in cardiac hypertrophy. *Circulation research*. 2008;103:1259-1269

16.   Kodiha M, Chu A, Lazrak O, Stochaj U. Stress inhibits nucleocytoplasmic shuttling of heat shock protein hsc70. *American journal of physiology. Cell physiology*. 2005;289:C1034-1041

17.   Kregel KC. Heat shock proteins: Modifying factors in physiological stress responses and acquired thermotolerance. *Journal of applied physiology (Bethesda, Md. : 1985)*. 2002;92:2177-2186

18.   Kumarapeli AR, Horak KM, Glasford JW, Li J, Chen Q, Liu J, Zheng H, Wang X. A novel transgenic mouse model reveals deregulation of the ubiquitin-proteasome system in the heart by doxorubicin. *FASEB journal : official*

publication of the Federation of American Societies for Experimental Biology. 2005;19:2051-2053

19.   Maron BJ, Sato N, Roberts WC, Edwards JE, Chandra RS. Quantitative analysis of cardiac muscle cell disorganization in the ventricular septum. Comparison of fetuses and infants with and without congenital heart disease and patients with hypertrophic cardiomyopathy. *Circulation.* 1979;60:685-696

20.   Marston S, Copeland O, Gehmlich K, Schlossarek S, Carrier L. How do mybpc3 mutations cause hypertrophic cardiomyopathy? *Journal of muscle research and cell motility.* 2012;33:75-80

21.   Marston S, Copeland O, Jacques A, Livesey K, Tsang V, McKenna WJ, Jalilzadeh S, Carballo S, Redwood C, Watkins H. Evidence from human myectomy samples that mybpc3 mutations cause hypertrophic cardiomyopathy through haploinsufficiency. *Circulation research.* 2009;105:219-222

22.   McLendon PM, Robbins J. Desmin-related cardiomyopathy: An unfolding story. *American journal of physiology. Heart and circulatory physiology.* 2011;301:H1220-1228

23.   McNamara JW, Li A, Lal S, Bos JM, Harris SP, van der Velden J, Ackerman MJ, Cooke R, Dos Remedios CG. Mybpc3 mutations are associated with a reduced super-relaxed state in patients with hypertrophic cardiomyopathy. *PloS one.* 2017;12:e0180064

24.   McNamara JW, Li A, Smith NJ, Lal S, Graham RM, Kooiker KB, van Dijk SJ, Remedios CGD, Harris SP, Cooke R. Ablation of cardiac myosin binding protein-c disrupts the super-relaxed state of myosin in murine cardiomyocytes. *Journal of molecular and cellular cardiology.* 2016;94:65-71

25.   Meiners S, Dreger H, Fechner M, Bieler S, Rother W, Gunther C, Baumann G, Stangl V, Stangl K. Suppression of cardiomyocyte hypertrophy by inhibition of the ubiquitin-proteasome system. *Hypertension (Dallas, Tex. : 1979).* 2008;51:302-308

26.   Mitch WE, Goldberg AL. Mechanisms of muscle wasting. The role of the ubiquitin-proteasome pathway. *The New England journal of medicine.* 1996;335:1897-1905

27.   Osaki J, Haneda T, Kashiwagi Y, Oi S, Fukuzawa J, Sakai H, Kikuchi K. Pressure-induced expression of heat shock protein 70 mrna in adult rat heart is coupled both to protein kinase a-dependent and protein kinase c-dependent systems. *Journal of hypertension.* 1998;16:1193-1200

28. Perng MD, Muchowski PJ, van Den IP, Wu GJ, Hutcheson AM, Clark JI, Quinlan RA. The cardiomyopathy and lens cataract mutation in alphab-crystallin alters its protein structure, chaperone activity, and interaction with intermediate filaments in vitro. *The Journal of biological chemistry*. 1999;274:33235-33243

29. Pfaffl MW. A new mathematical model for relative quantification in real-time rt-pcr. *Nucleic acids research*. 2001;29:e45

30. Powell SR, Davies KJ, Divald A. Optimal determination of heart tissue 26s-proteasome activity requires maximal stimulating atp concentrations. *Journal of molecular and cellular cardiology*. 2007;42:265-269

31. Predmore JM, Wang P, Davis F, Bartolone S, Westfall MV, Dyke DB, Pagani F, Powell SR, Day SM. Ubiquitin proteasome dysfunction in human hypertrophic and dilated cardiomyopathies. *Circulation*. 2010;121:997-1004

32. Previs MJ, Beck Previs S, Gulick J, Robbins J, Warshaw DM. Molecular mechanics of cardiac myosin-binding protein c in native thick filaments. *Science (New York, N.Y.)*. 2012;337:1215-1218

33. Razzaque MA, Gupta M, Osinska H, Gulick J, Blaxall BC, Robbins J. An endogenously produced fragment of cardiac myosin-binding protein c is pathogenic and can lead to heart failure. *Circulation research*. 2013;113:553-561

34. Sarikas A, Carrier L, Schenke C, Doll D, Flavigny J, Lindenberg KS, Eschenhagen T, Zolk O. Impairment of the ubiquitin-proteasome system by truncated cardiac myosin binding protein c mutants. *Cardiovascular research*. 2005;66:33-44

35. Schlossarek S, Englmann DR, Sultan KR, Sauer M, Eschenhagen T, Carrier L. Defective proteolytic systems in mybpc3-targeted mice with cardiac hypertrophy. *Basic research in cardiology*. 2012;107:235

36. Schlossarek S, Frey N, Carrier L. Ubiquitin-proteasome system and hereditary cardiomyopathies. *Journal of molecular and cellular cardiology*. 2014;71:25-31

37. Schlossarek S, Schuermann F, Geertz B, Mearini G, Eschenhagen T, Carrier L. Adrenergic stress reveals septal hypertrophy and proteasome impairment in heterozygous mybpc3-targeted knock-in mice. *Journal of muscle research and cell motility*. 2012;33:5-15

38. Schlossarek S, Singh SR, Geertz B, Schulz H, Reischmann S, Hubner N, Carrier L. Proteasome inhibition slightly improves cardiac function in mice with hypertrophic cardiomyopathy. *Frontiers in physiology*. 2014;5:484

39.   Solomon V, Goldberg AL. Importance of the atp-ubiquitin-proteasome pathway in the degradation of soluble and myofibrillar proteins in rabbit muscle extracts. *The Journal of biological chemistry*. 1996;271:26690-26697

40.   Stansfield WE, Tang RH, Moss NC, Baldwin AS, Willis MS, Selzman CH. Proteasome inhibition promotes regression of left ventricular hypertrophy. *American journal of physiology. Heart and circulatory physiology*. 2008;294:H645-650

41.   Stelzer JE, Fitzsimons DP, Moss RL. Ablation of myosin-binding protein-c accelerates force development in mouse myocardium. *Biophysical journal*. 2006;90:4119-4127

42.   Su H, Wang X. The ubiquitin-proteasome system in cardiac proteinopathy: A quality control perspective. *Cardiovascular research*. 2010;85:253-262

43.   Tardiff JC. Sarcomeric proteins and familial hypertrophic cardiomyopathy: Linking mutations in structural proteins to complex cardiovascular phenotypes. *Heart failure reviews*. 2005;10:237-248

44.   Thottakara T, Friedrich FW, Reischmann S, Braumann S, Schlossarek S, Kramer E, Juhr D, Schluter H, van der Velden J, Munch J, Patten M, Eschenhagen T, Moog-Lutz C, Carrier L. The e3 ubiquitin ligase asb2beta is downregulated in a mouse model of hypertrophic cardiomyopathy and targets desmin for proteasomal degradation. *Journal of molecular and cellular cardiology*. 2015;87:214-224

45.   van Dijk SJ, Dooijes D, dos Remedios C, Michels M, Lamers JM, Winegrad S, Schlossarek S, Carrier L, ten Cate FJ, Stienen GJ, van der Velden J. Cardiac myosin-binding protein c mutations and hypertrophic cardiomyopathy: Haploinsufficiency, deranged phosphorylation, and cardiomyocyte dysfunction. *Circulation*. 2009;119:1473-1483

46.   van Dijk SJ, Paalberends ER, Najafi A, Michels M, Sadayappan S, Carrier L, Boontje NM, Kuster DW, van Slegtenhorst M, Dooijes D, dos Remedios C, ten Cate FJ, Stienen GJ, van der Velden J. Contractile dysfunction irrespective of the mutant protein in human hypertrophic cardiomyopathy with normal systolic function. *Circulation. Heart failure*. 2012;5:36-46

47.   Vignier N, Schlossarek S, Fraysse B, Mearini G, Kramer E, Pointu H, Mougenot N, Guiard J, Reimer R, Hohenberg H, Schwartz K, Vernet M, Eschenhagen T, Carrier L. Nonsense-mediated mrna decay and ubiquitin-proteasome system

regulate cardiac myosin-binding protein c mutant levels in cardiomyopathic mice. *Circulation research.* 2009;105:239-248

48.   Yang Q, Sanbe A, Osinska H, Hewett TE, Klevitsky R, Robbins J. A mouse model of myosin binding protein c human familial hypertrophic cardiomyopathy. *The Journal of clinical investigation.* 1998;102:1292-1300

CHAPTER 4

MYBPC3 missense mutation locus influences protein stability *in vitro*

4.1 ABSTRACT

Mutations in cardiac myosin binding protein C (MYBPC3) are a frequent cause of hypertrophic cardiomyopathy (HCM), the most common inherited heart disease. Patient genotyping has uncovered two categories of pathogenic MYBPC3 mutations: truncating and non-truncating. Uniquely among other sarcomere genes harboring HCM-associated mutations, most MYBPC3 mutations are truncating and there is no evidence that mutation locus affects pathogenic mechanism. However, we identified three groups of non-truncating mutations that potentially represent mutation clusters within the C3, C6, and C10 domains of MYBPC3. While C3 and C6 mutant proteins make up a significant amount of total MYBPC3 in patient myocardium, at least one C10 mutant was undetectable in two unrelated patients, suggesting it does not directly affect sarcomere function and may act through a separate mechanism. We expressed C3, C6, and C10 non-truncating MYBPC3 mutations in neonatal rat ventricular cardiomyocytes to determine whether mutation locus influences subcellular localization and protein stability. All three individual C10 mutants we tested followed a pattern of cytosolic mislocalization, low expression, and accelerated

degradation, while the majority of C3 and C6 mutants behaved similar to WT MYBPC3. This data supports the hypothesis that mutation locus can significantly affect characteristics of non-truncating MYBPC3 mutants, potentially resulting in divergent pathogenic mechanisms.

4.2 INTRODUCTION

Hypertrophic cardiomyopathy (HCM) is the most common genetic heart disease and is generally considered a "sarcomeropathy." Characterized by left ventricular (LV) hypertrophy and fibrosis, HCM predisposes patients to heart failure, arrhythmias, and sudden cardiac death. Hundreds of individual causative mutations have been identified, yet underlying pathogenic mechanisms remain poorly understood. The most frequently mutated gene in HCM is *MYBPC3*, encoding cardiac myosin binding protein C (MYBPC3). MYBPC3 localizes in the sarcomere A-band, has both structural and regulatory function, and acts as a molecular "brake" on cross-bridge cycling[Previs, 2012]. Much of the literature has focused on truncating mutations and their physiological consequences rather than the significantly fewer in number non-truncating mutations. Non-truncating mutations merit further study because while there are many fewer individual missense vs. truncating mutations, they are not quite as rare in HCM patients. Although nonsense, frame-shift and splice-site mutations make up >90% of HCM-associated mutations in MYBPC3[Alfares, 2015], the Arg502Trp mutation represents the single most common mutation in HCM[Page, 2012, Saltzman, 2010]. As non-truncating mutations are likely associated with distinctly different pathogenic mechanisms (dominant-negative vs. haploinsufficiency), we sought to understand whether the primary mechanism is dependent on mutation locus.

Genotype analysis of HCM patients using the Sarcomeric Human Cardiomyopathy Registry (SHaRe) found that while truncating mutations occur throughout the *MYBPC3* gene, missense mutations may potentially cluster in regions encoding specific domains (unpublished data). Specifically, groups of missense mutations were found in the C3, C6, and C10 domains (See figure 1.2). The C10 domain is known to interact with light meromyosin and titin and is part of the binding region essential to sarcomere A-band incorporation of MYBPC3[Flashman, 2007, Freiburg, 1996, Gilbert, 1999, Miyamoto, 1999]. The C3 and C6 domains, however, have no definitive binding partners or functions associated with them.

We previously found that the in-frame duplication mutation Gly1248_Cys1253dup in C10 is extremely unstable in a neonatal rat ventricular cardiomyocyte (NRVM) culture system compared to WT MYBPC3 and even some truncated mutants (See Chapter 2, Figures 2.2 and 2.7)[Glazier, 2018]. It also failed to localize to the sarcomere despite retaining domains necessary for A-band localization (See Figure 2.3). Interestingly, the mutant protein could not be detected in myocardium from two unrelated HCM patients, in contrast to an Arg495Gln C3 mutant which made up ~70% of total MYBPC3 protein[Helms, 2014]. This C10 mutation most likely interrupts sarcomere binding, potentially making the mutant protein subject to rapid clearance from the cytosol. These characteristics are more consistent with truncating mutants, and may result in a loss-of-function mechanism rather than the dominant-negative mechanism generally associated with MYBPC3 missense mutations. We therefore hypothesized that the additional C10 mutants Leu1238Pro and Asn1257Lys would also fail to localize properly and have accelerated degradation rates. Conversely, we hypothesized that C3 and C6 mutants could incorporate properly and have similar degradation rates to WT MYBPC3.

To test these hypotheses and better understand whether the locus of non-truncating mutations dictates divergent molecular mechanisms of pathogenesis, we expressed MYBPC3 proteins with mutations in the relevant domains in NRVMs and determined their localization, stability, and degradation kinetics. Our results showed that C10 mutants had a consistent pattern of cytosolic mislocalization, low expression levels, and markedly fast degradation rates, while C3 and C6 mutants localized normally and tended to have comparable expression and degradation rates to WT MYBPC3. These results suggest that primary pathogenic mechanisms in HCM may not be universal in all missense mutation patients, which will be an important consideration when developing targeted therapies. Further, identification of the effects these groups of missense mutations have on the properties of MYBPC3 may help clarify the roles of domains C3 and C6 in regulating contraction.

4.3 METHODS

4.3.1 Isolation and culture of neonatal rat ventricular cardiomyocytes.

See section 2.3.1

4.3.2 Micropatterning of PDMS coverslips.

See section 2.3.2

4.3.3 Expression of FLAG-tagged WT and missense MYBPC3 constructs via recombinant adenovirus.

See section 2.3.3

4.3.4 Immunofluorescence of NRVMs.

See section 2.3.8

4.3.5 Cycloheximide pulse-chase assay.

NRVMs plated in 96-well plates at a density of $4x10^4$ cells/well were treated with FLAG-WT or FLAG-MYBPC3 missense adenovirus for 48 hours. Four wells in each plate were reserved as FLAG-negative controls and received no virus. Following viral treatment, media in quadruplicate wells of cells was changed with maintenance media containing 300µg/mL cycloheximide (CHX) (Sigma-Aldrich). Timepoints 0, 0.5, 1, 3, 6, 9 and 12 hours post addition of CHX were collected simultaneously. This was achieved by adding CHX at the appropriate time prior to completion of the timecourse (i.e., wells for the 3 hour timepoint received CHX 9 hours after the beginning of the timecourse with addition of CHX to wells for the 12 hour timepoint). Following CHX pulse chase, wells were rinsed three times with sterile PBS. Cells were then lysed in 1X AlphaLISA lysis buffer (PerkinElmer) by adding 50uL of lysis buffer per well and vigorously shaking the cell culture plate for 20 minutes at room temperature, followed by scraping. Samples were stored at -80°C in the original culture plate, sealed with an adhesive cover (MicroAmp® optical adhesive film, Applied Biosystems).

4.3.6 Optimization of AlphaLISA assay conditions.

To verify that experimental conditions resulted in data within the AlphaLISA assay's linear range of detection, we tested serial dilutions of lysate from cells transduced at MOI 10 for WT MYBPC3 and each missense mutation. Duplicate wells were analyzed for each condition. We found that for WT MYBPC3, C3 (Arg495Gln, Arg502Trp, Phe503Leu), and C6 (Trp792Arg, Arg810His) mutants, a 1:6 dilution resulted in an optimal signal-to-noise ratio while still within the linear range. For these proteins, the AlphaLISA assay was performed with a 1:6 dilution of lysate for all timepoints. However,

135

the C10 mutants (Gly1248_Cys1253dup, Leu1238Pro and Asn1257Lys) were only expressed at approximately 25% the level of WT MYBPC3, and dilution of these samples resulted in suboptimal signal-to-noise ratio. For C10 mutants, undiluted lysate remained within the linear range, and therefore these samples were not diluted in the AlphaLISA assay. These serial dilution curves were performed alongside each individual experiment to control for potential variability in adenoviral dosage within and between experiments.

4.3.7 AlphaLISA assay to detect degradation rates of MYBPC3 missense mutants.

To conjugate primary antibodies to AlphaLISA beads, antibodies were diluted 1:1000 in 1X AlphaLISA assay buffer with a 1:100 dilution of the appropriate bead (10:1 ratio of bead to antibody) and incubated for 1 hour at room temperature, protected from light. Mouse FLAG M2 antibody was incubated with anti-mouse AlphaScreen donor beads (PerkinElmer), while a rabbit polyclonal MYBPC3 antibody (custom, provided by Dr. Samantha Harris, University of Arizona) was incubated with anti-rabbit AlphaScreen acceptor beads (PerkinElmer). The AlphaLISA assay was carried out in an opaque white half-area 96 well plate (Corning). Each reaction well consisted of 5µL of cell lysate (diluted as described above), 10µL of FLAG antibody-conjugated donor beads, and 10µL of MYBPC3 antibody-conjugated acceptor beads. Conjugated beads were added to the wells under dimmed lighting conditions. The complete assay plate was covered with an adhesive foil seal and centrifuged for 1 minute at 1,000 rpm to eliminate bubbles. The plate was then incubated in the dark at room temperature for 18 hours. Data was collected using an EnVision 2105 multimode plate reader (PerkinElmer) with an excitation

wavelength of 680nm and emission detected at 615nm. Two independent experiments were completed.

4.3.8 Cycloheximide chase data analysis.

Background was defined as the average signal from the four FLAG-negative wells in each plate, and was subtracted from the raw signal. The fit of the linear range of serial dilution data for each mutant (1:4 through 1:32 dilutions for WT, C3 and C6 mutants, entire range for C10 mutants) was used to determine the quantity of FLAG-MYBPC3 in each sample. For each condition, the time 0 data were normalized to 1 to give a curve describing the relative abundance of FLAG-MYBPC3 over time. Data from two independent experiments were fit to a first-order exponential decay curve $[MYBPC3] = [MYBPC3]_0 e^{-kt}$ (with $[MYBPC3]_0$ normalized to 1), from which reaction constants k and half-lives $t_{1/2}$ (calculated as $t_{1/2} = \ln(2)/k$) were determined.

4.3.9 Statistics

Statistical analysis was done using GraphPad Prism software. Kruskal-Wallis nonparametric one-way ANOVA with Dunn's post hoc test for multiple comparisons were used for comparisons among WT MYBPC3 and mutant MYBPC3 groups. Outliers excluded from analysis were identified using GraphPad Prism's ROUT method with a Q coefficient of 1%. Cycloheximide chase data analysis was performed by fitting data to a first-order exponential decay curve as described above and determining if WT vs missense mutant data could be explained by identical or differing fit parameters (i.e. reaction constant k). p-values of <0.01 were considered statistically significant. Data is reported as mean±SEM unless otherwise noted.

4.4. RESULTS

4.4.1 Subcellular localization of MYBPC3 missense mutants in NRVMs is mutation locus-dependent.

Eight MYBPC3 missense mutations identified in HCM patients were engineered into the human *MYBPC3* gene with an N-terminal FLAG epitope. These mutations: three in the C3 domain, two in the C6 domain, and three in the C10 domain, are located in regions which may represent previously unidentified mutation clusters in MYBPC3 (Figure 4.1A). We then inserted these constructs into a mammalian expression vector for use in adenovirus. NRMVs were transfected with adenovirus at MOI 2. Immunofluorescence was performed on patterned NRVMs to determine whether the missense mutants localized correctly to the sarcomere (Figure 4.1B). Compared to FLAG-WT MYBPC3, all C3 and C6 mutants incorporated similarly into the sarcomere at the C-zone, colocalizing with endogenous MYBPC3. However, the three C10 mutants failed to show any sarcomere incorporation, instead localizing diffusely in the cytosol. This subcellular localization resembles the behavior of the truncating mutants discussed in Chapter 2, despite the presently tested mutants being full-length proteins.

4.4.2 Missense mutation locus influences steady-state expression of mutant protein.

We previously observed that the in-frame full-length Gly1248_Cys1253 mutation had unexpectedly low expression levels, an accelerated degradation rate, and did not localize to the sarcomere when expressed in NRVMs. Based on similar subcellular localization of other C10-domain mutants Leu1238Pro and Asn1257Lys, we

138

hypothesized that these mutants would also be expressed unstably, while C3- and C6-domain mutants would not. NRVMs expressing WT or missense mutant MYBPC3 were lysed and the AlphaLISA assay was used to detect steady-state FLAG-MYBPC3 signal. The AlphaLISA assay allows precise quantification of protein expression in a high-throughput format by using beads conjugated to two antibodies raised in different species which recognize the same target protein at separate epitopes. One antibody is conjugated to a "donor" bead while the other is conjugated to an "acceptor" bead. Excitation of the donor bead only when it is in proximity to the acceptor bead yields a light emission signal proportional to the quantity of target protein. This reduces spurious signal due to antibody cross-reactivity with other proteins. Antibodies against MYBPC3 and the FLAG epitope were used to specifically detect FLAG-MYBPC3 proteins. We found that all three C10 mutations consistently showed significantly reduced expression levels, at approximately ~25% of WT levels (Figure 4.2). In contrast, C3 and C6 mutations showed a general pattern of expression levels unchanged from that of WT MYBPC3, with the exception of the C3 mutant Phe503Leu, which was also had significantly reduced expression. Aside from Phe503Leu, steady-state protein expression of missense MYBPC3 mutants correlates with subcellular localization to the sarcomere, with non-incorporating mutants exhibiting reduced expression compared to WT.

4.4.3 Missense mutations in the C3 and C6 domains of MYBPC3 tend not to affect degradation rate.

We performed cycloheximide (CHX) pulse-chase analysis in NRVMs expressing MYBPC3 missense mutations to test whether mutation locus affected protein degradation rates and $t_{\frac{1}{2}}$. CHX was used to inhibit *de novo* protein synthesis in NRVMs. FLAG-

139

MYBPC3 quantity was determined in NRVM lysates at time points up to 12 hours post addition of CHX to the culture media using the AlphaLISA assay. First, we compared C3 mutants to WT-FLAG MYBPC3. Arg495Gln, Arg302Trp, and Phe503Leu were found to have half-lives not significantly different from that of WT MYBPC3 (5.50, 5.82, and 3.24hr vs 5.06hr, respectively) (Figure 4.3). Phe503Leu had the lowest $t_{1/2}$ out of the C3 mutants, which may be related to its decreased expression in relation to WT MYBPC3 (Figure 4.3D). C6 mutants Trp792Arg and Arg810His were found to have diverging effects on degradation. Trp792Arg had a $t_{1/2}$ which was reduced but not significantly different from that of WT (3.41hr) (Figure 4.4B). On the other hand, the Arg810His mutant significantly increased protein $t_{1/2}$ (8.92hr) (Figure 4.4C). Overall, C3 and C6 mutants were not associated with altered protein stability. See Table 4.1 for degradation curve fit parameters.

4.4.4 Missense mutations in the C10 domain of MYBPC3 are associated with significantly accelerated degradation rates.

We hypothesized that C10 mutants Leu1238Pro and Asn1257Lys would degrade significantly faster than WT or C3/C6 mutant MYBPC3, similarly to Glys1248_Cys1253dup as observed in Chapter 2. CHX pulse-chase with AlphaLISA analysis supported this hypothesis. All three C10 mutants had significantly decreased $t_{1/2}$ compared to WT MYBPC3, in the range of ~10-20 fold lower (Gly1248_Cys1253dup: 0.44hr, Leu1238Pro: 0.27hr; Asn1257Lys: 0.24hr) (Figure 4.5A-D). These findings correlate with the significantly reduced protein expression and lack of sarcomere incorporation we observed in C10 mutants. See Table 4.1 for degradation curve fit parameters.

4.5 DISCUSSION

The main findings of this study are (i) analysis of SHaRe registry data uncovered clusters of pathogenic missense mutations in the C3, C6, and C10 domains of MYBPC3 and (ii) protein localization and stability of MYBPC3 missense mutations are influenced by mutation locus. We also verified that the t½ of WT FLAG-MYBPC3 we observed from Western blot data in Chapter 2 (see Figure 2.7) was similar when measured by a different method and demonstrated the efficacy of the AlphaLISA assay to accurately detect FLAG-MYBPC3 at levels below the resolution of Western blotting. Based on these data, we speculate that C10 mutations may actually be associated with haploinsufficiency of MYBPC3, similarly what is observed in patients with truncating mutations[Jacques, 2008, Marston, 2009, van Dijk, 2012]. Conversely, C3- and C6-domain mutants are likely associated with a dominant-negative effect that alters contraction and the critical regulatory functions of MYBPC3.

The presence of pathogenic mutation clusters in C3 and C6 imply those loci contain residues important to function, binding or folding of MYBPC3. Yet despite the frequency of the Arg502Trp mutation and the apparent importance of the C3 and C6 domains, their roles of these domains remain unclear. Structural characterization of the C3 mutation Arg502Trp suggests the mutation alters the electrostatic properties of the domain, and the arginine 502 residue was found to be highly conserved across species[Zhang, 2014]. While there is no direct evidence that C3 binds to actin, transmission electron microscopy analysis of F-actin decorated with a C0-C3 fragment of MYBPC3 indicates they are in close proximity[Mun, 2011]. Mutations in C3 could potentially disrupt key interactions of the N-terminus of MYBPC3 with actin, or alter the flexibility of the protein,

which could both seriously impact function. Our results suggest that C3-domain mutations do not affect sarcomere incorporation and are stably expressed, which is in line with the hypothesis that altered function of full-length MYBPC3 can drive HCM pathogenesis through a dominant-negative mechanism causing contractile dysfunction.

Arginine 820 in the C6 domain is also conserved in mammals, and a naturally occurring Arg820Trp mutation causes feline HCM[Meurs, 2007]. Arg820Trp and Arg820Gln mutations have been identified in humans, but they were more associated with left ventricular non-compaction and dilated cardiomyopathy, respectively[Konno, 2003, Ripoll Vera, 2010]. The Trp792Arg mutation changes another highly conserved residue. Recently, Smelter et. al. analyzed this mutation in an engineered mouse cardiac tissue model and found it to be expressed at significantly lower levels compared to WT MYBPC3, suggesting instability despite correct sarcomere localization[Smelter, 2018]. They hypothesize that introduction of a charged arginine residue into the hydrophobic core of C6 causes misfolding of this fibronectin-like domain. These results conflict with our observations, which showed no significant signs of Trp792Arg being unstable compared to WT MYBPC3. This discrepancy could be explained by the use of different model systems with different genotypes: our experiments were performed using a monolayer of neonatal rat cardiomyocytes with full expression of endogenous MYBPC3, while Smelter et. al. generated 3D tissue cultures from MYBPC3 knockout neonatal mouse cardiomyocytes. Both studies used adenovirus to introduce mutant MYBPC3. Despite these differences, these encouraging findings support the idea that certain missense mutations result in instability of MYBPC3 and a loss-of-function based mechanism.
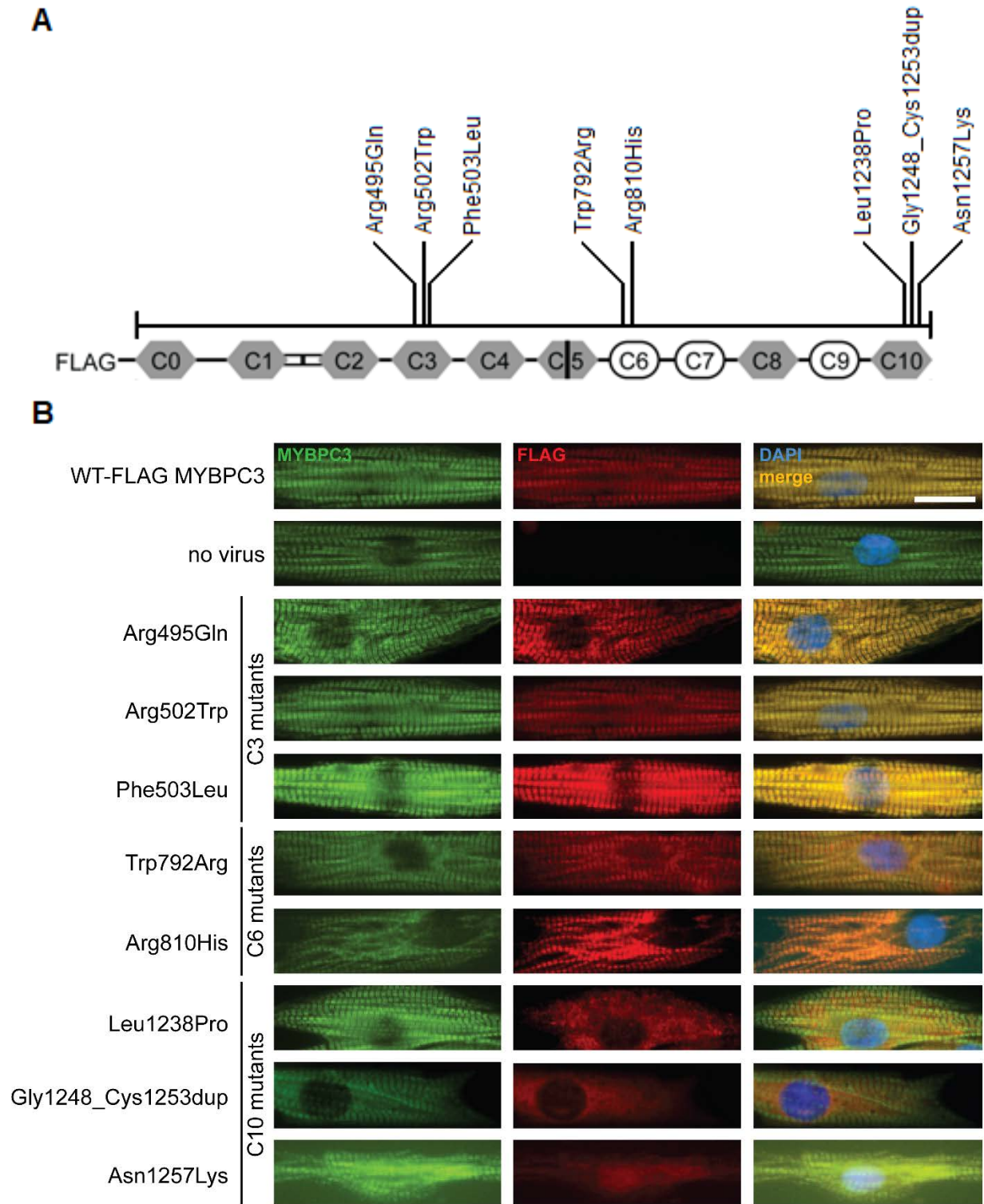
We observed significant instability of not C6 but C10 mutant proteins. The C10 domain has well-established binding partners and is necessary to anchor the C-terminus of MYBPC3 to the rod of the thick filament[Gilbert, 1999, Gilbert, 1996]. This corresponds with the failure of all three C10 mutants to incorporate into the sarcomere, which is probably a result of abolished MYBPC3 and light meromyosin/titin interactions. Aberrant cytosolic expression of C10 mutant MYBPC3 without protection from the sarcomere is a likely explanation for its susceptibility to rapid degradation and low expression levels. We therefore conclude that mutations in the putative C10 cluster are more likely to act by a mechanism distinct from other missense mutations. Ascertaining the precise mechanism associated with C10 mutations should be of high priority as personalized medicine moves forward, namely due to an extremely prevalent deletion mutation that is found in approximately 4% of the South Asian population, and potentially up to 1% of the entire population[Kuster, 2014]. This pathogenic variant replaces most of C10 with novel sequence and like the Gly1248_Cys1253dup mutation, it was not detectable in septal myectomy samples from two different HCM patients[Dhandapany, 2009]. We speculate that this mutant protein would also show accelerated degradation kinetics. Clearly, differentiating between molecular mechanisms associated with stable vs. unstable MYBPC3 mutations will be vital to development of targeted therapies for some of the most frequently occurring mutations in HCM.

4.6 ACKNOWLEDGEMENTS

FIGURE 4.1

Figure 4.1. C3 and C6-domain mutants localize to the C-zone, while C10-domain mutants mislocalize to cytoplasm. *(A)* Location of C3, C6 and C10 missense mutations within MYBPC3, showing potential mutation cluster regions. *(B)* Neonatal rat cardiomyocytes (NRVMs) were transiently transfected with FLAG-MYBPC3 adenovirus and immunofluorescence was performed on patterned NRVMs. FLAG-WT MYBPC3 and endogenous MYBPC3 correctly co-localize to the C-zone. This likewise occurs for C3 and C6-domain mutations. However, C10 domain mutations appear diffuse in the cytosol with little to no sarcomere localization. All conditions were tested at minimum in triplicate. Endogenous MYBPC3 (green), FLAG (red), DAPI (blue). Immunofluorescence micrographs, 60X magnification. Scale bar = 10µm.
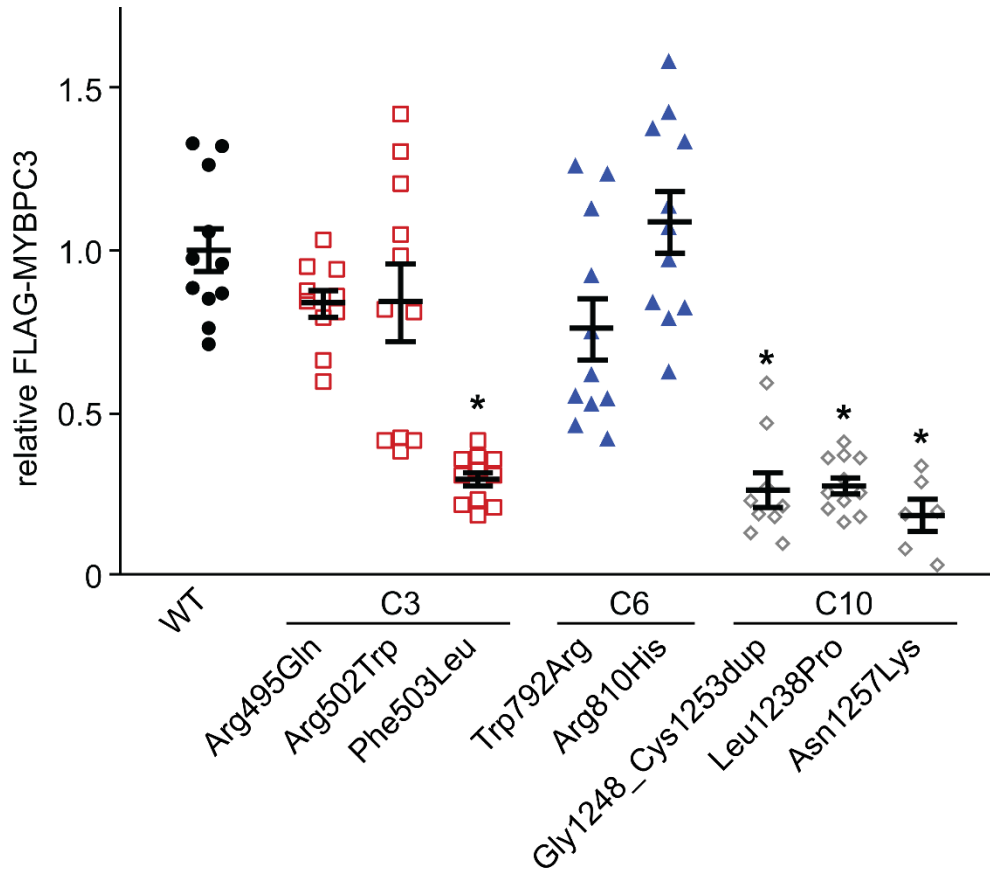
FIGURE 4.2

Figure 4.2. Expression levels of missense MYBPC3 mutants versus WT. The AlphaLISA assay was used to determine steady-state levels of adenovirally-transfected FLAG-MYBPC3 in NRVMs. C3- and C6-domain mutation levels were similar to WT levels, with the exception of F503L. Expression of all three C10-domain mutations was significantly reduced compared to WT, corresponding with their cytosolic mislocalization. Two independent experiments; Mean±SEM, n≥6. Kruskal-Wallis one-way ANOVA p<0.0001. *p<0.0001 vs control, Dunn's test for multiple comparisons.

FIGURE 4.3
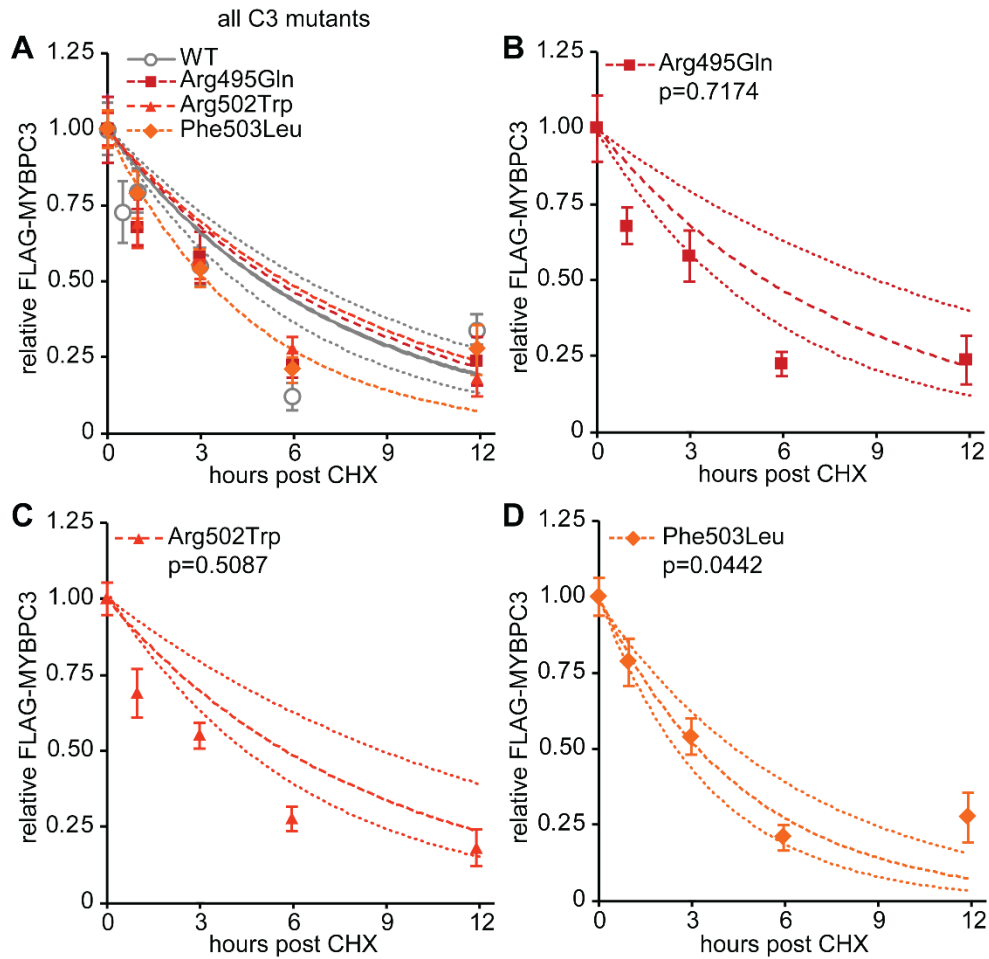
Figure 4.3. MYBPC3 missense mutations in the C3 domain do not significantly alter protein t½. *(A)* Overlaid cycloheximide pulse-chase analysis of the C3 mutants Arg495Gln (squares), Arg502Trp (triangles), Phe503Leu (diamonds), compared to FLAG-WT MYBPC3 (open circles, solid line) Gray dotted lines show 95% confidence intervals for WT fit. *(B-D)* Individual curve fits for mutants with 95% confidence interval. For each data point, n≥8 technical replicates from two independent experiments. Mean±SEM, p values represent significance of comparison of reaction constant *k* versus WT-FLAG MYBPC3. *p≤0.01. Dotted lines show 95% confidence intervals for *k*.

FIGURE 4.4
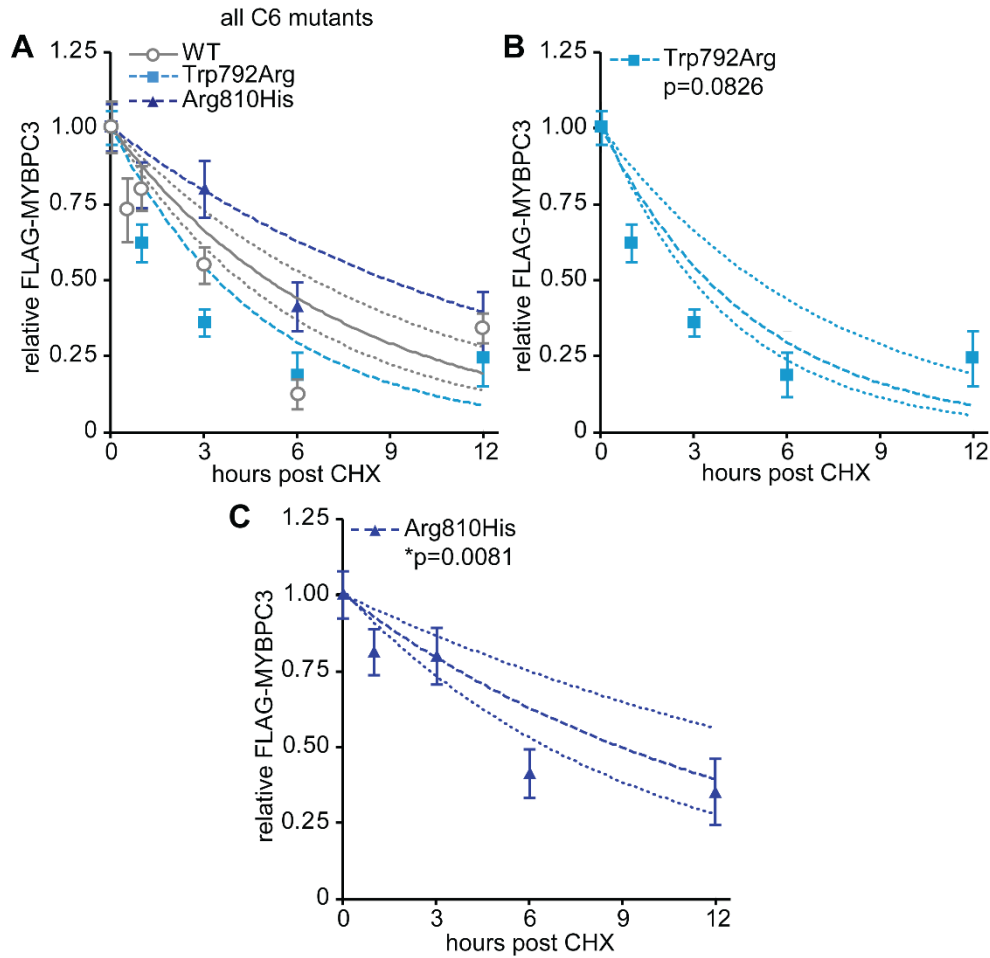
Figure 4.3. MYBPC3 missense mutations in the C6 domain do not significantly alter protein $t_{1/2}$. *(A)* Overlaid cycloheximide pulse-chase analysis of the C6 mutants Trp792Arg (squares) and Arg810His (triangles), compared to FLAG-WT MYBPC3 (open circles, solid line). WT data shown previously in Fig. 4.3. *(B-D)* Individual curve fits for mutants with 95% confidence interval. For each data point, n≥8 technical replicates from two independent experiments. Mean±SEM, p values represent significance of comparison of reaction constant *k* versus WT-FLAG MYBPC3. *p≤0.01. Dotted lines show 95% confidence intervals for *k*.

FIGURE 4.5
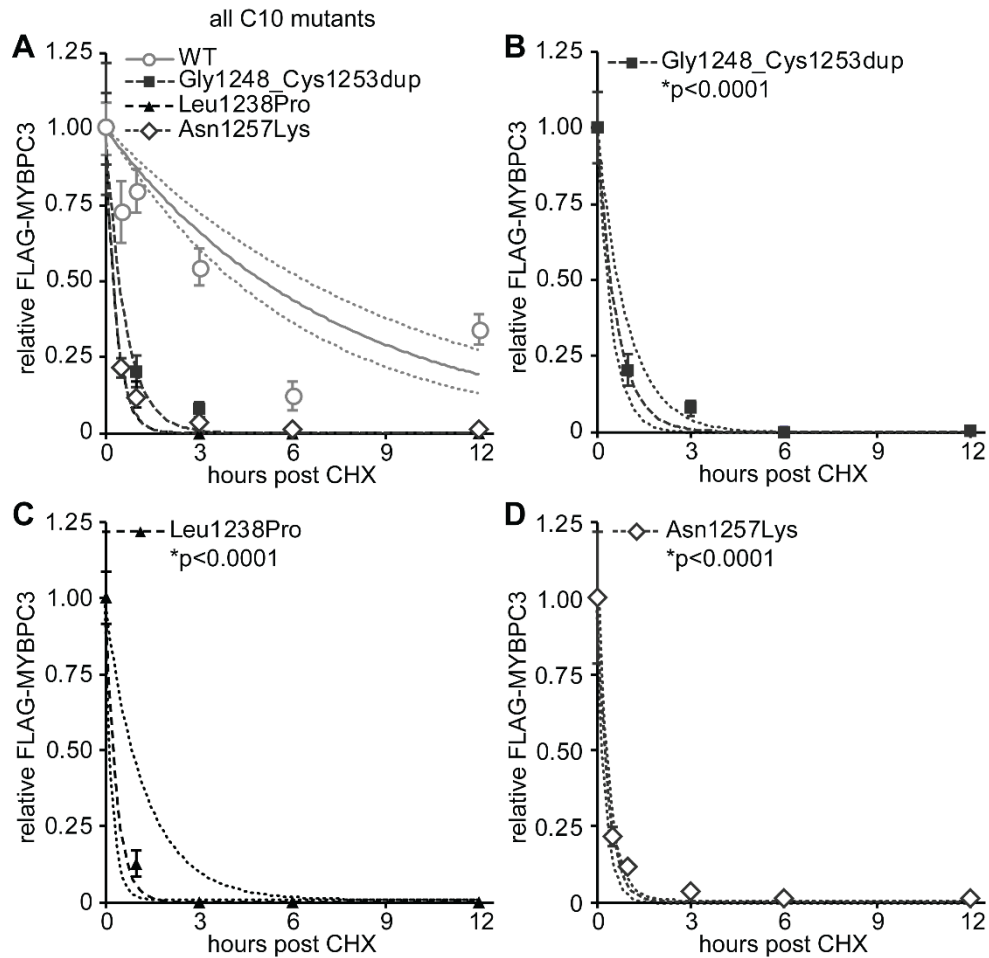
Figure 4.5. MYBPC3 missense mutations in the C10 domain severely reduce protein

$t_{\frac{1}{2}}$. *(A)* Overlaid cycloheximide pulse-chase analysis of the C10 mutants Gly1248_Cys1263dup (squares), Leu1238Pro (triangles), and Asn1257Lys (diamonds), compared to FLAG-WT MYBPC3 (open circles, solid line). WT data shown previously in Fig. 4.3. *(B-D)* Individual curve fits for mutants with 95% confidence interval. For each data point, n≥11 technical replicates from two independent experiments. Mean±SEM, p values represent significance of comparison of reaction constant *k* versus WT-FLAG MYBPC3. *p≤0.01. Dotted lines show 95% confidence intervals for *k*.

TABLE 4.1. Kinetic fit parameters for AlphaLISA cycloheximide pulse-chase data.

Domain	Protein	$t_{1/2}$ (hr)	$t_{1/2}$ 95% CI (hr)	k (hr^{-1}) ± SE	p value for k comparison vs. WT
	WT	5.06	4.15 to 6.50	0.137 ± 0.030	
	Arg495Gln	5.50	3.95 to 9.06	0.126 ± 0.049	0.7174
C3	Arg502Trp	5.82	4.35 to 8.81	0.214 ± 0.062	0.5087
	Phe503Leu	3.24	2.51 to 4.56	0.119 ± 0.040	0.0442
C6	Trp792Arg	3.41	2.58 to 5.04	0.203 ± 0.053	0.0826
	Arg810His	8.92	6.46 to 14.4	0.0777 ± 0.030	0.0081*
	Leu1238Pro	0.27	0.16 to 0.89	2.57 ± 1.8	<0.0001*
C10	Gly1248_Cys1253dup	0.44	0.32 to 0.66	1.58 ± 0.56	<0.0001*
	Asn1257Lys	0.24	0.18 to 0.37	2.89 ± 0.99	<0.0001*

Abbreviations. $t_{1/2}$: half-life; k: reaction constant; CI: confidence interval; SE: standard error

*p<0.01 for parameter k in first-order decay reaction fit for WT vs. respective mutant

4.7 REFERENCES

1. Alfares AA, Kelly MA, McDermott G, Funke BH, Lebo MS, Baxter SB, Shen J, McLaughlin HM, Clark EH, Babb LJ, Cox SW, DePalma SR, Ho CY, Seidman JG, Seidman CE, Rehm HL. Results of clinical genetic testing of 2,912 probands with hypertrophic cardiomyopathy: Expanded panels offer limited additional sensitivity. *Genetics in medicine : official journal of the American College of Medical Genetics.* 2015

2. Dhandapany PS, Sadayappan S, Xue Y, Powell GT, Rani DS, Nallari P, Rai TS, Khullar M, Soares P, Bahl A, Tharkan JM, Vaideeswar P, Rathinavel A, Narasimhan C, Ayapati DR, Ayub Q, Mehdi SQ, Oppenheimer S, Richards MB, Price AL, Patterson N, Reich D, Singh L, Tyler-Smith C, Thangaraj K. A common mybpc3 (cardiac myosin binding protein c) variant associated with cardiomyopathies in south asia. *Nature genetics.* 2009;41:187-191

3. Flashman E, Watkins H, Redwood C. Localization of the binding site of the c-terminal domain of cardiac myosin-binding protein-c on the myosin rod. *The Biochemical journal.* 2007;401:97-102

4. Freiburg A, Gautel M. A molecular map of the interactions between titin and myosin-binding protein c. Implications for sarcomeric assembly in familial hypertrophic cardiomyopathy. *European journal of biochemistry.* 1996;235:317-323

5. Gilbert R, Cohen JA, Pardo S, Basu A, Fischman DA. Identification of the a-band localization domain of myosin binding proteins c and h (mybp-c, mybp-h) in skeletal muscle. *Journal of cell science.* 1999;112 (Pt 1):69-79

6. Gilbert R, Kelly MG, Mikawa T, Fischman DA. The carboxyl terminus of myosin binding protein c (mybp-c, c-protein) specifies incorporation into the a-band of striated muscle. *Journal of cell science.* 1996;109 (Pt 1):101-111

7. Glazier AA, Hafeez N, Mellacheruvu D, Basrur V, Nesvizhskii AI, Lee LM, Shao H, Tang V, Yob JM, Gestwicki JE, Helms AS, Day SM. Hsc70 is a chaperone for wild-type and mutant cardiac myosin binding protein c. *JCI insight.* 2018;3

8. Helms AS, Davis FM, Coleman D, Bartolone SN, Glazier AA, Pagani F, Yob JM, Sadayappan S, Pedersen E, Lyons R, Westfall MV, Jones R, Russell MW, Day SM. Sarcomere mutation-specific expression patterns in human hypertrophic cardiomyopathy. *Circulation. Cardiovascular genetics.* 2014;7:434-443

9. Jacques A, Hoskins AC, Kentish JC, Marston SB. From genotype to phenotype: A longitudinal study of a patient with hypertrophic cardiomyopathy due to a

mutation in the mybpc3 gene. *Journal of muscle research and cell motility.* 2008;29:239-246

10. Konno T, Shimizu M, Ino H, Matsuyama T, Yamaguchi M, Terai H, Hayashi K, Mabuchi T, Kiyama M, Sakata K, Hayashi T, Inoue M, Kaneda T, Mabuchi H. A novel missense mutation in the myosin binding protein-c gene is responsible for hypertrophic cardiomyopathy with left ventricular dysfunction and dilation in elderly patients. *Journal of the American College of Cardiology.* 2003;41:781-786

11. Kuster DW, Sadayappan S. Mybpc3's alternate ending: Consequences and therapeutic implications of a highly prevalent 25 bp deletion mutation. *Pflugers Archiv : European journal of physiology.* 2014;466:207-213

12. Marston S, Copeland O, Jacques A, Livesey K, Tsang V, McKenna WJ, Jalilzadeh S, Carballo S, Redwood C, Watkins H. Evidence from human myectomy samples that mybpc3 mutations cause hypertrophic cardiomyopathy through haploinsufficiency. *Circulation research.* 2009;105:219-222

13. Meurs KM, Norgard MM, Ederer MM, Hendrix KP, Kittleson MD. A substitution mutation in the myosin binding protein c gene in ragdoll hypertrophic cardiomyopathy. *Genomics.* 2007;90:261-264

14. Miyamoto CA, Fischman DA, Reinach FC. The interface between mybp-c and myosin: Site-directed mutagenesis of the cx myosin-binding domain of mybp-c. *Journal of muscle research and cell motility.* 1999;20:703-715

15. Mun JY, Gulick J, Robbins J, Woodhead J, Lehman W, Craig R. Electron microscopy and 3d reconstruction of f-actin decorated with cardiac myosin-binding protein c (cmybp-c). *Journal of molecular biology.* 2011;410:214-225

16. Page SP, Kounas S, Syrris P, Christiansen M, Frank-Hansen R, Andersen PS, Elliott PM, McKenna WJ. Cardiac myosin binding protein-c mutations in families with hypertrophic cardiomyopathy: Disease expression in relation to age, gender, and long term outcome. *Circulation. Cardiovascular genetics.* 2012;5:156-166

17. Previs MJ, Beck Previs S, Gulick J, Robbins J, Warshaw DM. Molecular mechanics of cardiac myosin-binding protein c in native thick filaments. *Science (New York, N.Y.).* 2012;337:1215-1218

18. Ripoll Vera T, Monserrat Iglesias L, Hermida Prieto M, Ortiz M, Rodriguez Garcia I, Govea Callizo N, Gomez Navarro C, Rosell Andreo J, Gamez Martinez JM, Pons Llado G, Cremer Luengos D, Torres Marques J. The r820w mutation in the mybpc3 gene, associated with hypertrophic cardiomyopathy in cats, causes hypertrophic cardiomyopathy and left ventricular non-compaction in humans. *International journal of cardiology.* 2010;145:405-407

19.   Saltzman AJ, Mancini-DiNardo D, Li C, Chung WK, Ho CY, Hurst S, Wynn J, Care M, Hamilton RM, Seidman GW, Gorham J, McDonough B, Sparks E, Seidman JG, Seidman CE, Rehm HL. Short communication: The cardiac myosin binding protein c arg502trp mutation: A common cause of hypertrophic cardiomyopathy. *Circulation research*. 2010;106:1549-1552

20.   Smelter DF, de Lange WJ, Cai W, Ge Y, Ralphe JC. The hcm-linked w792r mutation in cardiac myosin-binding protein c reduces c6 fniii domain stability. *American journal of physiology. Heart and circulatory physiology*. 2018;314:H1179-H1191

21.   van Dijk SJ, Paalberends ER, Najafi A, Michels M, Sadayappan S, Carrier L, Boontje NM, Kuster DW, van Slegtenhorst M, Dooijes D, dos Remedios C, ten Cate FJ, Stienen GJ, van der Velden J. Contractile dysfunction irrespective of the mutant protein in human hypertrophic cardiomyopathy with normal systolic function. *Circulation. Heart failure*. 2012;5:36-46

22.   Zhang XL, De S, McIntosh LP, Paetzel M. Structural characterization of the c3 domain of cardiac myosin binding protein c and its hypertrophic cardiomyopathy-related r502w mutant. *Biochemistry*. 2014;53:5332-5342

CHAPTER 5

DISCUSSION

5.1 Summary of thesis work

A wealth of research over the years has cemented the assessment of cardiac myosin binding protein C (MYBPC3) as a critical regulator of contraction with significant roles in cardiac physiology. Despite its long-recognized status as the most frequently mutated gene in the most common inherited cardiomyopathy, definitive disease mechanisms associated with MYBPC3 mutations have not been firmly established. The overarching goal of this project was to work toward a better understanding of pathogenesis in MYBPC3-linked HCM. The work presented in this dissertation is pursuant to three specific aims: (i) to identify protein quality control-related factors involved in the handling and turnover of MYBPC3; (ii) to clarify whether pathogenic truncating MYBPC3 mutants are directly proteotoxic, and whether truncating mutations are sufficient to cause left ventricular remodeling in the absence of MYBPC3 haploinsufficiency; and (iii) to determine if protein stability, and therefore potential pathogenic mechanism, is dependent on mutation locus in non-truncating MYBPC3 mutants. These three questions are tied together around the central concept of sarcomere protein homeostasis. The conclusions drawn from our results accomplish the overarching goal and also offer insight into the

complex and incompletely understood subject of sarcomere maintenance and its physiological roles at the molecular, cellular, and organismal levels. To finish this dissertation, we will discuss the implications of this study on potential therapies and future directions in HCM research.

5.1.1 Novel interactions between MYBPC3 and molecular chaperone proteins

In Chapter 2, we used an unbiased affinity purification-mass spectrometry screen to detect MYBPC3 interacting proteins in NRVMs transduced with adenovirus to express FLAG-epitope tagged WT and mutant MYBPC3. Surprisingly, gene ontology analysis identified protein quality control-related interactors as the most enriched protein category, rather than myofilament proteins. This category included several molecular chaperones, proteins which assist in folding, repair and degradation of client proteins, most prominently the inducible and constitutive isoforms of heat shock protein 70kDa (HSP70 and HSC70, respectively). MYBPC3 is known to be degraded via the ubiquitin proteasome system (UPS)[Sarikas, 2005, Vignier, 2009], but mechanisms which target it for ubiquitination are unknown. After demonstrating physical interaction between MYBPC3 and HSP70 chaperones, we were also able to demonstrate functional interactions by using cycloheximide pulse-chase experiments to observe the effects of modulating HSP70/HSC70 expression and activity on the degradation kinetics of WT and mutant MYBPC3. Suppression of HSC70 expression and activation of HSP70 resulted in significant changes in protein $t_{½}$, strongly implying HSP70s act upstream of the UPS to target MYBPC3 for degradation through interactions with E3 ligases like C-terminus of HSC70 interacting protein (CHIP)[McDonough, 2003]. To our knowledge these are the first chaperones found to interact with MYBPC3. While evaluation of functional interactions

between MYBPC3 and chaperone proteins was limited to the HSP70-family in this study, we also consider the small heat shock proteins (sHSP) αB-crystallin and HSP27 compelling candidates for factors involved in MYBPC3 turnover. In contrast to the HSP70s, the sHSPs showed loss of interaction with mutant MYBPC3. αB-crystallin and HSP27 are among those sHSPs highly expressed in the heart[Golenhofen, 2004, Hollander, 2004]. Both of these chaperones have previously established interactions with titin which can be induced by mechanical damage and unfolding of immunoglobulin-like domains[Kotter, 2014]. These interactions are relevant because MYBPC3 contains eight immunoglobulin domains with high structural similarity to those in titin[Otey, 2009]. It is unknown whether MYBPC3 immunoglobulin-like domains unfold in response to stretch *in vivo,* but atomic force microscopy experiments suggest they will unfold under relatively modest mechanical loads[Karsai, 2011]. Therefore, αB-crystallin and HSP27 could be recruited to refold MYBPC3 in a similar fashion to titin. Future studies should address functional interactions between MYBPC3 and sHSPs perhaps under both normal and chronic stretch conditions. The significance of identifying chaperones and co-chaperones associated with MYBPC3 lies in the discovery of pathways that could be targeted to control expression of MYBPC3 in disease contexts, particularly to restore expression to normal levels in haploinsufficient states.

5.1.2 Truncated MYBPC3 is not directly proteotoxic in cardiomyocytes

In Chapter 3, we investigated proteostasis at the cellular and whole-organ levels by challenging cardiomyocytes with expression of truncated MYBPC3 proteins. Previous studies found evidence that expression of truncated mutants was sufficient to disrupt proteostasis by causing impaired UPS function and aggregation of ubiquitinated

proteins[Bahrudin, 2008, Sarikas, 2005]. Combined with later findings of significantly reduced proteasome enzymatic activity in septal myectomy tissue from HCM patients[Predmore, 2010, Thottakara, 2015], this data generated the hypothesis that truncated MYBPC3 is inherently proteotoxic and a "poison peptide" effect contributes to HCM pathogenesis. *In vivo* modeling of "pure" haploinsufficient mice (heterozygous MYBPC3 knock-out) versus mice with both haploinsufficiency and truncated protein expression (heterozygous truncating knock-in) seemed to support this hypothesis, as myocardial UPS dysfunction was only reproduced in the heterozygous knock-in mice[Schlossarek, 2012, Schlossarek, 2012]. However, this premise has been repeatedly called into question by attempts to detect truncated proteins in patient tissue which have consistently failed[Jacques, 2008, Marston, 2009, van Dijk, 2009]. The above studies showed that truncated MYBPC3 expression may be necessary to induce UPS dysfunction, but not ventricular remodeling. Haploinsufficiency without truncated MYBPC3 was found to be sufficient to elicit cardiac hypertrophy, but the inverse situation had never been tested. We demonstrated that truncated MYBPC3 is in fact not sufficient to cause hypertrophic remodeling or disrupt proteostasis in non-haploinsufficient models. Using a more diverse panel of mutations than previous studies[Sarikas, 2005], we found no evidence of UPS dysfunction, protein aggregates, or HSP70-related protein folding stress responses in NRVMs with acute expression of truncated mutants. Neither were UPS dysfunction or aggregates present in the hearts of transgenic mice with conserved MYBPC3 stoichiometry chronically expressing truncated protein. Finally, rigorous structural and functional assessment of transgenic murine hearts over 12 months identified no cardiac disease phenotype. These results move toward resolving the haploinsufficiency vs. "poison peptide" debate in MYBPC3-linked HCM. Future studies

should try to clarify whether "pure" haploinsufficiency is sufficient to cause UPS dysfunction without a "second hit." The heterogeneity of HCM phenotypes suggests influence of unknown modifier genes; variants in proteasome subunits or other protein quality control-related genes could affect whether loss of proteostasis develops subsequent to hypertrophic remodeling. As mouse models with MYBPC3 mutations generally display very mild phenotypes, isogenic induced pluripotent-derived stem cell lines or large animal models may be better choices of model systems. A porcine HCM model carrying a mutation in *MYH7* has been generated and exhibits a robust phenotype[del Rio Carlos, 2017, Green Eric, 2017]. Mutations in MYBPC3 would optimistically produce a similar phenotype in pigs.

5.1.3 *Putative missense mutation clusters in MYBPC3 reveal locus-dependent variability in protein stability.*

In Chapter 3, SHaRe registry patient genotype data revealed three regions of potential "hot spots" for non-truncated MYBPC3 mutations in the C3, C6, and C10 domains. Non-truncating mutations in MYBPC3 make up <10% of individual mutations thus far identified[Alfares, 2015], and are generally assumed to share a common dominant-negative pathogenic mechanism whereby they incorporate into the sarcomere and alter contractile function. This assumption has recently been challenged based on a missense mutation that significantly alters protein stability and may instead cause haploinsufficiency[Smelter, 2018]. Additionally, in Chapter 2 we found that an in-frame duplication mutation had an extremely accelerated degradation rate compared to WT MYBPC3, and was unable to localize to the sarcomere[Glazier, 2018]. In patients the mutant protein was not detectable, as is consistently seen with truncating mutations[Helms, 2014].

We assessed the subcellular localization and expression levels of three C3, two C6, and three C10 non-truncating mutants adenovirally-transduced into NRVMs. We next used a streamlined, microplate-based version of the cycloheximide pulse-chase method employed in Chapter 2 to compare degradation kinetics of the different mutants. Our results support the hypothesis that distinct pathogenic mechanisms exist within the subcategory of MYBPC3 missense mutations that are dictated by mutation locus. Most significantly, all three C10-domain mutants showed cytosolic mislocalization, low expression and protein $t_{1/2}$ 10- to 20-fold lower than WT MYBPC3. If these characteristics are recapitulated *in vivo,* a dominant-negative mechanism is very unlikely. In general, we found the C3- and C6-domain mutants to have expression and protein $t_{1/2}$ not significantly different from WT MYBPC3, and all five of these localized properly to the C-band. This pattern is more in line with the dominant-negative mechanism. Our lab is currently expanding this study to include *in silico* structural analysis of these mutants using Iterative Threading Assembly Refinement (I-TASSER)[Yang, 2015] and structure-based prediction of protein stability (STRUM)[Quan, 2016] methods to predict protein structure and the Gibb's free energy gap differences between WT and mutant proteins (ΔΔG). Preliminary results further distinguish between the two groups of mutations, with C3 mutants predicted to have little to no change in stability, while C10 mutants all have ΔΔG≤-1, indicating destabilization. Future, more mechanistically-targeted directions should emphasize ruling out direct effects on contractile function associated with C10-domain mutants through comparison to "pure" haploinsufficient models or by showing that conditional suppression of the C10 mutant allele results in no change in phenotype. Being able to predict pathogenic mechanisms based on mutation locus will facilitate development of targeted

therapies in MYBPC3-linked HCM and make identification of appropriate interventions more efficient.

5.2 MYBPC3 mutations and unifying pathogenic mechanisms in HCM

Despite the range of evidence in support of the two main hypotheses discussed previously, an intermediate mechanistic link between haploinsufficiency and/or proteotoxicity and whole-organ cardiac remodeling remains undefined, as does a unifying pathogenic mechanism across various HCM genotypes. As with HCM caused by a subset of mutations in other sarcomere genes, Ca^{2+} sensitivity of the myofilament is increased in MYBPC3-linked HCM[van Dijk, 2009]. Increased Ca^{2+} sensitivity, potentially leading to hypercontractility, impaired relaxation, and alterations in Ca^{2+}-dependent signaling pathways, has been suggested as a unifying pathogenic mechanism in HCM. Another compelling hypothesis proposes HCM is the result of energetic deficits stemming from overuse of ATP by myosin due to altered contractility[Ashrafian, 2003].

Both of these broader mechanisms are theoretically consistent with haploinsufficiency of MYBPC3 being the primary insult. Partial extraction of MYBPC3 from rat cardiomyocytes has been shown to result in increased Ca^{2+} sensitivity, and total ablation of MYBPC3 is associated with increased Ca^{2+} sensitivity in some mouse models[Fraysse, 2012, Hofmann, 1991]. Haploinsufficiency of MYBPC3 would blunt the "braking" function, leading to a higher rate of cross-bridge cycling in the C-zone. This would presumably also apply to C10-domain non-truncating mutations. Evidence in support of this includes recent findings in both mouse and human cardiomyocytes that MYBPC3 may stabilize the super-relaxed conformation of myosin, in which actin binding and ATP

161

hydrolysis are severely restricted[McNamara, 2017, McNamara, 2016]. These reports demonstrated accelerated ATP turnover and a decrease in the proportion of super-relaxed myosin heads in patient cells and MYBPC3-knockout murine cells, respectively. Whether proteotoxicity of truncated MYBPC3 or proteasome dysfunction could affect overall myocyte Ca^{2+} homeostasis or energy balance is less straightforward, but many processes involved in PQC are ATP-dependent including proteasome-mediated degradation and HSP70 chaperone folding cycles, while Ca^{2+} homeostasis in the endoplasmic reticulum is also vital for maintaining ER proteostasis. Another viable hypothesis suggests that UPS impairment could block the normal degradation of hypertrophic signaling factors, such as calcineurin[Li, 2004], NFAT[Tang, 2010], and MAPK phosphatase-1[Xie, 2009], causing inappropriate activation of pro-hypertrophic signaling. Overall, however, our data does not support that truncated MYBPC3 can elicit these effects on its own. Given that mutations in most other sarcomere genes act by directly altering contractile function, it is difficult to place proteotoxicity of truncated MYBPC3 within a hypothetical larger framework of converging mechanisms.

5.3 The risk of treating absence of evidence as evidence of absence regarding truncated protein expression

The evidence increasingly supports haploinsufficiency of MYBPC3 in patient myocardium, while truncated mutant proteins remain undetected. Nevertheless, we must acknowledge that more sensitive techniques could be employed before accepting the current absence of evidence to mean evidence of absence. Published studies typically used SDS-PAGE and Western blotting to look for truncated proteins, with lower detection

limits established to be 1.5-3.0% of the total MYBPC3 protein[Marston, 2009, Rottbauer, 1997, van Dijk, 2009]. Our lab has attempted to detect truncated proteins by cutting out bands from polyacrylamide gels at the predicted molecular weight of the given protein and analyzing protein composition by mass spectrometry (unpublished data). This method also failed to detect any mutant protein, but it is entirely possible that the mutation ran at a different weight than predicted. As we have observed, proteasome inhibition blocks degradation of MYBPC3 mutants, and could be used to try to bring out expression in patient-derived induced pluripotent stem cell-derived cardiomyocytes. We could also take advantage of frameshift mutants that produce novel amino acid sequences and use mass spectrometry to detect peptides containing these unique sequences. Lastly, the ribo-seq technique could identify whether prematurely terminated MYBPC3 transcripts are ever translated by sequencing of transcript fragments being actively translated and therefore protected from RNase treatment by the ribosome[Ingolia, 2009]. This method has already been successfully used to demonstrate that titin truncating variants which were not detected by SDS-PAGE were indeed translated[Schafer, 2016].

5.4 Future Directions

5.4.1 Potential therapeutic interventions in MYBPC3-linked HCM

Our study found that truncating MYBPC3 mutations could not produce phenotypes when isolated from the haploinsufficiency observed in HCM patients. Recognition that haploinsufficiency plays a central role in disease pathogenesis for MYBPC3 mutation-linked HCM raises interesting possibilities for disease-modifying therapies. Currently, medical management is supportive. Treatments include beta blockers, calcium channel

blockers, surgical myectomy for symptomatic left ventricular outflow tract obstruction, implantable cardiac defibrillators for prevention of sudden cardiac death, and heart transplantation for a small subset of patients who progress to decompensated heart failure. There is a great interest in exploring therapies that could prevent the emergence and/or progression of HCM. MYBPC3 carriers showed the greatest benefit in a small randomized trial of the Ca^{2+} channel blocker diltiazem in sarcomere gene mutation carriers, with reductions in LV wall thickness and mass, improved diastolic filling, and lower cardiac troponin I levels in those taking diltiazem compared with controls[Ho, 2015]. However, correcting the fundamental defect that triggers pathological remodeling in HCM is the ultimate goal for disease prevention. For MYBPC3 mutation carriers, developing strategies to normalize MYBPC3 protein levels could hold tremendous promise. In cellular and mouse models, increasing WT MYBPC3 levels prevents the development of hypertrophy and other HCM phenotypic characteristics[Mearini, 2014, Merkulov, 2012, Monteiro da Rocha, 2016]. These studies raise the possibility of gene delivery of wild-type MYBPC3 via viral vectors into patients with HCM as a potential therapeutic option. Alternatively, with the advent of CRISPR technology, gene correction has been proposed as a treatment option. As a proof of concept CRISPR-mediated repair of a MYBPC3 mutation was recently successful performed in a human embryo[Kaul, 2018] (Figure 5.1A). Another method of gene editing is exon skipping. This strategy has been employed successfully for Duchenne muscular dystrophy[Aartsma-Rus, 2009, Aartsma-Rus, 2017]. In a mouse model carrying biallelic MYBPC3 mutations, antisense oligonucleotide-induced exon skipping produced an alternative transcript that restored partial protein expression and function[Gedicke-Hornung, 2013]. However, this strategy is likely not applicable for heterozygous mutations given that

the WT allele would also undergo exon skipping, leaving no full-length WT MYBPC3. Despite the obvious enthusiasm for applying gene corrective approaches to the treatment of Mendelian diseases like HCM, there are many technical obstacles and safety concerns that limit its applicability in the near future. For these reasons, a more attractive approach to targeted therapy for HCM is small molecule therapeutics. An allosteric myosin modulator (mavacamten) that inhibits myosin ATPase activity has been developed[Green, 2016, Kawas, 2017] (Figure 5.1D) and is currently in clinical trials in HCM patients. However, it is not yet clear whether mavacamten will be effective for those who carry mutations in genes other than myosin. For MYBPC3 mutation carriers, the possibility of targeting haploinsufficiency therapeutically using small molecules could be very attractive for preventing or attenuating disease progression. One potential approach would be to employ read-through strategies (Figure 5.1B). Small molecule drugs have been developed that enable ribosomal read-through of nonsense mutations in mRNA resulting in the production of full length protein. Altaluren, one such small molecule, is being tested in phase 3 clinic trials for the treatment of Duchene Muscular Dystrophy[McDonald, 2017].

5.3.2 Targeting PQC of MYBPC3 as a method to restore normal stoichiometry

As we uncover a more complete understanding surrounding how nonsense mediated mRNA decay, the ubiquitin proteasome system, and molecular chaperones regulate and control MYBPC3 protein levels, we may identify novel targets that can be regulated to restore wild-type MYBPC3 protein levels (Figure 5.1C). Towards this goal, it has already been demonstrated that proteasome inhibition and inhibition of nonsense-mediated mRNA decay can increase MYBPC3 protein levels[Vignier, 2009]. However, this approach could also increase levels of mutant protein which may not incorporate into the

sarcomere or have deleterious effects. Thus, the phenotypic consequences of increased mutant protein levels must be defined. Further, these systems may change levels of other cellular proteins resulting in off-target effects. A potentially more specific approach is to alter the activity of specific molecular chaperones. While identification of HSP70/HSC70 as MYBPC3 chaperones is an important first step towards this, these chaperones are highly ubiquitous and involved in numerous critical cell functions and inhibition would also affect myriad other protein clients. Identification of specific co-chaperones or E3 ligases that assist with HSC70-medated MYBPC3 degradation may allow more finely-tuned regulation of MYBPC3 expression.

5.3.3 Other factors influencing haploinsufficiency of MYBPC3

5.3.3.1 Correlation between WT MYBPC3 levels and HCM phenotypes

An interesting unresolved question is whether MYBPC3 mutation carriers remain asymptomatic until a certain threshold of haploinsufficiency is reached. As we develop modulators of MBYPC3 protein homeostasis, it is also important to recognize that the dynamic relationship between MYBPC3 protein levels and HCM phenotypes remains undefined. More accurate techniques to measure and quantify mRNA and protein levels will facilitate a more refined understanding of this relationship. Some potential useful technologies include the use of human SNPs and high-density DNA arrays to detect allelic imbalance[Mei, 2000] and quantitative mass spectrometry-based analytical methods[Panuwet, 2016]. The development of chemical probes that can dynamically control MYBPC3 protein levels or allow for the quantification of MYBPC3 protein levels within live cardiac tissue could significantly impact on our ability to evaluate how MYBPC3 protein level and disease phenotypes are linked. Identification of modifier genes involved in PQC may help

166

explain some of the phenotypic heterogeneity in HCM. Impairment in protein folding stress responses increases with age and, such modifier genes could affect age of disease onset. For example, HSP70 polymorphisms have tentatively been shown to influence clinical manifestation of HCM in South Asian patient cohorts[Rangaraju, 2014, Rangaraju, 2013].

5.3.3.2 Effects of stress on MYBPC3 expression

Some recent studies have raised the question of whether stress can trigger reduction in MYBPC3 levels and remodeling in asymptomatic individuals, which may also explain the variable age of onset of MYBPC3-linked HCM[Strande, 2015]. Schlossarek et al. found that adrenergic challenge via one week of treatment with isoprenaline and phenylephrine induced ventricular hypertrophy and proteasome dysfunction in previously phenotype-negative heterozygous MYBPC3 mutant mice[Schlossarek, 2012]. Additionally, Barefield et al. observed reduction in wild-type MYBPC3 expression in heterozygous, but not wild-type, mice following both transverse aortic constriction surgery and, surprisingly, sham surgery[Barefield, 2015]. These findings tentatively suggest that stress may influence MYBPC3 expression particularly in truncating mutation carriers. A number of sources of cellular stress activate unfolded protein response pathways, including heat stress, oxidative stress, inflammation, and metabolic dysfunction[Morimoto, 1993]. Additional studies are needed to determine whether stressors such as chronic β-adrenergic stimulation, cardiovascular stress separate from HCM, and trauma can exacerbate or even initiate maladaptive cardiac remodeling by influencing expression of MYBPC3.

5.5 Concluding Remarks

In summary, this dissertation explored connections between MYBPC3 and proteostasis networks in order to better understand how MYBPC3 mutations cause hypertrophic cardiomyopathy and what role protein quality control plays in disease pathogenesis. Our findings challenge two important hypotheses: first, that truncating mutations can cause HCM by disrupting cardiomyocyte proteostasis; and second, that non-truncating mutations share a common dominant-negative mechanism that directly affects contraction independent of mutation locus. On the contrary, we observed that non-truncating mutations in the light meromyosin binding C10 domain of MYBPC3 are rendered acutely unstable compared to other mutations in C3 and C6, and likely result in haploinsufficiency instead. Although we were not able to associate truncated MYBPC3 expression to proteotoxicity or hypertrophic remodeling, our affinity purification-mass spectrometry screen implicated the important molecular chaperone HSC70 as a regulator of MYBPC3 degradation, the first chaperone found to be associated with MYBPC3. These results de-emphasize the role of proteotoxicity in the pathogenesis of HCM, but open the door to new lines of inquiry regarding how therapeutic interventions might restore MYBPC3 sarcomere stoichiometry in haploinsufficient hearts. A more detailed understanding of the mechanisms which regulate MYBPC3 protein homeostasis could potentially lead to a successful treatment strategy for HCM, where natural protein quality control mechanisms could be leveraged to selectively restore MYBPC3 protein homeostasis and overcome haploinsufficiency.

FIGURE 5.1
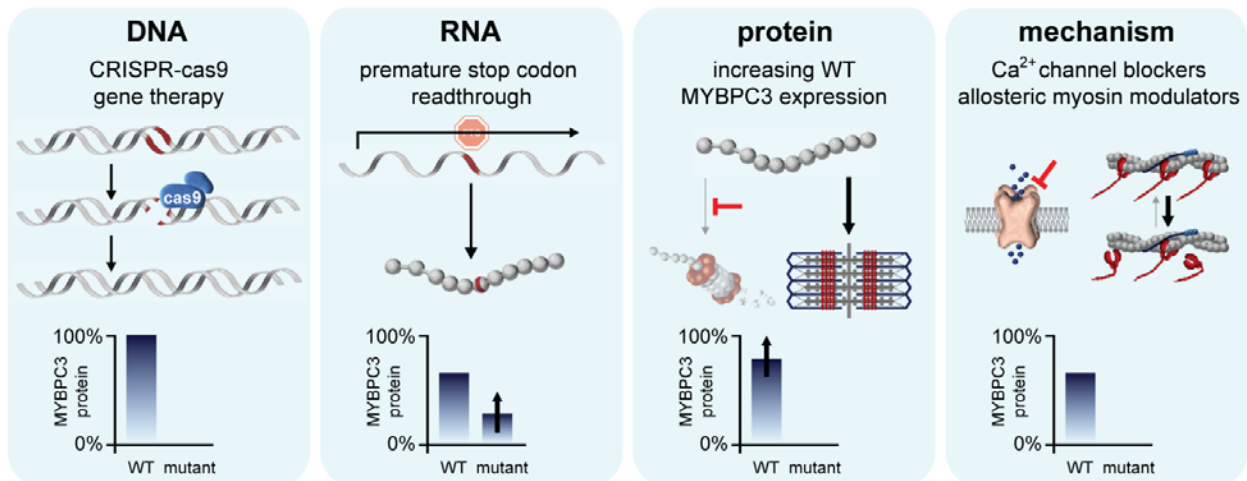
Figure 5.1. **Potential therapeutic approaches to correcting or ameliorating the effects of MYBPC3 haploinsufficiency in HCM at different mechanistic stages.** Such approaches could include: correction of the mutant allele through gene editing technology, restoring full expression of wild-type MYBPC3; stop codon readthrough for truncating mutations, resulting in expression of a mutant but functional full-length protein; increasing expression of the wild-type protein by modulating its turnover; and targeting of downstream maladaptive mechanisms without affecting MYBPC3 protein expression.

5.5 REFERENCES

1.   Aartsma-Rus A, Fokkema I, Verschuuren J, Ginjaar I, van Deutekom J, van Ommen GJ, den Dunnen JT. Theoretic applicability of antisense-mediated exon skipping for duchenne muscular dystrophy mutations. *Human mutation.* 2009;30:293-299

2.   Aartsma-Rus A, Straub V, Hemmings R, Haas M, Schlosser-Weber G, Stoyanova-Beninska V, Mercuri E, Muntoni F, Sepodes B, Vroom E, Balabanov P. Development of exon skipping therapies for duchenne muscular dystrophy: A critical review and a perspective on the outstanding issues. *Nucleic acid therapeutics.* 2017;27:251-259

3.   Alfares AA, Kelly MA, McDermott G, Funke BH, Lebo MS, Baxter SB, Shen J, McLaughlin HM, Clark EH, Babb LJ, Cox SW, DePalma SR, Ho CY, Seidman JG, Seidman CE, Rehm HL. Results of clinical genetic testing of 2,912 probands with hypertrophic cardiomyopathy: Expanded panels offer limited additional sensitivity. *Genetics in medicine : official journal of the American College of Medical Genetics.* 2015

4.   Ashrafian H, Redwood C, Blair E, Watkins H. Hypertrophic cardiomyopathy:A paradigm for myocardial energy depletion. *Trends in genetics : TIG.* 2003;19:263-268

5.   Bahrudin U, Morisaki H, Morisaki T, Ninomiya H, Higaki K, Nanba E, Igawa O, Takashima S, Mizuta E, Miake J, Yamamoto Y, Shirayoshi Y, Kitakaze M, Carrier L, Hisatome I. Ubiquitin-proteasome system impairment caused by a missense cardiac myosin-binding protein c mutation and associated with cardiac dysfunction in hypertrophic cardiomyopathy. *Journal of molecular biology.* 2008;384:896-907

6.   Barefield D, Kumar M, Gorham J, Seidman JG, Seidman CE, de Tombe PP, Sadayappan S. Haploinsufficiency of mybpc3 exacerbates the development of hypertrophic cardiomyopathy in heterozygous mice. *Journal of molecular and cellular cardiology.* 2015;79:234-243

7.   del Rio Carlos L, Henze Marcus P, Wong Fiona L, Evanchik Marc J, Divekar A, Gifford Lindsey M, Ferhaan A, Green Eric M. Abstract 20770: A novel mini-pig genetic model of hypertrophic cardiomyopathy: Altered myofilament dynamics, hyper-contractility, and impaired systolic/diastolic functional reserve in vivo. *Circulation.* 2017;136:A20770-A20770

8.   Fraysse B, Weinberger F, Bardswell SC, Cuello F, Vignier N, Geertz B, Starbatty J, Kramer E, Coirault C, Eschenhagen T, Kentish JC, Avkiran M, Carrier L. Increased myofilament ca2+ sensitivity and diastolic dysfunction as early

consequences of mybpc3 mutation in heterozygous knock-in mice. *J Mol Cell Cardiol.* 2012;52:1299-1307

9. Gedicke-Hornung C, Behrens-Gawlik V, Reischmann S, Geertz B, Stimpel D, Weinberger F, Schlossarek S, Precigout G, Braren I, Eschenhagen T, Mearini G, Lorain S, Voit T, Dreyfus PA, Garcia L, Carrier L. Rescue of cardiomyopathy through u7snrna-mediated exon skipping in mybpc3-targeted knock-in mice. *EMBO molecular medicine.* 2013;5:1128-1145

10. Glazier AA, Hafeez N, Mellacheruvu D, Basrur V, Nesvizhskii AI, Lee LM, Shao H, Tang V, Yob JM, Gestwicki JE, Helms AS, Day SM. Hsc70 is a chaperone for wild-type and mutant cardiac myosin binding protein c. *JCI insight.* 2018;3

11. Golenhofen N, Perng MD, Quinlan RA, Drenckhahn D. Comparison of the small heat shock proteins alphab-crystallin, mkbp, hsp25, hsp20, and cvhsp in heart and skeletal muscle. *Histochemistry and cell biology.* 2004;122:415-425

12. Green EM, Wakimoto H, Anderson RL, Evanchik MJ, Gorham JM, Harrison BC, Henze M, Kawas R, Oslob JD, Rodriguez HM, Song Y, Wan W, Leinwand LA, Spudich JA, McDowell RS, Seidman JG, Seidman CE. A small-molecule inhibitor of sarcomere contractility suppresses hypertrophic cardiomyopathy in mice. *Science (New York, N.Y.).* 2016;351:617-621

13. Green Eric M, Weiss Robert M, Divekar A, Bartholomew Ingle Sadie R, Henze M, Kawas R, Gifford L, Davis Melissa K, Rohret F, Thedens Daniel R, Rodriguez Hector M, Evanchik Marc J, Anderson Robert L, Sieren J, Rogers Christopher S, Meyerholz David K, Ahmad F. Abstract 16: A minipig genetic model of hypertrophic cardiomyopathy. *Circulation research.* 2017;121:A16-A16

14. Helms AS, Davis FM, Coleman D, Bartolone SN, Glazier AA, Pagani F, Yob JM, Sadayappan S, Pedersen E, Lyons R, Westfall MV, Jones R, Russell MW, Day SM. Sarcomere mutation-specific expression patterns in human hypertrophic cardiomyopathy. *Circulation. Cardiovascular genetics.* 2014;7:434-443

15. Ho CY, Lakdawala NK, Cirino AL, Lipshultz SE, Sparks E, Abbasi SA, Kwong RY, Antman EM, Semsarian C, Gonzalez A, Lopez B, Diez J, Orav EJ, Colan SD, Seidman CE. Diltiazem treatment for pre-clinical hypertrophic cardiomyopathy sarcomere mutation carriers: A pilot randomized trial to modify disease expression. *JACC. Heart failure.* 2015;3:180-188

16. Hofmann PA, Hartzell HC, Moss RL. Alterations in ca2+ sensitive tension due to partial extraction of c-protein from rat skinned cardiac myocytes and rabbit skeletal muscle fibers. *The Journal of general physiology.* 1991;97:1141-1163

17. Hollander JM, Martin JL, Belke DD, Scott BT, Swanson E, Krishnamoorthy V, Dillmann WH. Overexpression of wild-type heat shock protein 27 and a nonphosphorylatable heat shock protein 27 mutant protects against ischemia/reperfusion injury in a transgenic mouse model. *Circulation*. 2004;110:3544-3552

18. Ingolia NT, Ghaemmaghami S, Newman JR, Weissman JS. Genome-wide analysis in vivo of translation with nucleotide resolution using ribosome profiling. *Science (New York, N.Y.)*. 2009;324:218-223

19. Jacques A, Hoskins AC, Kentish JC, Marston SB. From genotype to phenotype: A longitudinal study of a patient with hypertrophic cardiomyopathy due to a mutation in the mybpc3 gene. *Journal of muscle research and cell motility*. 2008;29:239-246

20. Karsai A, Kellermayer MS, Harris SP. Mechanical unfolding of cardiac myosin binding protein-c by atomic force microscopy. *Biophysical journal*. 2011;101:1968-1977

21. Kaul S, Heitner SB, Mitalipov S. Sarcomere gene mutation correction. *European heart journal*. 2018;39:1506-1507

22. Kawas RF, Anderson RL, Ingle SRB, Song Y, Sran AS, Rodriguez HM. A small-molecule modulator of cardiac myosin acts on multiple stages of the myosin chemomechanical cycle. *The Journal of biological chemistry*. 2017;292:16571-16577

23. Kotter S, Unger A, Hamdani N, Lang P, Vorgerd M, Nagel-Steger L, Linke WA. Human myocytes are protected from titin aggregation-induced stiffening by small heat shock proteins. *The Journal of cell biology*. 2014;204:187-202

24. Li HH, Kedar V, Zhang C, McDonough H, Arya R, Wang DZ, Patterson C. Atrogin-1/muscle atrophy f-box inhibits calcineurin-dependent cardiac hypertrophy by participating in an scf ubiquitin ligase complex. *The Journal of clinical investigation*. 2004;114:1058-1071

25. Marston S, Copeland O, Jacques A, Livesey K, Tsang V, McKenna WJ, Jalilzadeh S, Carballo S, Redwood C, Watkins H. Evidence from human myectomy samples that mybpc3 mutations cause hypertrophic cardiomyopathy through haploinsufficiency. *Circulation research*. 2009;105:219-222

26. McDonald CM, Campbell C, Torricelli RE, Finkel RS, Flanigan KM, Goemans N, Heydemann P, Kaminska A, Kirschner J, Muntoni F, Osorio AN, Schara U, Sejersen T, Shieh PB, Sweeney HL, Topaloglu H, Tulinius M, Vilchez JJ, Voit T, Wong B, Elfring G, Kroger H, Luo X, McIntosh J, Ong T, Riebling P, Souza M, Spiegel RJ, Peltz SW, Mercuri E. Ataluren in patients with nonsense mutation

duchenne muscular dystrophy (act dmd): A multicentre, randomised, double-blind, placebo-controlled, phase 3 trial. *Lancet (London, England).* 2017;390:1489-1498

27.   McDonough H, Patterson C. Chip: A link between the chaperone and proteasome systems. *Cell stress & chaperones.* 2003;8:303-308

28.   McNamara JW, Li A, Lal S, Bos JM, Harris SP, van der Velden J, Ackerman MJ, Cooke R, Dos Remedios CG. Mybpc3 mutations are associated with a reduced super-relaxed state in patients with hypertrophic cardiomyopathy. *PLoS One.* 2017;12:e0180064

29.   McNamara JW, Li A, Smith NJ, Lal S, Graham RM, Kooiker KB, van Dijk SJ, Remedios CGD, Harris SP, Cooke R. Ablation of cardiac myosin binding protein-c disrupts the super-relaxed state of myosin in murine cardiomyocytes. *Journal of molecular and cellular cardiology.* 2016;94:65-71

30.   Mearini G, Stimpel D, Geertz B, Weinberger F, Kramer E, Schlossarek S, Mourot-Filiatre J, Stoehr A, Dutsch A, Wijnker PJ, Braren I, Katus HA, Muller OJ, Voit T, Eschenhagen T, Carrier L. Mybpc3 gene therapy for neonatal cardiomyopathy enables long-term disease prevention in mice. *Nature communications.* 2014;5:5515

31.   Mei R, Galipeau PC, Prass C, Berno A, Ghandour G, Patil N, Wolff RK, Chee MS, Reid BJ, Lockhart DJ. Genome-wide detection of allelic imbalance using human snps and high-density DNA arrays. *Genome research.* 2000;10:1126-1137

32.   Merkulov S, Chen X, Chandler MP, Stelzer JE. In vivo cardiac myosin binding protein c gene transfer rescues myofilament contractile dysfunction in cardiac myosin binding protein c null mice. *Circ Heart Fail.* 2012;5:635-644

33.   Monteiro da Rocha A, Guerrero-Serna G, Helms A, Luzod C, Mironov S, Russell M, Jalife J, Day SM, Smith GD, Herron TJ. Deficient cmybp-c protein expression during cardiomyocyte differentiation underlies human hypertrophic cardiomyopathy cellular phenotypes in disease specific human es cell derived cardiomyocytes. *Journal of molecular and cellular cardiology.* 2016;99:197-206

34.   Morimoto RI. Cells in stress: Transcriptional activation of heat shock genes. *Science (New York, N.Y.).* 1993;259:1409-1410

35.   Otey CA, Dixon R, Stack C, Goicoechea SM. Cytoplasmic ig-domain proteins: Cytoskeletal regulators with a role in human disease. *Cell motility and the cytoskeleton.* 2009;66:618-634

36.   Panuwet P, Hunter RE, Jr., D'Souza PE, Chen X, Radford SA, Cohen JR, Marder ME, Kartavenka K, Ryan PB, Barr DB. Biological matrix effects in quantitative

tandem mass spectrometry-based analytical methods: Advancing biomonitoring. *Critical reviews in analytical chemistry*. 2016;46:93-105

37. Predmore JM, Wang P, Davis F, Bartolone S, Westfall MV, Dyke DB, Pagani F, Powell SR, Day SM. Ubiquitin proteasome dysfunction in human hypertrophic and dilated cardiomyopathies. *Circulation*. 2010;121:997-1004

38. Quan L, Lv Q, Zhang Y. Strum: Structure-based prediction of protein stability changes upon single-point mutation. *Bioinformatics (Oxford, England)*. 2016;32:2936-2946

39. Rangaraju AML, Satyanarayana; Calambur, Narasimhan; Nallari, Pratibha. Modifier genes in hypertrophic cardiomyopathy patients of south indian cohort. *International Journal of Genetics and Genomics*. 2014;2:84-91

40. Rangaraju AS, ML; Ananthapur, Venkateshwari; Swapna, Nalla; Narasimhan, Calambur; Nallari, Pratibha Heat shock protein 70 polymorphism in hypertrophic cardiomyopathy of south indian cohort. *Journal of Indian College of Cardiology*. 2013;3:9-15

41. Rottbauer W, Gautel M, Zehelein J, Labeit S, Franz WM, Fischer C, Vollrath B, Mall G, Dietz R, Kubler W, Katus HA. Novel splice donor site mutation in the cardiac myosin-binding protein-c gene in familial hypertrophic cardiomyopathy. Characterization of cardiac transcript and protein. *The Journal of clinical investigation*. 1997;100:475-482

42. Sarikas A, Carrier L, Schenke C, Doll D, Flavigny J, Lindenberg KS, Eschenhagen T, Zolk O. Impairment of the ubiquitin-proteasome system by truncated cardiac myosin binding protein c mutants. *Cardiovascular research*. 2005;66:33-44

43. Schafer S, de Marvao A, Adami E, Fiedler LR, Ng B, Khin E, Rackham OJL, van Heesch S, Pua CJ, Kui M, Walsh R, Tayal U, Prasad SK, Dawes TJW, Ko NSJ, Sim D, Chan LLH, Chin CWL, Mazzarotto F, Barton PJ, Kreuchwig F, de Kleijn DPV, Totman T, Biffi C, Tee N, Rueckert D, Schneider V, Faber A, Regitz-Zagrosek V, Seidman JG, Seidman CE, Linke WA, Kovalik J-P, O'Regan D, Ware JS, Hubner N, Cook SA. Titin-truncating variants affect heart function in disease cohorts and the general population. *Nature genetics*. 2016;49:46

44. Schlossarek S, Englmann DR, Sultan KR, Sauer M, Eschenhagen T, Carrier L. Defective proteolytic systems in mybpc3-targeted mice with cardiac hypertrophy. *Basic research in cardiology*. 2012;107:235

45. Schlossarek S, Schuermann F, Geertz B, Mearini G, Eschenhagen T, Carrier L. Adrenergic stress reveals septal hypertrophy and proteasome impairment in

heterozygous mybpc3-targeted knock-in mice. *Journal of muscle research and cell motility*. 2012;33:5-15

46. Smelter DF, de Lange WJ, Cai W, Ge Y, Ralphe JC. The hcm-linked w792r mutation in cardiac myosin-binding protein c reduces c6 fniii domain stability. *American journal of physiology. Heart and circulatory physiology*. 2018;314:H1179-H1191

47. Strande JL. Haploinsufficiency mybpc3 mutations: Another stress induced cardiomyopathy? Let's take a look! *Journal of molecular and cellular cardiology*. 2015;79:284-286

48. Tang M, Li J, Huang W, Su H, Liang Q, Tian Z, Horak KM, Molkentin JD, Wang X. Proteasome functional insufficiency activates the calcineurin-nfat pathway in cardiomyocytes and promotes maladaptive remodelling of stressed mouse hearts. *Cardiovascular research*. 2010;88:424-433

49. Thottakara T, Friedrich FW, Reischmann S, Braumann S, Schlossarek S, Kramer E, Juhr D, Schluter H, van der Velden J, Munch J, Patten M, Eschenhagen T, Moog-Lutz C, Carrier L. The e3 ubiquitin ligase asb2beta is downregulated in a mouse model of hypertrophic cardiomyopathy and targets desmin for proteasomal degradation. *Journal of molecular and cellular cardiology*. 2015;87:214-224

50. van Dijk SJ, Dooijes D, dos Remedios C, Michels M, Lamers JM, Winegrad S, Schlossarek S, Carrier L, ten Cate FJ, Stienen GJ, van der Velden J. Cardiac myosin-binding protein c mutations and hypertrophic cardiomyopathy: Haploinsufficiency, deranged phosphorylation, and cardiomyocyte dysfunction. *Circulation*. 2009;119:1473-1483

51. Vignier N, Schlossarek S, Fraysse B, Mearini G, Kramer E, Pointu H, Mougenot N, Guiard J, Reimer R, Hohenberg H, Schwartz K, Vernet M, Eschenhagen T, Carrier L. Nonsense-mediated mrna decay and ubiquitin-proteasome system regulate cardiac myosin-binding protein c mutant levels in cardiomyopathic mice. *Circulation research*. 2009;105:239-248

52. Xie P, Guo S, Fan Y, Zhang H, Gu D, Li H. Atrogin-1/mafbx enhances simulated ischemia/reperfusion-induced apoptosis in cardiomyocytes through degradation of mapk phosphatase-1 and sustained jnk activation. *The Journal of biological chemistry*. 2009;284:5488-5496

53. Yang J, Yan R, Roy A, Xu D, Poisson J, Zhang Y. The i-tasser suite: Protein structure and function prediction. *Nature methods*. 2015;12:7-8